Detecting Particles Properties From Their Kinematics in Granular Flows

SUDIP LAUDARI

Supervisor: Pierre Rognon
Associate Supervisor: Benjy Marks

A thesis submitted in fulfilment of
the requirements for the degree of
Doctor of Philosophy

School of Civil Engineering
Faculty of Engineering
The University of Sydney
Australia

2 August 2024

Statement of originality

This is to certify that to the best of my knowledge, the content of this thesis is my own work. This thesis has not been submitted for any degree or other purposes. I certify that the intellectual content of this thesis is the product of my own work and that all the assistance received in preparing this thesis and sources have been acknowledged.

Sudip Laudari

Abstract

This Thesis introduces a method for detecting the physical properties of particles in granular flows. It aims to establish a proof of concept that particles kinematics contain information regarding their physical properties, and can therefore be used as a proxy to detect them. To reach this aim, we used a combination of simulated granular flows involving different particles, and machine learning classifiers to try and detect particles of differing properties based on the knowledge of their kinematics.

This approach is first applied to the case of individual particles dropped on an inclined plane. It is found that monitoring particles position and velocity as they bounce and roll enables to detect properties such as density, stiffness, friction and adhesion. This means that this method could significantly enhance traditional *sensor-based* sorting used in mineral progressing, as these properties are difficult or impossible to detect using conventional sensors during motion.

The kinematic-based classification is then applied to silo flows and flows in a rotating drums involving mixtures of two particle sizes. Results show that the size of large and small particles can be effectively detected based on their kinematics. Moreover, they show that the size of the smaller particles can be detected from the kinematics of the larger particles. These findings are particularly relevant to optimising industrial processes involving comminution using ball mills; the method proposed here indicate that large crusher kinematics can be used to monitor the size of smaller particles during comminution.

The conclusions of this thesis pave the way to enhancing a number of industrial processes requiring in-situ detection of particles properties. Furthermore, it is likely that kinematic-based detection of particle property would apply to a range of particulate fluids including suspensions, emulsions or foams.

Acknowledgements

First and foremost, I express my heartfelt gratitude to my supervisors, Prof. Pierre Rognon and Dr. Benjy Marks, for giving me the opportunity to work on this project. Their unwavering support, invaluable guidance, and deep insights have been the foundation of this research and have inspired me to reach my potential.

I am sincerely thankful for the invaluable feedback and thoughtful suggestions from my thesis committee members, which have added depth and rigor to my work.

Special thanks to Prof. Itai Einav, Dr. Francois Guillard, and the entire Granular group for their invaluable insights and support during our group meetings. These sessions have always been a source of learning and skill improvement, greatly enriching my academic journey. I am also deeply grateful to the faculty and staff of the Civil Engineering Department for their dedication to excellence and consistent support throughout my research journey.

To my beloved wife Nurana Samadova and my family: your unwavering love and belief in me have been my constant source of strength. Your patience and encouragement have lightened every challenging step of this journey. A warm acknowledgment goes to all my friends and colleagues. Your unwavering support and shared moments of joy have made this academic voyage both memorable and meaningful. Lastly, a profound thank you from the bottom of my heart to everyone who has touched my PhD journey in any manner. Your faith and support have been instrumental.

CONTENTS

List of Figures

CHAPTER 1

Introduction

Granular materials encompass a spectrum of particles including fine desert sand grains, fragmented rocks, seeds and grains. These particles exhibit a large diversity in physical property such as their size, size distribution, shape, density, stiffness and adhesion. These in turn underpin rich rheological properties. Granular materials are infamous for behaving like a solid, like a liquid or like a gas depending on the external stresses and on the particle properties. Establishing the link between the particle properties and their collective flow properties is key to many application, and remains a significant scientific challenge. Figure 1.1 illustrates this two ways relation.

A significant body of research has focused on predicting the flow behaviour from known particle properties, which is illustrated by the top arrow on figure 1.1. Applications of these discoveries includes the prediction of the flow dynamics of natural events such as landslides and snow avalanches. They also include the design of more efficient industrial processes in many sectors involving handling granular matter. Mineral processing is a notorious example, as it requires conveying, crushing, sorting and mixing vast quantities of bulk materials.

The reverse relation is to predict the particles properties based on observable flow dynamics, as illustrated by the bottom arrow on figure 2.1 (image source [1]). Research pertaining to this question is at its infancy. It is the focus of this Thesis. The hypothesis is that, given that particle properties influence the way the move, the way they move may contain some information on their properties.

The goal of this Thesis is to establish a proof of this concept, by exploring which particle properties can be inferred from their kinematics, if any, and how. Kinematics includes

trajectory, velocity and acceleration. Particle properties include there size density, stiffness, friction and adhesion.

The anticipated practical application driving this study is to provide a new method for sensing particle properties that would be difficult to measure directly while they move. Such a method would strongly benefit large scale industrial processes such as *sensor-based* particle sorting and *ball-milling*.

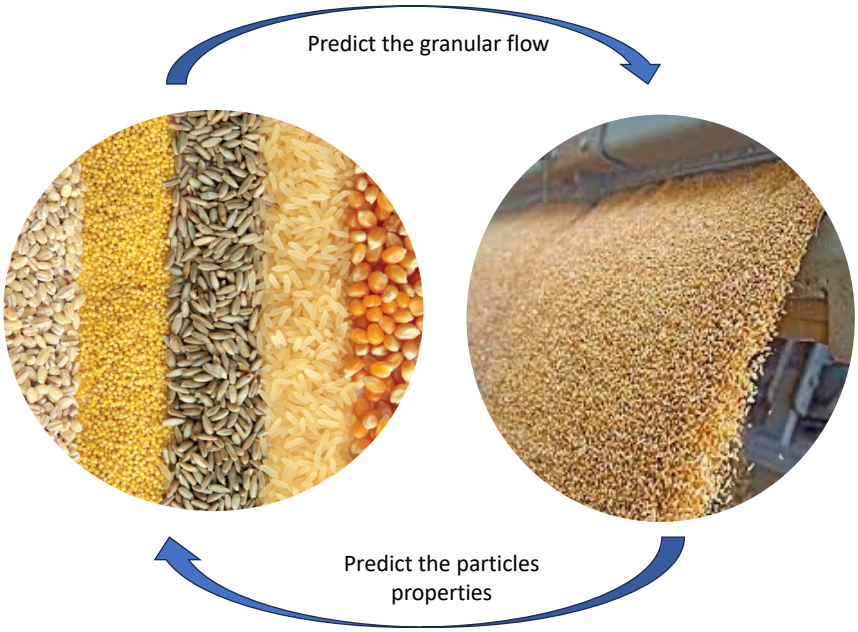

FIGURE 1.1: **Relation between particle properties and granular flows.** Many applications require the ability to predict the flow properties knowing the grain properties, illustrated by the top arrow. This Thesis focuses on much more uncharted reverse relation illustrated by the bottom arrow: can particle properties be deduced from their kinematic within the flow.

Sensor-based sorting: consists of separating two kinds of particles by presenting them individually to a sensor while they move and using this sensor to classify the particle, usually as either “valuable” or “waste”. However, most particle mechanical properties cannot be measured while they move. This Thesis will investigate whether the particle kinematics, which can be measured by conventional imaging, may be used as a proxy to infer these properties.

Ball-milling: consists of crushing large particles into small, often powder size particles by making them flow in a rotating drum containing large steel balls acting as crushers.

The key challenge in this process is to monitor in-situ the particle size. There is no sensor available that can perform this task, greatly due to the harsh mechanical environment. However, it was recently showed that accelerometer could be embedded into crushers and monitor their acceleration. This Thesis will investigate whether the crusher of acceleration contains information on the size of the smaller particles, and whether it can be used as a proxy to sense them.

To investigate the potential of kinematic-based sensing, this Thesis developed a two steps approach. First, granular flows are simulated using a discrete element methods with different kinds of particles. Second, a machine learning classifier is trained and tested to assess its ability to detect a specific particle kind based on their recorded kinematics. The following report details this method and application to different configuration. It is structured as follows:

- Chapter 2 - reviews the literature with a focus on applicaiton needing sorting of granular materials and granular rheology.
- Chapter 3 - details the methodology, including DEM simulations and machine learning techniques.
- Chapter 4 - applies this method to the case of individual particle falling on an inclined plane. The aim is to show how mechanical properties can be inferred from their kinematics, thus advancing the possibilities of sensor-based sorting.
- Chapter 5 and 6 - applies this method to flows in silo and in rotatiing drum comprising two different particle sizes. The goal is to demonstrate that the particle size can be deduced from their kinematic. Chapter 6 specifically focuses on the ball-mill application, and explore whether the kinematics of large crushers in rotating drum can be used as a proxi to sense the size of smaller particles.
- Chapter 7- applies the method using experimental data where a large particles is immersed in a packing of small particles that is subjected to shaking.
- Chapter 8 - summarizes the key findings of this Thesis and their implication.

CHAPTER 2

Literature Review

In this chapter, we explore grain flow behavior and how this affects sorting methods. We start by looking at existing sorting methods, what they are used for, and the problems they face. Next, we focus on various flow regimes and how this influences sorting. We also look into how machine learning can improve sorting. The discussion points out the importance of continually updating sorting technologies to make them adaptable and dependable, especially while classifying grains based on their kinematics properties.

2.1 Application of Sorting

The diverse applications of sorting extend far beyond simple organizational tasks, playing a significant role in our daily lives and various work processes. Often without our conscious recognition, we rely on sorting techniques that are crucial for enhancing efficiency and sustainability across different sectors. Among these, the sorting of grains stands out as a prime example. This process not only guarantees the quality of our food but also improves production efficiency and supports sustainable farming practices, affecting virtually every aspect of our consumption and usage of agricultural products. It underscores the importance of sorting in elevating quality, increasing efficiency, and fostering environmental sustainability.

Particularly in agriculture, sorting technologies are indispensable within the supply chain, ensuring that consumers receive only the highest quality seeds and grains. These efforts contribute to sustainable farming practices and strengthen food security [2]. Employing advanced optical machines allows for the precise identification and classification of agricultural products based on characteristics such as color, shape, and ripeness. This capability is crucial for ensuring food safety and maintaining high-quality standards in our food supply [3]. Through these examples, we see how integral sorting is to our daily lives, especially in ensuring the quality and safety of the food we consume.

In the pharmaceutical industry, sorting ensures that tablets are uniform, which is crucial for the correct dosage and drug effectiveness which are the key factors in patient care and treatment outcomes [4]. Similarly, the mining sector benefits from sorting technologies like X-ray and near-infrared sensors, which are used to separate valuable minerals efficiently. This not only saves on processing costs but also helps to protect the environment by reducing waste [5, 6]. Beside these industries, there are other industries which also benefit from sorting technologies. For instance, the construction industry, it relies on sorting to obtain materials such as sand and gravel that meet specific quality standards, thus guaranteeing the structural integrity and longevity of buildings and infrastructure [7]. Further, recycling sees a significant boost from these technologies, which help separate materials like plastics, metals, and paper, aiding circular economy efforts and reducing reliance on virgin materials [8]. They also play a key

role in waste management by segregating organic from inorganic waste, contributing to lower greenhouse emissions and producing compost for agriculture [9]. In manufacturing, sorting ensures component quality and material purity, essential for the production of high-tech goods [10].

This diverse application of sorting and technologies shows their importance in everyday tasks extending far beyond merely organizing materials. They are essential for guaranteeing the quality and dependability of products in numerous sectors. Understanding the kinematics of grains, specifically their movement and flow, is especially critical. By examining their behavior and kinematic properties, we can devise more accurate sorting methods tailored to the distinct requirements of each grain type, whether for planting, processing, or packaging.

2.2 Sorting Techniques: Evolution and Limitations

The process of sorting granular materials has significantly evolved, transitioning from basic manual techniques to advanced technological solutions across various industries. Initially, sorting was primarily manual, relying on visual inspection or mechanical processing to categorize particles by size, shape, color, and density [11]. Later, an innovative approaches revolutionize sorting techniques by utilizing electrostatic induction, where particles are charged for separation in electric fields, demonstrating a creative strategy to leverage physical properties for sorting [12]. For instance, a traditional sorting method involves the use of conveyor belts equipped with scanning cameras and detectors, as illustrated in figure 2.1. Studies also highlight the persistent use of these traditional techniques, where scanning cameras and conveyor belts play a crucial role in sorting particles by color and size [13]. Additionally, the utilization of structures like pipes and chutes aids in segregation [14, 15], and research into how particles interact within vertical pipes provides insight into their behavior [16]. Further, the incorporation of stationary or mobile obstacles to manage material flow exemplifies the diversity of traditional sorting approaches, which can vary in their ability to separate or combine materials [17, 18].

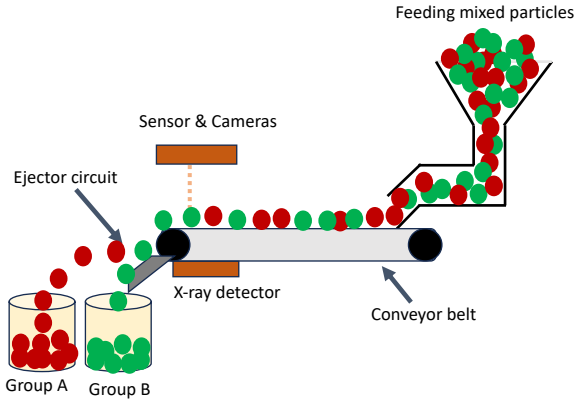

FIGURE 2.1: **Conventional Particle Sorting System** - A visualization of a sorting setup using conveyor belt, sensors, cameras, and an X-ray detector for particle segregation and sorting.

Additionally, the development of advanced sorting technologies that integrate machine vision, sensing technologies, and machine learning offers improvements over the limitations of traditional methods, as evidenced in the literature [19, 20, 21]. Machine vision systems, for example, utilize advanced image processing algorithms to classify particles based on visual characteristics, while sensor technologies such as optical, laser-based, and acoustic offer real-time insights into particle size, shape, and composition. Machine learning, with its ability to digest large datasets, enables the automated classification of particles by learning from their features and movements [22, 23]. These innovations not only enhance sorting accuracy but also cater to the high-volume demands of industrial applications.

The evolution of particle sorting technologies marks a significant transition from traditional methods to more advanced techniques that emphasize the dynamic behaviors and kinematic properties of particles. This shift underscores the growing complexity of sorting challenges that require a nuanced understanding of particle motion. Traditional technologies, while effective to a certain extent, often fall short in capturing the full spectrum of particle kinematics, pointing to a critical area of research and development. The focus is increasingly on leveraging the trajectories and motion patterns of particles to refine sorting and segregation processes. A deeper understanding of granular flow regimes and their kinematic signatures is key to unlocking these advancements. Each regime presents unique patterns of movement and interactions among particles, offering rich insights into their inherent properties. By

analyzing velocities, accelerations, and trajectories, we can uncover new dimensions of material characteristics. Such knowledge paves the way for innovative sorting methods that are not only more efficient but also capable of meeting the specific needs of various industries. This continuous exploration and application of kinematic principles promise to revolutionize sorting technologies, making them more adaptable and precise.

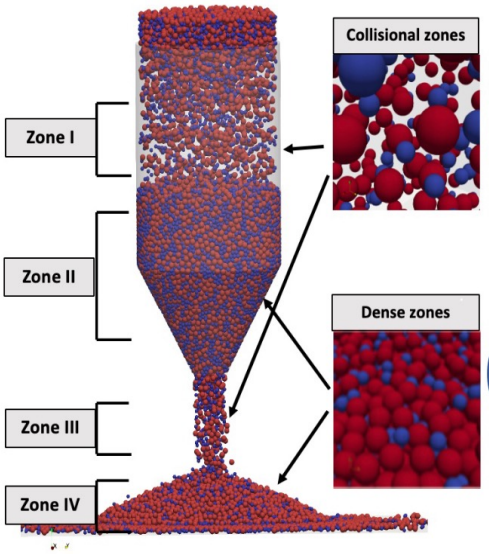

FIGURE 2.2: Silo configuration and different flow regimes. We utilized particles kinematics to detect size of large and small particles.

The subsequent sections will delve deeper into granular flow regimes, examining their kinematic properties and how these can be systematically analyzed to correlate with particle characteristics. This exploration is pivotal to our second research work (chapter-5), which investigates the implications of kinematic properties in different flow regimes, specifically within silo configurations (see figure 2.2). Through this lens, we aim to uncover the potential of kinematics for improving industrial sorting processes, setting the stage for a new era of operational efficiency and accuracy.

2.3 Understanding Kinematics in Granular Flow Regimes

The way we sort granular materials, like grains or sand, greatly depends on understanding how they move in different flow patterns. This area of study focuses on motion without worrying

about what causes it. In granular flows, where particles move and interact, recognizing these patterns is crucial. For example, in a dense flow, particles move slowly, mainly touching and pushing against each other. Sorting systems for this kind of flow need to handle these constant contacts well. On the other hand, in a fast-moving "gaseous" flow, particles bounce off each other quickly. Here, sorting systems must quickly adjust to the fast, unpredictable movements. There is also a "liquid" flow, a mix of the two, where particles are close together but still moving, making sorting a bit trickier because it has to deal with both pushing contacts and quick movements [24, 25, 26, 27].

To simulate these kinematic behaviors, various approaches have been developed. Among them, the Discrete Element Method (DEM) is particularly prominent for its accuracy in modeling the motion and interaction of particles. DEM was first introduced by Cundall and Strack in their pioneering work [28]. Their groundbreaking study laid the foundation for using numerical methods to analyze granular assemblies, providing a robust framework to understand particle dynamics. Cundall and Strack's model treats each particle as a discrete entity and calculates its trajectory based on Newton's laws of motion, incorporating contact forces between particles. This method allows for the detailed examination of particle interactions, such as collisions and frictional contacts, which are essential for accurately predicting the behavior of granular materials. Their work demonstrated that DEM could effectively model complex phenomena like the formation of force chains and the distribution of stresses within a granular assembly. This has made DEM a crucial tool in studying granular flows in various contexts, from industrial processes to natural events like landslides and avalanches. Over the years, DEM has evolved and been refined, incorporating more sophisticated contact models and computational techniques, but the fundamental principles established by Cundall and Strack remain central to its application [28].

In DEM simulations, the trajectories of particles are computed by solving Newton's second law of motion. The force interactions, especially the contact forces between particles, are modeled using various contact mechanics theories, such as the Hertz-Mindlin no-slip model and other advanced contact models. This approach allows for detailed visualization and analysis of granular flows, providing critical insights into particle dynamics that are essential

for developing effective sorting technologies. For example, DEM has been used extensively to study the behavior of granular materials in various industrial processes, such as hopper discharge, mixing, and milling operations [29]. It has also been applied to understand the flow behavior in natural phenomena like landslides and avalanches [30]. These studies have demonstrated the robustness of DEM in capturing the complex interactions and motion of particles under different conditions. While DEM has been highly successful, other methods, such as continuous and multi-scale strategies, have also shown promise, especially for dense granular flows. Continuous approaches like the Navier-Stokes equations adapted for granular flows and multi-scale methods that combine DEM with continuum models help to bridge the gap between micro-scale particle interactions and macro-scale flow behavior [31, 32]. These methods can efficiently handle larger systems and more complex scenarios, providing a comprehensive understanding of granular flow regimes.

Incorporating these diverse approaches enhances our ability to simulate and analyze the kinematics of granular materials across different flow regimes. By leveraging the strengths of DEM, continuous models, and multi-scale strategies, we can develop more accurate and robust models that inform the design of advanced sorting technologies. Understanding these flow patterns is important for several reasons. First, it helps us create sorting technologies that are more efficient by designing them specifically for each type of flow. Second, it provides a deeper understanding of granular material behavior, opening up new methods for particle sorting and improvements in various industrial processes. Lastly, knowing more about these flows improves the accuracy of sorting, which is crucial for meeting the high standards required in many industries. This multidisciplinary approach not only refines existing techniques but also opens new avenues for research and application across diverse sectors.

The upcoming subsections will delve deeper into the characteristics of the dense, gaseous, and intermediate flow regimes and explore their specific implications for particle sorting. By examining the specific characteristics of each flow regime, we gain insights into the influence of particle kinematics on sorting outcomes. This knowledge enables us to understand flow behavior in different flow regimes and propose more effective sorting strategies tailored to

these distinct regimes. Our aim is to not only enhance existing sorting technologies but also to develop innovative methodologies capable of navigating the complexities of granular flows. This effort is crucial for advancing our understanding of how particle motion can indicate their inherent properties, thereby filling a significant gap in current sorting technology applications across various industries.

2.3.1 Dense Quasi-Static Regime

In the dense quasi-static regime, particles are closely packed, and their movement is mainly slow due to the friction between them. This friction affects how particles move and interact, leading to specific patterns of movement that are essential for understanding how materials flow in this regime [33].

Research has shown that the shape of particles significantly affects flow dynamics in this regime. Various factors, such as gravity, the particles' material characteristics (like Young's modulus), and their size play crucial roles in determining flow behavior [34]. One key finding is how kinetic sieving and squeeze expulsion drive segregation, especially in conditions like shallow avalanches seen in silos and drums, allowing particles to separate based on size [35]. These processes, along with gravity and velocity shear, help larger and rougher particles move to the front of a dense flow.

In this regime, the study of non-spherical particles reveals their unique impact on flow due to their ability to rotate, offering insights into sorting technologies [36]. Similarly, particle size, shape, and density differences can cause layers to form within the flow, which is crucial for sorting efficiency [35]. Another phenomena in regimes is particles Jamming, particularly in tight spaces like hoppers, which presents challenges in sorting. Understanding granular kinematics can help overcome [37] such challenges. Additionally, the effects of external forces, such as vibration and rotation, on sorting efficiency highlight the importance of considering particles' kinematic behaviors in sorting technology development [38, 39].

Grasping the kinematics in the dense quasi-static regime is key to enhancing sorting technologies. By delving into particle interactions and their conditions, we unlock insights into their properties, paving the way for more sophisticated and flexible sorting methods.

2.3.2 Gaseous Regime

In the gaseous regime, particles move quickly and are spread out, often colliding, which contributes to a dynamic and complex environment. These collisions result in unpredictable particle trajectories, complicating the sorting process that typically relies on physical attributes like size and mass [40, 41]. Furthermore, unique conditions such as microgravity enhance clustering effects from inelastic collisions. Factors including the particles' density, their material's ability to rebound (restitution properties), and their size significantly impact the way particles come together or separate, affecting segregation outcomes [42].

The key to enhancing sorting processes in the gaseous regime lies in understanding the kinematic properties of particles, specifically, their velocities, directional changes, and trajectories. This understanding is crucial because of the unpredictable nature of particle movement, necessitating advanced analytical tools and methods for precise sorting outcomes. By closely analyzing movement and collision patterns, we can develop more effective segregation techniques, allowing for the efficient sorting of various particle types [11]. Recent advances have made significant strides in this direction, particularly with the development of methods for 3D tracking of particles, such as rod-like shapes. These techniques, which leverage video analysis and computational algorithms, offer deeper insights into particle dynamics, facilitating the creation of more sophisticated sorting strategies suited to the complexities of the gaseous regime [43].

2.3.3 Intermediate Liquid Regime

In the intermediate liquid regime, the behavior of particles is significantly influenced by the balance between kinetic energy and its dissipation. This balance is crucial for determining how particles move, cluster, and are ultimately sorted. Velocity fluctuations and shear-induced

rearrangements play pivotal roles in defining the efficiency of sorting processes. The ability to understand and monitor these dynamic changes is essential for developing sorting methods that are precise and flexible [44]. Furthermore, the intricacies of the intermediate liquid regime call for a sophisticated understanding of granular flow behavior. Research indicates that the quasi-fluid state of granular materials in this regime impacts sorting efficiency, with factors such as fluid viscosity and particle-fluid interactions becoming key considerations. Advanced computational models, particularly those combining the Discrete Element Method (DEM) with Computational Fluid Dynamics (CFD), have offered significant insights into these interactions, as highlighted by Zhou et al. [45]. These models are instrumental in predicting granular material behavior under conditions akin to the intermediate liquid regime, aiding in the development of sorting systems that are well-suited to the dynamic nature of these flows.

This regime poses distinct challenges in sorting granular materials, blending the features of both dense and gaseous flow dynamics. It marks a crucial phase for the application of sorting technologies, bridging the gap between the slow, dense movements of particles and the rapid, collision-based dynamics of more dispersed states. Mastering sorting in this intricate environment demands a thorough grasp of kinematic properties, such as velocity, acceleration, and the trajectories of particles. This knowledge is vital for crafting sorting strategies that can effectively contend with the fluid-like conditions and unique challenges presented by the intermediate liquid regime.

2.4 Application of Machine Learning

The integration of Artificial Intelligence (AI) into a wide range of academic fields represents a significant leap forward in research methods. AI's impact has been especially notable in areas such as image processing and time series data analysis, contributing greatly to disciplines like computer science and medical science. This section focuses on the application of Machine Learning (ML) not only in physics but also across various other domains, underscoring the

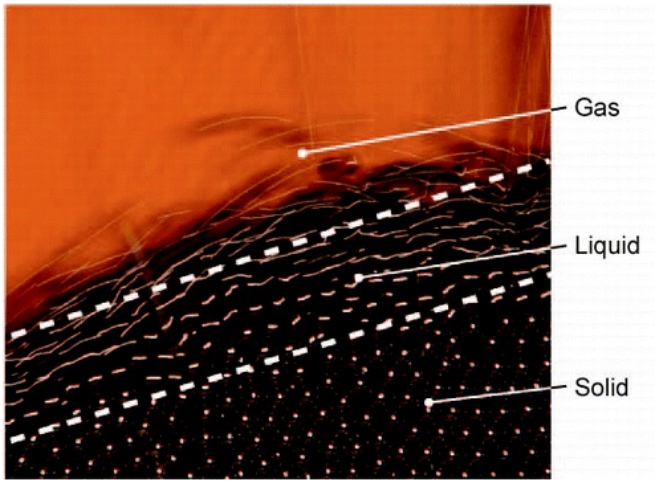

FIGURE 2.3: **Granular flow regimes**: The transition from solid to liquid, and finally to gas-like states illustrates the behaviors of particles[46].

versatility and transformative potential of ML technologies in enhancing research and analysis across diverse fields.

Building on the broad integration of AI and ML across disciplines, their applications extend deeply into fields such as physics, chemistry, engineering, and mathematics, significantly enhancing our analytical capabilities. Techniques from AI and ML have been leveraged for feature selection, enabling the identification of microstructural properties within granular materials, marking a step forward in materials science [47]. In the realm of fluid mechanics, ML assists in modeling and optimizing fluid flow, holding the promise to transform research with its advanced processing power [48]. The development of methods to analyze flow defects in various geometries showcases the versatility of ML, applying algorithms like the Support Vector Machine to categorize particles based on hardness or softness for more precise analysis [49].

The breadth of AI's application is further illustrated by examples in literature, ranging from granular physics to fluid dynamics [50, 51]. Noteworthy is the work by CX Ren et al. (2019), which utilizes a distributed gradient boosting algorithm, specifically the Extreme Gradient Boosting (XGBoost) model, to estimate the frictional state within sheared granular media. This research exemplifies how combining DEM simulations with ML can uncover predictive insights from the velocity signals of individual particles, offering a novel approach

to understanding granular media dynamics. Similarly, in chemical science, ML algorithms have been pivotal in modeling soft materials, pushing the envelope in molecular property prediction and chemical discovery [52]. Moreover, advancements in machine learning and data science have revolutionized flow cytometry techniques, enhancing the accuracy of cell marking, viability assessment, and the sorting of rare objects in blood flow [53].

The advancements in ML have significantly opened new avenues in scientific research, equipping experts with cutting-edge tools that bolster precision and enrich our grasp of intricate systems. By harnessing the predictive power of ML, researchers can now dissect and understand the complexities inherent in various fields, including the granular domain. This application of ML facilitates a deeper understanding of granular flow dynamics, enhances fluid mechanics, and broadens the scope for innovations across numerous scientific areas. ML enables us to efficiently tackle and make sense of these complex systems like never before. The following section delves into the application of ML in sorting granular particles, showcasing its potential to revolutionize this field.

2.5 Machine Learning in Sorting Granular Particles

The integration of ML and AI into the sorting of granular particles has marked a significant evolution across various sectors, making processes more efficient and precise. ML algorithms are particularly adept at identifying complex patterns within large datasets, a capability that proves invaluable when dealing with granular materials of varying properties. This is evident in several pioneering applications. For example, a novel system designed for sorting transparent polycarbonate granules utilizes machine vision and pneumatic separation, leveraging the k-Nearest Neighbors algorithm to effectively detect defects [54]. This innovation overcomes the challenge of handling transparent materials, highlighting ML's role in improving separation accuracy.

Similarly, the technique has been extended to enhance sensor-based sorting of cohesive materials, employing area-scan cameras and multi-object tracking for accurate object path prediction and material characterization, thus significantly reducing sorting errors [55]. The

versatility of ML in sorting applications is further demonstrated through the development of an automated grain sorting system that uses Convolutional Neural Networks (CNN) and a Jetson Nano camera to efficiently identify and remove defects, showcasing ML's effectiveness in reducing human error and optimizing operations [56]. Moreover, ML models are instrumental in advancing recycling processes, addressing global waste challenges by improving the separation and classification of recyclable materials [57]. The technology also finds applications in agriculture, where it integrates with machine vision to analyze crop images, enhancing productivity amidst shrinking agricultural land [58]. The mining industry benefits from AI's precision in extracting valuable minerals, thereby boosting efficiency and minimizing environmental impacts [59]. In the pharmaceutical sector, ML is revolutionizing areas such as drug formulation and discovery, cancer diagnosis, and protein structure prediction, streamlining the development of therapeutic formulations through advanced techniques like generative models and reinforcement learning [60].

Deep learning, a subset of ML, has significantly advanced sorting applications through the use of CNNs, which excel in image-based sorting systems. These models can precisely identify and classify particles by their visual attributes, enhancing sorting accuracy and leading to more sophisticated methodologies across various industries [61, 62, 63, 64]. This shift towards data-driven decision-making in material handling signifies not just a technological upgrade but a fundamental change in approach, underscoring the importance of analyzing granular flow kinematics to enhance sorting accuracy and efficiency.

The integration of Machine Learning (ML) and Artificial Intelligence (AI) into sorting processes marks a significant transition towards data-driven decision-making in material handling. This innovative shift is not merely a technological enhancement but represents a fundamental change in approach, emphasizing the analysis of granular flow kinematics to improve sorting accuracy and efficiency. By utilizing ML algorithms to analyze and predict particle properties based on their dynamic behavior during sorting, this methodology stands to revolutionize sorting practices across various industries. The potential of ML to transform traditional sorting techniques into more efficient, precise, and environmentally sustainable

operations underscores the importance of marrying theoretical knowledge with practical applications, thereby advancing the field of sorting technologies.

2.6 Summary

Sorting and segregation of granular particles play essential roles in numerous industries, including agriculture, pharmaceuticals, mining, and recycling. These processes are pivotal to ensuring quality control, improving efficiency, and minimizing environmental impacts by accurately separating materials based on distinct characteristics. Despite the development of various technologies and methods for sorting and segregation, our review highlights a notable gap: the under utilization of kinematic properties of particles, such as velocity, trajectory, and acceleration, in sorting processes.

Kinematic properties are fundamental to understanding the behavior of granular materials, yet traditional sorting techniques primarily focus on static attributes like size, shape, color, and density. This approach may overlook the dynamic nature of particle motion, which can offer critical insights into their properties, especially in complex flow conditions. To bridge this gap, we advocate for a methodology that prioritizes the sensing of kinematic properties in granular sorting. By harnessing the power of advanced Machine Learning (ML) and Artificial Intelligence (AI) algorithms, we can gain a deeper insight into particle behavior. This knowledge can lead to the creation of cutting-edge sorting technologies that identify and classify particles based on their motion dynamics, significantly enhancing sorting precision and effectiveness.

CHAPTER 3

Methodology

This chapter elaborates on the methodological framework utilized in this research, specifically designed to enhance the sorting of granular particles. Our approach includes using Discrete Element Method (DEM) simulations to collect data, preprocessing this data, and applying Machine Learning (ML) models. This method helps us achieve our main goal: understanding particle properties from their movements in different granular flow conditions.

3.1 Data Collection via DEM Simulations

Our methodology begins with using the Discrete Element Method (DEM) to simulate granular particle behaviors. DEM is known for its accuracy in modeling particle interactions and movements, making it essential for capturing the complex dynamics of granular materials. For our research, we utilized the LIGGGHTS software [65], an open-source tool that extends the capabilities of LAMMPS (Large-scale Atomic/Molecular Massively Parallel Simulator) specifically for granular materials. This allows for detailed visualization and comprehensive analysis of granular flow.

The LIGGGHTS software provides a robust framework for simulating the behavior of particles in various scenarios, which is critical for understanding and predicting the behavior of granular materials in industrial processes. By leveraging the power of DEM within LIGGGHTS, we can accurately model the trajectories, interactions, and forces between particles. This capability is particularly important in applications such as mineral processing, agriculture, and pharmaceuticals, where the flow and interaction of granular materials play a crucial role.

In this analysis, the trajectory of each particle is determined by solving Newton's second law of motion. The force interactions, particularly contact forces between particles, are modeled using the Hertz-Mindlin no-slip contact model, which accurately calculates both normal and tangential contact forces. The basic equations governing the DEM are as follows [65]:

$$\mathbf{F}_c^{ij} = \mathbf{F}_n^{ij} + \mathbf{F}_t^{ij} \tag{3.1}$$

where $\mathbf{F}_c^{ij}$ is the total contact force between particles i and j, consisting of a normal component $\mathbf{F}_n^{ij}$ and a tangential component $\mathbf{F}_t^{ij}$. The normal force is given by the Hertzian contact theory as:

$$\mathbf{F}_n^{ij} = \frac{4}{3} E^* \sqrt{R^* \delta^{ij}} \mathbf{n}^{ij} \tag{3.2}$$

where E^* is the effective Young's modulus, R^* is the effective radius, δ^{ij} is the overlap between particles, and $\mathbf{n}^{ij}$ is the unit normal vector at the contact point. The tangential force, based on the Mindlin model, is:

$$\mathbf{F}_t^{ij} = -k_t \mathbf{u}_t^{ij} - \eta_t \mathbf{v}_t^{ij} \tag{3.3}$$

where k_t is the tangential stiffness, $\mathbf{u}_t^{ij}$ is the tangential displacement, η_t is the tangential damping coefficient, and $\mathbf{v}_t^{ij}$ is the relative tangential velocity.

These simulations provide granular flow data with high fidelity, capturing aspects like particle trajectory, rotation, and interaction forces, which are indispensable for a nuanced understanding of granular behavior. The high-fidelity data generated through these simulations enable us to develop more accurate models for predicting and optimizing industrial processes involving granular materials.

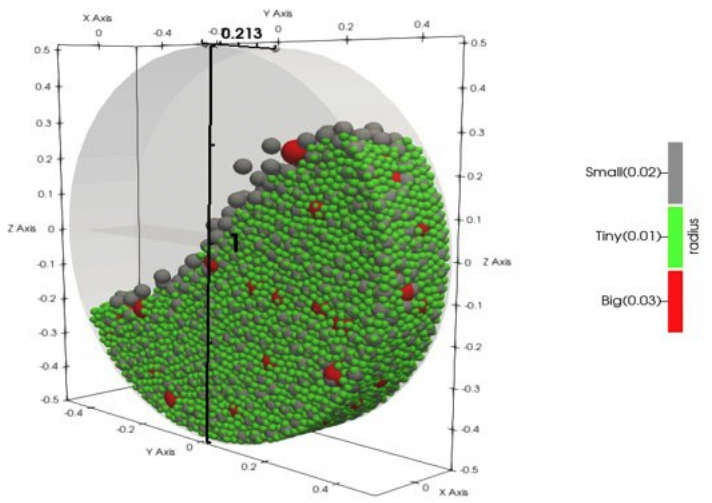

FIGURE 3.1: A visualization of particle simulation in the milling process using the Discrete Element Method (DEM).

Additionally, we used iterative time steps small enough to approach the actual solution accurately during simulation process. For this, we employed the `fix/check/timestep/gran` function, which checks whether our time steps are sufficiently small in both positive and negative ranges. It utilizes Rayleigh time and Hertzian time for the simulation, helping

ensure that our simulations do not have convergence issues. The system size is chosen based on preliminary tests to balance computational cost and accuracy. Simulations are run on high-performance computing clusters, with typical computation times ranging from several hours to days, depending on the system's complexity, particle size, and the number of particles involved. For chapter 4, DEM simulations were conducted using a simple personal computer with an 8-core, 7th Gen Intel(R) Core(TM) i5-12700F at 2.10 GHz. For chapters 5 and 6, simulations were performed on a more powerful system with a 20-core (with 32GB RAM), 12th Gen Intel(R) Core(TM) i7-12700F at 2.10 GHz, providing enhanced computational capabilities.

We focused on granular media commonly found in industrial processes, such as ores, coffee beans, and grains. The grain sizes range from 0.5 mm to 5 mm in diameter, typically with spherical shapes. Their densities range from 2500 to 5000 kg/m³, and the elastic stiffness (Young's modulus) is approximately 5×10^6 N/m². The coefficient of restitution varies between 0.5 and 0.8, and the surface roughness is characterized by a coefficient of friction ranging from 0.3 to 0.6. More information related to DEM simulation scripts is provided in the appendix section of this thesis. These properties are critical for accurately simulating the behavior of granular materials, as they directly influence the interactions and movements of the particles. For example, the coefficient of restitution affects how particles bounce off each other and surfaces, while surface roughness impacts friction and adhesion. By incorporating these detailed material properties into our DEM simulations, we can achieve a more realistic and comprehensive understanding of granular flow dynamics.

Furthermore, the choice of DEM parameters and the accuracy of the simulations are crucial for various applications. In mineral processing, accurate simulations can help optimize the design of equipment such as crushers and separators. In agriculture, understanding the flow of grains can improve the efficiency of storage and handling systems. In pharmaceuticals, precise modeling of powder flow can enhance the manufacturing of tablets and other solid dosage forms.

Overall, our use of DEM simulations provides a powerful tool for investigating the complex behaviors of granular materials. This enables us to gather detailed data that can inform and

improve sorting techniques in various industrial applications, ultimately leading to more efficient and effective processes.

3.2 Data Preprocessing

Another important step of this research is data preprocessing. The initial step in data preprocessing involves refining the raw data obtained from DEM simulations. This stage is crucial for enhancing the quality of the dataset by removing noise and irrelevant information. In this step, we used Python 3.11.6. with libraries Pandas, Sikit-learn, Numpy to refine raw data and extract features. We focused on extracting essential features that are significant for our analysis, such as the forces in the x, y, and z directions, acceleration, velocities and more.

The mathematical representation of the force vector is given by: $\vec{F} = F_x\hat{i} + F_y\hat{j} + F_z\hat{k}$ where, F_x, F_y, and F_z are the components of the force in the respective directions, and $\hat{i}$, $\hat{j}$, and $\hat{k}$ are the unit vectors along the x, y, and z axes.

Following the extraction of directional forces, we proceed to calculate the magnitude of the force $|\vec{F}| = \sqrt{F_x^2 + F_y^2 + F_z^2}$. Similarly, the magnitude of acceleration is calculated using the magnitude of force.

To prepare a concise dataset for machine learning training, data normalization and standardization techniques are applied depending on the model training iterative approach and model accuracy. These techniques adjust the scale of the data and transform it into a format that is more suitable for machine learning algorithms. Normalization is typically done using the min-max scaling, which can be expressed as:

$$x' = \frac{x - \min(x)}{\max(x) - \min(x)} \tag{3.4}$$

where x is an original value, x' is the normalized value, and $\min(x)$ and $\max(x)$ are the minimum and maximum values in the data, respectively.

Standardization, on the other hand, is carried out using the z-score method, given by:

$$z = \frac{(x - \mu)}{\sigma} \tag{3.5}$$

where μ is the mean of the data, and σ is the standard deviation of the data.

Another step in data preprocessing is to reducing dimension of the data. Since there exists many methods, we used one of the common approach which is Principal Component Analysis[66]. The process of PCA involves several critical steps. It begins with the standardization of data to ensure each feature contributes equally to the analysis. This is followed by computing the covariance matrix, which helps understand how variables in the data are correlated. PCA then involves finding the eigenvalues and eigenvectors of this matrix. The eigenvectors determine the directions of the new feature space, while the eigenvalues determine their magnitude. The principal components are selected based on these eigenvalues, with those corresponding to the highest eigenvalues chosen as they represent the directions of maximum variance in the data. Finally, the original data is transformed into this new feature space, which leads to a reduced number of features. This reduction simplifies the complexity of the data, making it easier to analyze and visualize, while ensuring that most of the significant information is retained. It enhances the efficiency of machine learning models by reducing computational costs and helps in mitigating the risk of overfitting by eliminating redundant features. Applying these preprocessing steps is essential for ensuring that the machine learning algorithms function optimally and yield meaningful insights from the dataset and avoiding model over fitting and bias problem.

3.3 ML Model Development & Prediction

The third pivotal step in our methodology is the implementation of Machine Learning (ML) models. ML, a subset of artificial intelligence (AI), enables predictive analytics by allowing computers to learn from data. This learning can be supervised, where models predict outcomes based on labeled data, or unsupervised, where models discern data patterns without predefined labels. Reinforcement learning, another category, optimizes decision-making through rewards-based learning from environmental interactions. These methodologies are

particularly promising for managing the dynamic nature of granular flows and enhancing the efficiency of sorting processes.

For our study, we primarily engaged with supervised learning algorithms, such as Support Vector Machines (SVM), Random Forests, and Neural Networks. These models were trained on data characterized by features representative of granular particle kinematics. An example of our ML development process is illustrated in Figure 3.2.

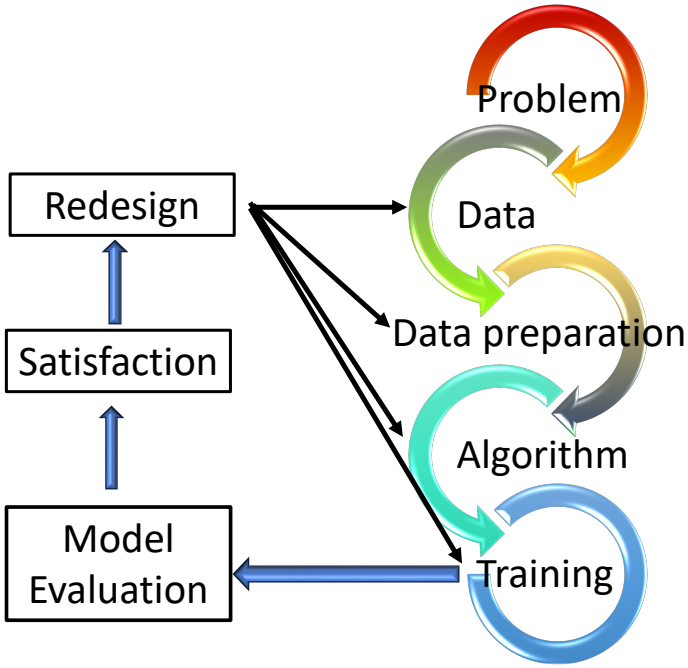

FIGURE 3.2: Overview of the machine learning development cycle. The iterative stages of building a machine learning model from problem definition to model evaluation and redesign.

3.3.1 Artificial Neural Network (ANN)

The initial foray into ML implementation was through an Artificial Neural Network (ANN). This network is composed of an input layer that receives the data, multiple hidden layers that process the data, and an output layer that delivers the prediction. The ANN architecture deployed in our initial work is depicted in figure 3.3.

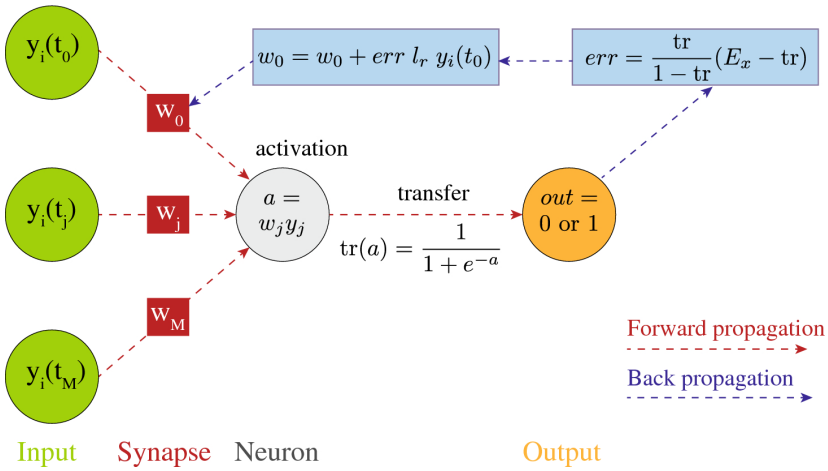

FIGURE 3.3: **Artificial Neural Network (ANN):** An overview of the ANN model depicting the flow from input to output through layers of interconnected neurons.

The ANN processes data in a sequential manner, starting with the input layer. The data then undergoes a forward pass where each neuron applies an activation function, such as the Rectified Linear Unit (ReLU), to the weighted sum of its inputs. ReLU is given by $f(x) = \max(0, x)$. The backward pass involves updating the weights to minimize the loss function, often a mean squared error (MSE), using gradient descent. The update rule for a weight w_{ij} is given by $w_{ij} \leftarrow w_{ij} - \eta \frac{\partial \mathcal{L}}{\partial w_{ij}}$, where η is the learning rate and $\mathcal{L}$ is the loss function. Activation functions like the Sigmoid function, $\text{Sigmoid}(x) = \frac{1}{1+e^{-x}}$, introduce non-linearity and are crucial in the network's ability to model complex relationships.

3.3.2 Random Forest Algorithm

Complementing our use of ANNs, the Random Forest algorithm offers a robust alternative. It creates an ensemble of decision trees from bootstrapped subsets of the dataset and makes predictions by aggregating the outcomes of these trees. The combined approach of these trees enhances the model's accuracy and reduces overfitting. A representative decision tree from the Random Forest ensemble is shown in figure 3.4.

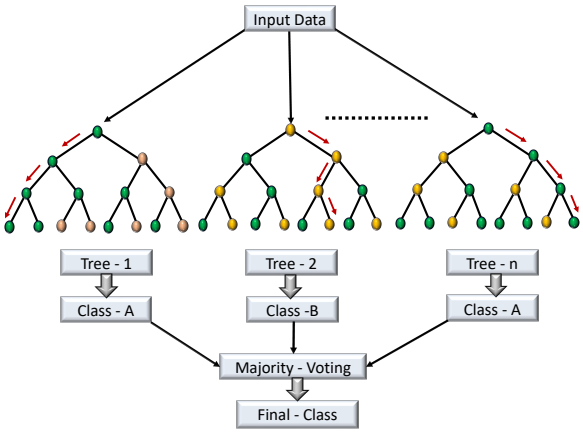

FIGURE 3.4: **Random Forest Architecture**. This diagram represents the ensemble learning process of a Random Forest, illustrating how multiple decision trees (Tree-1 to Tree-n) contribute to a consensus prediction through majority voting.

The Random Forest model's strength lies in its collective decision-making process. Each tree votes, and the most common outcome (in classification tasks) or the mean prediction (in regression tasks) is taken as the final result. This ensemble method effectively captures the diverse aspects of granular kinematics data, providing a reliable prediction mechanism.

3.3.3 Model Prediction, Testing, and Addressing Overfitting

We carefully tested our models using a specific dataset that constituted 20% of our total data, unseen by the model during training, to evaluate their predictive performance. This step was crucial to ensure our models accurately capture the dynamics of granular flow behavior.

To strengthen our machine learning models and prevent overfitting, we employed techniques such as cross-validation and regularization. Cross-validation involves partitioning the data into subsets, training the model on some subsets while validating it on others, which helps in verifying the model's robustness and generalizability.

For our analysis, we utilized different machine learning algorithms tailored to specific studies:

(1) In chapter 4, we used simple Artificial Neural Networks (ANN) with backpropagation. The hyperparameters were tuned by controlling the number of hidden layers and nodes, using a learning rate of 0.001 and the sigmoid activation function. The number of hidden layers and nodes determines the capacity of the network to learn complex patterns. The learning rate controls the step size at each iteration while moving towards a minimum of the loss function, and the sigmoid activation function helps in mapping the output between 0 and 1. We experimented with different epoch values, ranging from 200 to 300, to identify the optimal setup for each case. The number of epochs determines how many times the learning algorithm will work through the entire training dataset, which helps in finding the best fit.

(2) In chapter 5 and 6, we employed Random Forest algorithms. We tuned hyperparameters such as the number of estimators (`n_estimators`) set between 200 and 300, and the maximum depth of trees (`max_depth`) set between 7 and 9, depending on the accuracy and specifics of each case. The number of estimators defines the number of trees in the forest, which helps in improving the model's robustness and accuracy. The maximum depth of trees limits how deep the tree can grow during training, which helps in controlling overfitting. Additionally, we used grid search to find the best parameters; however, this approach proved to be computationally expensive. Grid search involves systematically working through multiple combinations of parameter values, cross-validating as it goes to determine which combination provides the best performance.

By adopting this comprehensive approach to machine learning, we aim to accurately predict granular flow kinematics, which is essential for effective particle sorting.

3.4 Summary

This chapter outlines our methodical approach, beginning with DEM simulations for generating data akin to complex scenarios encountered in industries like mining, where collecting real-world data poses significant challenges. By simulating these environments, we could

gather detailed data necessary for our study. We then applied machine learning techniques to this data, uncovering hidden patterns in granular flow and the kinematic properties of granular materials. Our approach not only demonstrates improved efficiency in sorting tasks but also makes the process quicker, easier, and less labor-intensive. We are confident that these methods will pave the way for the development of more sophisticated sorting techniques and contribute to the advancement of rheological models.

CHAPTER 4

Classifying Grains Using Behaviour-Informed Machine Learning

Sorting granular materials is crucial in various industries, including mineral processing, agriculture, and waste recycling. Traditionally, sorting methods have focused on identifying differences in grain properties such as size, color, density, and chemical composition. However, some essential grain properties cannot be directly observed in-situ, leading to challenges in achieving effective sorting. Our research seeks to explore whether it is possible to discern differences in the trajectories of granular particles based on their intrinsic behavior, and whether these insights can help overcome the limitations of current sorting techniques. To establish a proof of concept, we first compared this approach to the one proposed by Maier et al. (2018) [67]. In literature, different particles using conveyor belt and scanning cameras were utilized to capture high resolution images. Such approaches are time consuming, expensive and requires human maneuver.

To address these questions, we introduce a novel approach using a simple neural network. This network analyzes the observable kinematics of grains how they move and interact to identify contrasts in a broad spectrum of grain properties. This includes not just size, density, and color, but also crucial factors like stiffness, friction, energy dissipation, and adhesion. Our method, based on behavior-based classification, significantly broadens the range of granular materials that can be accurately sorted. Moreover, the potential applications of this research go beyond granular materials; the same techniques could improve the sorting of other particulate substances, such as cells and droplets in microfluidic devices, by exploiting patterns in their behavior. Which highlights the potentiality of kinematics based classification by establishing relationship between particles properties and their kinematics without relying in any images or any expensive equipment.

The following paper is comprised of a main material. In the paper, published in *Scientific Reports* was supervised by professor Pierre Rognon and Dr. Benjy Mark. Citation: {Laudari, S., Marks, B. & Rognon, P. Classifying grains using behaviour-informed machine learning. Sci Rep 12, 13915 (2022)}

Classifying grains using behaviour-informed machine learning

Sudip Laudari, Benjy Marks, and Pierre Rognon
Particles and Grains Laboratory, School of Civil Engineering,
The University of Sydney, Sydney, NSW 2006, Australia
(Dated: February 1, 2024)

Sorting granular materials such as ores, coffee beans, cereals, gravels and pills is essential for applications in mineral processing, agriculture and waste recycling. Existing sorting methods are based on the detection of contrast in grain properties including size, colour, density and chemical composition. However, many grain properties cannot be directly detected in-situ, which significantly impairs sorting efficacy. We show here that a simple neural network can infer contrast in a wide range of grain properties by detecting patterns in their observable kinematics. These properties include grain size, density, stiffness, friction, dissipation and adhesion. This method of classification based on behaviour can significantly widen the range of granular materials that can be sorted. It can similarly be applied to enhance the sorting of other particulate materials including cells and droplets in microfluidic devices.

I. INTRODUCTION

"To separate the wheat from the chaff" is a significant issue for many industries dealing with granular materials. The aim can be to extract high-grade ores from gangue, to remove defective pills, fruits and nuts, or to separate different waste materials for recycling [1–3]. In mining applications, several mechanical separation methods exist including flotation and rotating tumbler. For some materials, however, these methods are ineffective and sensor-based techniques must be employed. They involve presenting individual grains to a sensor for classification. The challenge is then to classify a vast quantity of moving grains into separate categories.

This classification can be based on measurements of the physical properties of the grains such as size, colour, shape, density and chemical composition by using, amongst others, optical or X-ray sensors [4]. However, poor contrast in these measured properties often means that classification is inaccurate or impossible. A similar classification challenge exists with other particulate materials, for instance when detecting rare pathogenic objects suspended in blood flows, or when sorting droplets and cells in microfluidic devices [5, 6].

Often, the grains to be sorted differ by a range of mechanical properties including elastic modulii, contact friction and adhesion. However, these micro-mechanical properties are not practically measurable while grains are moving, and can therefore not be directly used as a basis for sorting. Nonetheless, they may have some observable influence on the motion of the grains. As a result, a contrast in the physical properties of the grains may be indirectly perceived by detecting a contrast in their trajectories. The experiments and analysis presented by Maier et al. have validated this hypothesis [7]. The tests involved wooden spheres and hemispheres, as well as wax balls and cotton balls falling down a moving conveyor belt. By using a multiple object tracking algorithm, the trajectory of each grain could be measured from area-scanned camera images. Subsequently, a random forest machine learning algorithm was found to enable an efficient grain classification based on some selected features of their trajectories, including the maximum and mean velocities at different locations.

The potential for machine learning to address questions related to granular materials has only recently started to be exploited. For instance, machine learning based on image analysis was proposed to relate third body (the interfacial layer of material between contacting particles) morphology to contact rheology [8], to relate the grain velocity field to the frictional state of a sheared layer undergoing stick-slip [9], to enable prediction of the discharge time of granular flows in hoppers [10], and to infer micromechanical parameters from X-ray imaging [11]. Machine learning methods that do not rely on images were found to enable prediction of seismicity of laboratory-scale earthquakes, specifically of their stick-slip stress time series [12], and to enable optimal bulk-feeder system selection based on grain micromechanical properties [13]. More generally, a Support Vector Machine method was shown to enable the prediction of particle rearrangement from the knowledge of their microstructure in a variety of flowing soft materials [14].

However, research on machine learning applied to sorting granular materials remains embryonic. In particular, the capabilities of a kinematic-based classification are unexplored beyond the first evidence presented in [7]. This work seeks to further demonstrate the potential of using the kinematic signature of moving grains to indirectly detect contrast in their physical properties.

II. RESULTS AND DISCUSSION

The Discrete Element Method (DEM) code LIGGGHTS [15] was used to simulate a database of approximately 5×10^4 grain trajectories in the canonical configuration represented in Figure 1a. Grains free-fall a distance $h \in [H - \Delta H, H + \Delta H]$, and bounce or roll onto an inclined surface. This configuration is chosen for its simplicity and for its potential to yield

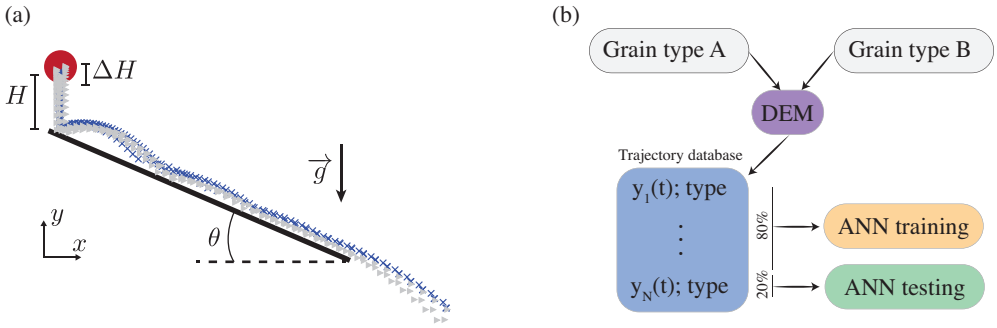

FIG. 1: Grain classification based on behaviour. (a) Schematic representation of the simulated system where grains are dropped one at the time on an inclined plane. Grains free fall from a height selected at random with the range $H \pm \Delta H$ and bounce or roll onto a planar surface inclined at $\theta = 40°$. Symbols represent two families of trajectories corresponding to grains of type A ($\times$) and type B ($\blacktriangleright$) with different properties. (b) Flow chart depicting the method of analysis where an artificial neural network is trained and tested using simulated trajectories.

different trajectories depending on the micro-mechanical properties of the grains.

In the following we seek to achieve a binary classification between grains of type A and B based on their simulated trajectory. Properties of type A grains are summarised on Table I and remain constant for all tests. Type B grains differ from type A by one of these properties, which will be specified below. The initial position h of the grains is randomly selected within the range $H \pm \Delta H$, which mimics the effect of a feeder discharging grains into the sensing zone at a random position. As a result, identical grains do not follow a unique trajectory. Rather, each grain type is associated to a family of trajectories. Figure 1a shows that the trajectory families of two grain types may significantly overlap. This means that classifying grains based on simple, explicit criteria such as maximum bounce height and average velocity is not necessarily straightforward or possible.

As an alternative, we have assessed the ability of a machine learning method to achieve this classification. Amongst other possibilities including Random Forests and Support Vector Machine, we chose a simple Artificial Neural Network (ANN); we observed that using a random forest classifier led to similar classification results. The training and testing of the neural network is based on datasets of 100 trajectories of grain type A and 100 trajectories of grain type B, as illustrated in Figure 1b. Positions are recorded at a frequency of 100 Hz for a period of two seconds from the release of the particle. As a way to stringently probe the ANN classification ability, the information sent to the network is restricted to the time series of one component of the grain position $y(t)$. The assumption is that sending additional information such as other position components, velocity and acceleration time series, would only enhance the classification. Using a k-fold cross validation, 80% of the trajectories are used for training and 20% for testing. The prediction accuracy of the trained network is measured by the proportion ϵ of the test trajectories for which the network prediction was correct. The value of ϵ can take lie between 0 (the network is always wrong) and 1 (the network is always right). A value of $\epsilon = 0.5$ is expected for predictions made randomly. It constitutes a benchmark: the network is deemed to have some predicting ability when the accuracy ϵ is greater than 0.5. Both the DEM and the ANN are well established numerical methods, and their specifics are detailed in Method Section IV.

Figure 2 depicts the classification accuracy obtained when grains of type B differ from grains of type A by one of the following properties: radius, coefficient of restitution, coefficient of friction, stiffness, adhesion or density; all other properties being the same. The initial heigh of fall is selected at random in the range 0.12 m $\pm$ 20%. The contrast between the two grain types is measured by the ratios R_B/R_A, e_B/e_A, μ_B/μ_A etc. A ratio of 1 means that the two grain types are in fact identical and therefore indistinguishable. A ratio greater than one means that the grain types are different and that there may be different trajectories.

In Figure 2a the accuracy of the network is shown for grain types featuring a contrast in size (radii R_A and R_B). The network accuracy steadily increases from approximately 0.5 in the limit of a size ratio equal to 1, up to nearly 1 when the size ratio is large enough. We propose the following empirical function to capture this trend:

TABLE I: Properties of type A grains: radius R, density ρ, elastic stiffness k, coefficient of restitution e, coefficient of friction μ and cohesion c. Type B grains feature a difference in one these parameters. Grains are not cohesive ($c = 0$) in all tests except for those presented in Figure 2e.

R [m]	ρ [kg/m^3]	k [N/m]	e	μ	c [J/m^3]
0.01	2500	5×10^6	0.5	0.4	0 or 10^4

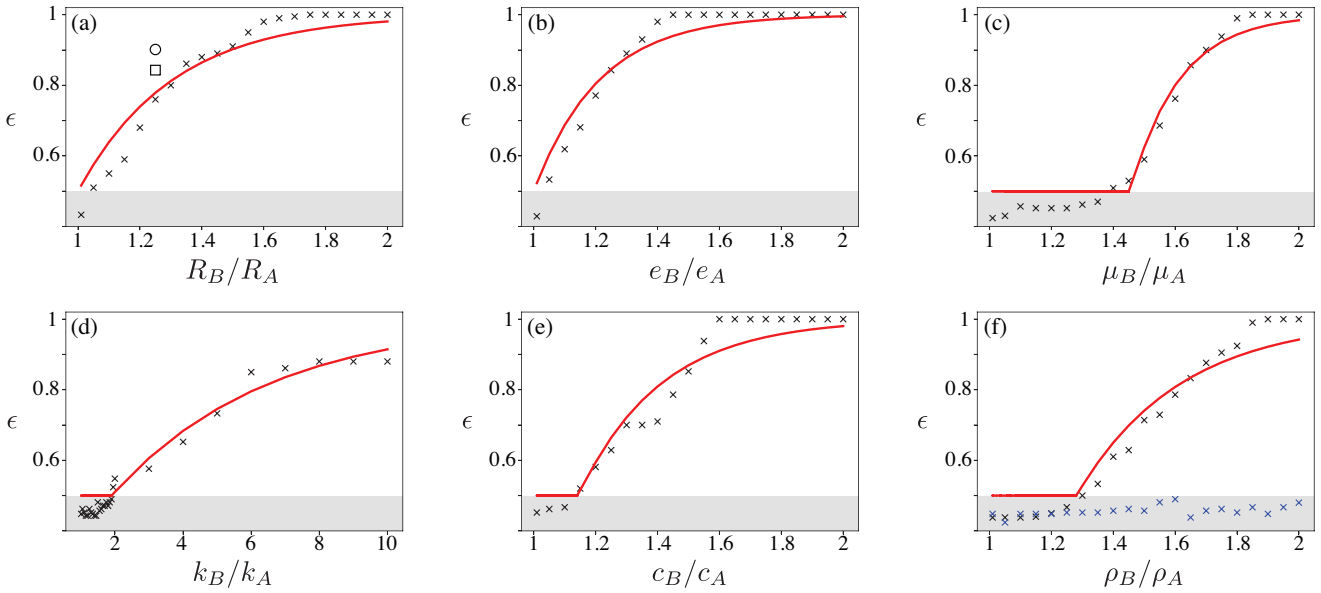

FIG. 2: Prediction accuracy ϵ for grain types with differing properties. (a) radius, (b) coefficient of restitution, (c) coefficient of friction, (d) stiffness (e) cohesion and (f) density without (blue) and with (black) a background drag force (fluid viscosity $\eta = 10^{-3}$ Pa s). Each symbol represents the ANN prediction obtained by training and testing against 200 trajectories of two grain types. Properties of grain type A are summarised in Table I.Grains of type B differ by one properties ($\times$), or two properties including coefficient of restitution $e_B = 1.25e_A$ ($\circ$) or coefficient of friction $\mu_B = 1.35\mu_A$ ($\square$).

Red lines correspond to best fits of the accuracy using Equation (1) or (2). Grey areas denote accuracy lower than that of a random classification ($\epsilon = 0.5$).

$$\epsilon(r) = 1 - \frac{1}{2}\exp\left(-\frac{r-1}{r_c}\right), \tag{1}$$

where r is the level of contrast between the two differing properties, in this case $r = R_B/R_A$. The fitting parameter $r_c > 1$ characterises the network classification accuracy for a given level of contrast r. This exponential function is chosen to match two limits. Firstly, $r = 1$ means that grain types are perfectly identical and are therefore indistinguishable: the network accuracy is then expected to be no better than that of a random classification: $\epsilon(r = 1) = 0.5$. Secondly, $r \to \infty$ means that the grain types are so different that the network should be able to correctly classify all grains: $\epsilon(r \to \infty) = 1$. The choice of an exponential function to interpolate these two limits is arbitrary and other functions could capture the data equally well. The data presented in Figure 2a are best fit by Equation (1) using a value of $r_c = 0.33$. Figure 2b evidences a similar behaviour when grains differ by their coefficient of restitution ($r = e_B/e_A$). The empirical function (1) appears to capture this increase in accuracy with a value of $r_c = 0.16$.

Figure 2c shows a qualitatively different behaviour when the contrasting property is the coefficient of friction. For relatively low ratios μ_B/μ_A, the accuracy remains at about 0.5, meaning that the network could not detect sufficient differences in the trajectories of the grains to enable classification. The accuracy starts increasing for larger ratios. We propose to capture this by introducing a threshold value r_t greater than 1 into Equation (1):

$$\epsilon(r) = \begin{cases} 1 - \frac{1}{2}\exp\left(-\frac{r-r_t}{r_c}\right), & \text{if } r \geq r_t \\ 0.5, & \text{otherwise.} \end{cases} \tag{2}$$

This expression reduces to Equation (1) for $r_t = 1$. The measured accuracy are best fit with $r_t = 1.45$ and $r_c = 0.52$. Figures 2 d and e display similar behaviour when the contrasting property is the grain stiffness or cohesion, which is best fit by Equation (2) with $r_t = 1.79$, $r_c = 4.93$ and $r_t = 1.09$, $r_c = 0.32$ respectively.

In contrast with all the other mechanical parameters, figure 2f shows that the accuracy never exceeds 0.5 when grain types have different densities, meaning that classification by density is not possible.

These results indicate that a classification based on grain trajectory is often possible using an ANN. They further show that the prediction accuracy depends on the nature as well as the intensity of the difference in micro-mechanical parameters of the grains. This can qualitatively be explained by the expected influence, or lack of influence, of these parameters on the trajectories. For instance, different grain sizes would impact the effective

free fall distance $H - R$ before the first impact. Different coefficients of restitution or different coefficients of friction would lead to different amounts of kinetic energy dissipation at impact. In contrast, grain density does not affect grain free fall in the absence of a background fluid, and does not affect the energy dissipated at impact. With no effect on the grain trajectory, classification is then impossible. To have density influence the grain trajectory, one can introduce a background fluid producing a drag force, such as a Stokes drag $\overrightarrow{F^{drag}} = -6\pi R\eta\overrightarrow{v}$, where η is the fluid viscosity and $\overrightarrow{v}$ the grain velocity. The terminal velocity of a free falling grain is then expected to be given by $\frac{mg}{6\pi R\eta}$, which depends on the density via the grain mass m. Figure 2f confirms that density then influences the trajectories in a way that is detectable by the ANN.

The classification accuracy is contingent on the existence of uncontrolled processes influencing the grain trajectory, which we refer to as sources of noise. In the tests presented above, noise was exclusively introduced by randomly selecting the grain initial position within $H \pm \Delta H$. In absence of a noise source, grains from the same type would exhibit identical trajectories. Distinguishing the trajectories of two grain types would then not necessarily require machine learning; it could simply be achieved by using an explicit criterion, for instance by comparing their maximum velocity. A noise source makes classification significantly more challenging, as each grain type is associated to a family of trajectories, as illustrated in Figure 1a. Whereas a classification based on a single criterion may not be generally possible, machine learning appears to be capable of sensing the effect of micro-mechanical parameters amongst that noise, provided that these effects are sufficiently salient. This qualitatively explains why, for a fixed level of noise ΔH, the classification accuracy increases with the contrast intensity, as observed in Figure 2. The classification accuracy for a fixed contrast is expected to decrease when the noise is increased. To test this hypothesis, we have repeated the tests presented in Figure 2a — involving a contrast in radius — for various level of noise ΔH. Figure 3a indicates that the exponential increase in Equation (1) of the accuracy is preserved at all noise levels; however, the parameter r_c increases approximately linearly with the level of noise ΔH, which reflects how noise hinders classification.

In practice, other factors may impact the classification when measuring the position of the grains using an optical camera and a particle tracking algorithm [7, 16]. They include a level of imprecision on the position and a limit to the frequency of image acquisition [17]. To assess the robustness of the classification to these factors, we have mimicked them in our simulated trajectories. Firstly, Figure 3b shows the classification accuracy obtained when adding random numbers in the range $\pm\delta$ to all positions, considering grain types of differing radii with $r = 2$. The classification gradually decreases with an increasing level of noise, but remains close to 1 for sub millimetric noise. Secondly, Figure 3b shows the effect of the trajectory sampling frequency f on the same trajectories using $\delta = 0$. The classification accuracy remains close to 1 when the sampling frequency is large enough ($f \gtrsim 25\,\mathrm{Hz}$, $f^{-1} \lesssim 40\,\mathrm{ms}$), and decreases at lower frequencies as less and less information are provided to the network. These two results suggest that classification is possible over a range of position sampling rate and precision that are well within the capabilities of standard imaging techniques.

Furthermore, grains may differ by more than one properties. One could expect that having some contrast in more than one property should facilitate classification. To test this hypothesis, we considered grains differing only by their size ($R_B = 1.125R_A$) as a benchmark and added a contrast in friction coefficient ($\mu_B = 1.135\mu_A$) or in coefficient of restitution ($e_B = 1.125e_A$). Results shown of figure 2 confirms that additional contrast leads to enhanced classification accuracy.

III. CONCLUSION

"Tell me who you are and I will predict how you behave" is the motto of traditional material modelling. In the context of individual particle sorting we found here that machine learning enables us to reverse this motto to "Tell me how you behave and I will deduce who you are". This behaviour-based classification can potentially improve a number of sorting processes by indirectly detecting contrast in micro-mechanical properties which would otherwise be difficult to measure. This method should be applicable to processes involving various particulate materials (e.g. grains, droplets, bubbles, cells) moving in various configurations such as down inclined planes, out of silos or through microfluidic devices. The behaviour-based classification, evidenced here for individual grains, could also be applied to classifying bulk materials comprised of many interacting grains, where the dynamics is related to grain micro-mechanical properties [18, 19]. Recent advanced in X-ray sensors for measuring the velocity within bulk flows would also enable such classification [17, 20, 21].

Remarkably, we found that classification is possible using the simplest network architecture, which involves a single neurone and does not perceive any order in time series. Further still, this network was only provided with minimal information on grain trajectories. It is likely that classification capabilities would be enhanced by using more advanced networks, for instance convolutional networks, and by including more information in their training such as grain velocity and acceleration time series. Furthermore, using machine learning methods with higher interpretability such as random forests could allow for insights on which features of the trajectory are perceived and useful for classification.

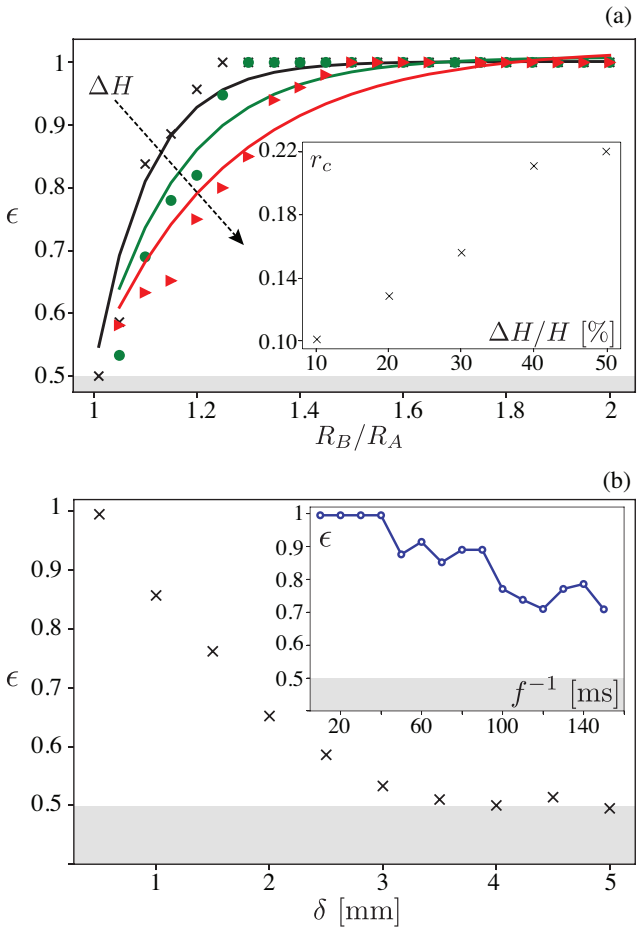

FIG. 3: Classification robustness to external noise. (a) Classification accuracy obtained for different levels of noise on the initial grain position $\Delta H/H = 10\%$ (×), 20% (•) and 50% (▶) using grain types of differing radius; lines are the best fits using Equation (1); (inset) corresponding values of the fitting parameter r_c. (b) Classification accuracy obtained when adding a noise of magnitude δ on all positions $y(t)$, or when decreasing the position sampling frequency f (inset); results correspond to grain types of differing radii, $R_B = 2R_A$ and $\Delta H/H = 20\%$. Grey areas correspond to accuracy lower than 0.5.

IV. METHOD

Discrete element method - DEM consists of a numerical integration of Newton's second law of motion for individual grain translation and rotation, by discretising them over small time steps dt. In our simulations, grains are spherical and are subject to gravity. They interact with the surface by an elasto-dissipative and frictional contact characterised by a normal stiffness k, a coefficient of restitution e and a coefficient of friction μ. In some instances, an adhesive force following the linear-elastic JKR model is introduced; this adhesive force is proportional the contact surface area A via a surface energy term c [22, 23]. The normal component of the grain-to-surface contact force is $f_n = k\delta_n - \zeta\dot{\delta}_n - cA$, where δ_n is the deflection of the contact and ζ is a viscous parameter yielding some energy dissipation during a normal contact. The tangential contact force involves an elastic component that is capped by a Coulomb friction: $f_t = \min(k\delta_t;\ \mu k\delta_n)$.

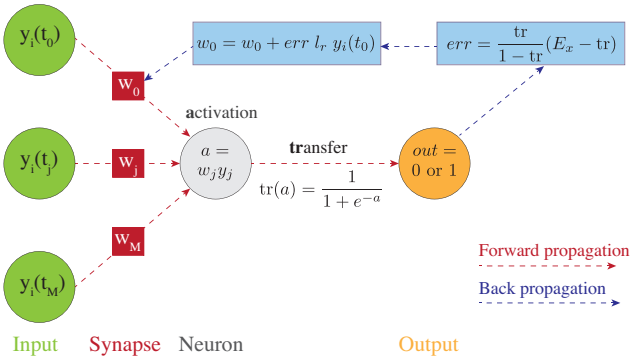

FIG. 4: Artificial Neural Network used to classify trajectories, using a feedforward and back propagation training method. The network is comprised of a single neurone and several synapses whose weight w evolves during the training to optimise the network prediction. The cycle shown corresponds to one training *epoch*.

Artificial Neural Network- We considered the simple network architecture presented in Figure 4. It is comprised of a single neurone, which is connected to the input features by synapses. The features are a series of grain positions $y_i(t_j)$. The index i refers to a particular grain within a trajectory set; t_j is a particular time at which the grain position was recorded, M is the total number of positions presented to the network for one grain trajectory, which is 200 in all the tests but those of figure 3b-inset, where the number of features was gradually reduced. The network translates this series of position into a grain type via the weight of each synapse w_i, an activation function $a = \sum_i a_i w_i$ and a transfer function $\mathrm{tr}(a) = 1/(1+e^{-a})$ known as the sigmoid function which rescales the activation function between 0 and 1. This result is converted into an output, which is a prediction for the grain type: $\mathrm{tr} \leqslant 0.5$ is interpreted as type A and $\mathrm{tr} > 0.5$ type B. The permutative nature of the activation function means that this network is insensitive to the order with which the positions $y(t)$ are presented.

Training the network consists of identifying a set of weights w_i which leads to some optimal network predictions across a number of trajectories. We use an algorithm known as feedforward-backpropagation to perform the training, which involves the following steps.

Initially, the weights w_i of the network are allocated a random value between 0 and 1. For each trajectory, a feedforward step is applied which consists of using

the network to make a prediction on the type of grain. This prediction is compared to the true grain type of the trajectory j under consideration, $E_j = 0$ or 1, via an error function $err = (E_j - \mathrm{tr}) * \mathrm{tr}/(1 - \mathrm{tr})$. The subsequent back-propagation step uses this error to update the weights according to a stochastic gradient descent method, via the function: $w_i^{new} = w_i^{old} + err\, l_r y_i$, where l_r is referred to as *learning rate*. This feedfowrad-backpropagation cycle is repeated on all trajectories of the training set. This corresponds to one training iteration, commonly referred to as one *epoch*. The two hyper parameters of the training are the number of epochs and the learning rate. We found that using 200 epochs and a learning rate ranging from 0.09 to 0.4 yielded optimum network accuracy while avoiding instances of overfitting. Overfitting is characterised by a training accuracy that steadily improves with the number of epochs while the testing accuracy worsens.

[1] V. Narendra and S. Hareesha, "Prospects of computer vision automated grading and sorting systems in agricultural and food products for quality evaluation," *International Journal of Computer Applications*, vol. 1, 02 2010.

[2] W. Kępys, "Opto-pneumatic separators in waste management," *Inzynieria Mineralna*, vol. 17, pp. 63–67, 01 2016.

[3] J. Lessard, J. de Bakker, and L. McHugh, "Development of ore sorting and its impact on mineral processing economics," *Minerals Engineering*, vol. 65, pp. 88–97, 10 2014.

[4] C. Robben and H. Wotruba, "Sensor-based ore sorting technology in mining—past, present and future," *Minerals*, vol. 9, no. 9, 2019.

[5] L. Mazutis, J. Gilbert, W. L. Ung, D. A. Weitz, A. D. Griffiths, and J. A. Heyman, "Single-cell analysis and sorting using droplet-based microfluidics," *Nature protocols*, vol. 8, no. 5, pp. 870–891, 2013.

[6] D. V. Voronin, A. A. Kozlova, R. A. Verkhovskii, A. V. Ermakov, M. A. Makarkin, O. A. Inozemtseva, and D. N. Bratashov, "Detection of rare objects by flow cytometry: Imaging, cell sorting, and deep learning approaches," *International Journal of Molecular Sciences*, vol. 21, no. 7, 2020.

[7] G. Maier, F. Pfaff, F. Becker, C. Pieper, R. Gruna, B. Noack, H. Kruggel-Emden, T. Längle, U. Hanebeck, S. Wirtz, V. Scherer, and J. Beyerer, "Motion-based material characterization in sensor-based sorting," *tm - Technisches Messen*, vol. 85, 01 2018.

[8] R. Jaza, G. Mollon, S. Descartes, A. Paquet, and Y. Berthier, "Lessons learned using machine learning to link third body particles morphology to interface rheology," *Tribology International*, vol. 153, p. 106630, 2021.

[9] C. X. Ren, O. Dorostkar, B. Rouet-Leduc, C. Hulbert, D. Strebel, R. A. Guyer, P. A. Johnson, and J. Carmeliet, "Machine learning reveals the state of intermittent frictional dynamics in a sheared granular fault," *Geophysical Research Letters*, vol. 46, no. 13, pp. 7395–7403, 2019.

[10] Z. Liao, Y. Yang, C. Sun, R. Wu, Z. Duan, Y. Wang, X. Li, and J. Xu, "Image-based prediction of granular flow behaviors in a wedge-shaped hopper by combing dem and deep learning methods," *Powder Technology*, vol. 383, pp. 159–166, 2021.

[11] H. Cheng, T. Shuku, K. Thoeni, P. Tempone, S. Luding, and V. Magnanimo, "An iterative bayesian filtering framework for fast and automated calibration of dem models," *Computer methods in applied mechanics and engineering*, vol. 350, pp. 268–294, 2019.

[12] B. Rouet-Leduc, C. Hulbert, N. Lubbers, K. Barros, C. J. Humphreys, and P. A. Johnson, "Machine learning predicts laboratory earthquakes," *Geophysical Research Letters*, vol. 44, no. 18, pp. 9276–9282, 2017.

[13] J. Torres-Serra, A. Rodríguez-Ferran, and E. Romero, "Classification of granular materials via flowability-based clustering with application to bulk feeding," *Powder Technology*, vol. 378, pp. 288–302, 2021.

[14] E. Cubuk, S. Schoenholz, J. Rieser, B. Malone, J. Rottler, D. Durian, E. Kaxiras, and A. Liu, "Identifying structural flow defects in disordered solids using machine-learning methods," *Physical review letters*, vol. 114, 09 2014.

[15] C. Kloss, C. Goniva, A. Hager, S. Amberger, and S. Pirker, "Models, algorithms and validation for open-source dem and cfd–dem," *Progress in Computational Fluid Dynamics, an International Journal*, vol. 12, no. 2-3, pp. 140–152, 2012.

[16] T. Miller, P. Rognon, B. Metzger, and I. Einav, "Eddy viscosity in dense granular flows," *Physical review letters*, vol. 111, no. 5, p. 058002, 2013.

[17] Z. Maranic, F. Guillard, J. Baker, I. Einav, and B. Marks, "A granular thermometer," *Granular Matter*, vol. 23, no. 2, pp. 1–15, 2021.

[18] G. M. gdrmidi@ polytech. univ-mrs. fr http://www. lmgc. univ-montp2. fr/MIDI/, "On dense granular flows," *The European Physical Journal E*, vol. 14, pp. 341–365, 2004.

[19] M. Macaulay and P. Rognon, "Inertial force transmission in dense granular flows," *Physical Review Letters*, vol. 126, no. 11, p. 118002, 2021.

[20] J. Baker, F. Guillard, B. Marks, and I. Einav, "X-ray rheography uncovers planar granular flows despite non-planar walls," *Nature communications*, vol. 9, no. 1, pp. 1–9, 2018.

[21] E. Andò, B. Marks, and S. Roux, "Single-projection reconstruction technique for positioning monodisperse spheres in 3d with a divergent x-ray beam," apr 2021.

[22] K. L. Johnson, K. Kendall, and a. Roberts, "Surface energy and the contact of elastic solids," *Proceedings of the royal society of London. A. mathematical and physical sciences*, vol. 324, no. 1558, pp. 301–313, 1971.

[23] P. G. Rognon, J.-N. Roux, M. Naaim, and F. Chevoir, "Dense flows of cohesive granular materials," *Journal of Fluid Mechanics*, vol. 596, pp. 21–47, 2008.

CHAPTER 5

Insights on the Internal Dynamics of Bi-Disperse Granular Flows from Machine Learning

---

After establishing a method to showcase contrast in granular particle trajectories using single particles in our previous research, we now delve deeper into the complex world of granular flows. This research is motivated by the need to understand the intricate dynamics of granular materials in more complicated scenarios, such as bulk flow in silos, where grains exhibits a wide range of forces and velocities.

In this study, we focus on bi-disperse flows, where granular materials consist of both small and large grains. Traditional statistical methods have given us insights into how dynamics scale with grain size in uniform (monodisperse) flows. However, in a more realistic scenario where grain sizes vary, as in bi-disperse flows, understanding the interaction and behavior of different-sized grains becomes crucial.

Our approach employs machine learning classifiers to analyze characteristics like velocity, acceleration, and force, aiming to distinguish between small and large grains. Surprisingly, we find that classification based solely on velocity is ineffective, suggesting that both small and large grains exhibit similar velocities statistically. In the dense zones of the flow, even force-based classification encounters limitations, indicating that grains of different sizes experience similar forces. However, when we combine force and acceleration data, the classifier successfully differentiates between grain sizes. This success highlights the classifier's sensitivity to the correlation between force and acceleration - essentially, Newton's second law - allowing it to discern grain sizes based on their mass.

The importance of this research lies in its potential to enhance our understanding of granular flows, a common yet complex phenomenon in various industrial processes. By leveraging machine learning, we can unravel the nuanced behaviors of granular materials in bi-disperse flows, providing insights that are critical for improving processing, handling, and sorting in industries dealing with these materials. This study marks a significant step forward from our previous work, moving from analyzing individual particle trajectories to understanding the collective behavior in more complex granular systems.

The following paper is comprised of a main material. In the paper, published in *Granular Matters* was supervised by professor Pierre Rognon and Dr. Benjy Mark.

Citation: Laudari, S., Marks, B. & Rognon, P. Insights on the internal dynamics of bi-disperse granular flows from machine learning. Granular Matter 25, 73 (2023)

Granular Matter (2023) 25:73
https://doi.org/10.1007/s10035-023-01357-4

ORIGINAL REPORT

Insights on the internal dynamics of bi-disperse granular flows from machine learning

Sudip Laudari[1] · Benjy Marks[1] · Pierre Rognon[1]

Received: 16 February 2023 / Accepted: 11 July 2023 / Published online: 18 August 2023

Abstract
In granular flows, grains exhibit heterogeneous dynamics featuring large distributions of forces and velocities. Conventional statistical methods have previously revealed how these dynamical properties scale with the grain size in monodisperse flows. We explore here whether they differ between small and large grains in bi-disperse flows. In simulated silo flows comprised of dense and collisional zones, we use a machine learning classifier to attempt to distinguish small from large grains based on features such as velocity, acceleration and force. Results show that a classification based on grain velocity is not possible, which suggests that large and small grains feature statistically similar velocities. In the dense zones, classification based on force only fails too, indicating that small and large grains are subjected to similar forces. However, classification based on force and acceleration succeeds. This indicates that the classifier is sensitive to the correlation between forces and acceleration, i.e. Newton's second law, and can thus detect differences in grain size via their mass. These results highlight the potential for machine learning to assist with better understanding the behaviour of granular flows and similar disordered fluids.

Keywords Granular flows · machine-learning · kinematics · segregation

1 Introduction

The internal dynamics of granular flows is never steady and uniform. The velocity and contact forces of grains vary greatly in space and time, even when the granular packing is subjected to a steady and uniform shear [1–4]. Conventional statistics have previously enabled the characterisation of the the distribution of these quantities. In dense flows, they revealed a bi-modal distribution of contact forces with a mean scaling as Pd^2, where P is the pressure and d the grain size, and extreme forces exceeding this by an order of magnitude. They also revealed a normal distribution of grain velocities, with a standard deviation scaling as $\dot{\gamma}d$ in collisional flows [5–7] and $\dot{\gamma}d/\sqrt{I}$ in dense flows [8–12], where $\dot{\gamma}$ is the shear strain rate and I the inertial number. Understanding this dynamical heterogeneity is key to predicting the behaviour of granular flows as a continuum. For instance, several theories explain the $\mu(I)$ rheology [13–15] and non-local models in terms of force network and grain kinematic [16–19].

Granular flows comprised of different grain sizes exhibit a more complex internal dynamics, which may give rise to some segregation [20]. Typically, larger grains migrate preferentially in zones of lower shear rate. This is the case in silo flows where large grains tends to concentrate in the center of the silo [21, 22] and may therefore be first to discharge. In bi-disperse flows, size segregation is understood to be driven by the differences in velocity fluctuations and contact force between species [23, 24]; these differences become more pronounced for larger size ratios. Segregation is counteracted by the remixing arising from shear-induced diffusion [25]. As a result, segregation develops only for large enough size differences. However, in mixture with moderate grain size differences, whether and how the dynamics of small grains might differ from that of larger grains remains to be established. We propose here to explore the potential

Sudip Laudari, Benjy Marks and Pierre Rognon have contributed equally to this work.

✉ Pierre Rognon
pierre.rognon@sydney.edu.au

Sudip Laudari
sudip.laudari@sydney.edu.au

Benjy Marks
benjy.marks@sydney.edu.au

[1] Particles and Grains Laboratory, School of Civil Engineering, The University of Sydney, Sydney, NSW 2006, Australia

for machine learning methods to assist with addressing this question.

Machine learning (ML) methods are designed to make predictions based on a training set of data, while being oblivious of any causal relationship. They have recently been used to predict the behaviour of granular matter. Image-based ML has related grain morphology to the effect on interfacial friction in tribology [26], to relate the grain velocity field to the frictional state of a sheared layer undergoing stick–slip [27], to predict of the discharge time of granular flows in hoppers [28], and to infer micromechanical parameters from X-ray imaging [29, 30]. ML not based on images were found to enable prediction of seismicity of laboratory-scale earthquakes, specifically of their stick–slip stress time series [31], and to enable optimal bulk-feeder system selection based on grain micro-mechanical properties [32]. They were also found effective at classifying different types of grains based on their kinematics while falling on an inclined plane [33] and to the behaviour of a packing undergoing compression from grain kinematics and contact texture [34]. Most relevant to granular rheology, a Support Vector Machine method was shown to enable the prediction of particle rearrangement from the knowledge of their microstructure in a variety of flowing soft materials [35].

In this Paper, we explore how the predictive power of machine learning can be used to better understand the internal dynamics of granular flows. We conducted discrete element method simulations of bidisperse granular flows in a silo configuration. The strategy consists of training a Machine Learning classifier to distinguish large grains from small grains, based on information such as contact forces, grain velocities and acceleration. Instances where classification fails are taken to mean that the dynamical features are similar between small and large grains. On the contrary, a successful classification would mean that the dynamical features present some noticeable differences between grain species.

The paper is organised as follows: the specifics of the DEM and ML methods are presented in Sect. 2 and the ML classification results are discussed in Sect. 3.

2 Methods

The method is comprised of the two steps illustrated in Fig. 1: first simulating a granular flow comprised of two grain sizes in a silo and then the use of a random forest classifier to attempt to classify small and large grains based on selected dynamical properties.

2.1 Granular flows in silo

We use the discrete element method (LIGGGHTS [36]) to simulate the flow of a bidisperse mixture of grains in a silo. The mixture is comprised of 14, 000 grains of diameter $d = 20$ mm or 30 mm. The proportion of small and large grains is equal in number. The density of the grains is $\rho = 2500\,\mathrm{kg/m^3}$. They interact via visco-dissipative elastic contact characterised by a linear stiffness $k = 10^7\,\mathrm{N/m}$, a coefficient of friction of 0.3 and a coefficient of restitution of 0.3. Gravity is set at $9.81\,\mathrm{m/s^2}$ and there is no long range interaction or contact adhesion.

Grains are gradually fed during a period of 5 s by placing them randomly and without contact at the top of the

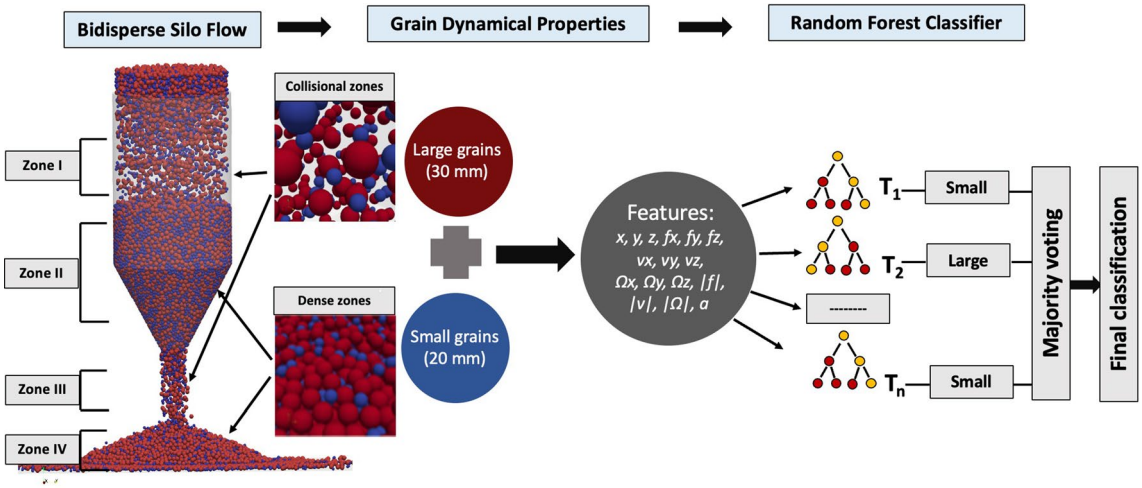

Fig. 1 Methodology: a bidisperse mixture is simulated in a silo configuration. Properties including grain velocity, acceleration and contact forces are then used to train a random forest classifier to distinguish large and small grains. Different combinations of properties are used to identify which present statistical differences between grain species. The random forest classifier is composed of 100 trees, each considering a subset of the features and producing a vote for classification. The final classification is the one receiving the most votes

silo (see Fig. 1). They then free fall (zone I), form a dense flow above the silo outlet (zone II), exit the silo (zone III) and form a heap on the ground (zone IV). These zones are depicted on Fig. 1.

In zones I and II, the flow is collisional with large inter-particle spacing and some binary collisions. In zones III and IV, the flow is dense or stopped with multiple, sustained contacts. The cylindrical part of the silo is 2 m tall and 1.52 m in diameter. The constriction is 0.97 m tall. The outlet is 0.43 m in diameter and is located 1.5 m above the ground. In the analysis below, the zones locations relative to the ground are: 4.1–3.6 m for I, 3–1.9 m for II, 1.2–0.8 m for III and 0.4–0 m for IV.

Individual grain properties including position $\{x, y, z\}$, translational velocity $\{v_x, v_y, v_z\}$, rotational velocity $\{\Omega_x, \Omega_y, \Omega_z\}$ and the net force they are subjected to $\{f_x, f_y, f_z\}$ (sum of contact forces and self weight) are recorded throughout the flow, for a period of 25 s. The present analysis focuses on classification using a discharge time of 25 s. We have checked that similar classification accuracy could be obtained considering period of time as short as 1 s.

2.2 Random forest classifier

We trained and tested a random forest classifier using one or more features including the time series of grain velocity, angular velocity, acceleration, and total force. The dataset was split into two parts: 80% of the grains were used to train the classifier, and the remaining 20% were used to test its predictive ability once trained. This process was repeated five times by taking random samplings of grains for training and testing. During the testing phase, a prediction was made for each grain in the testing sets, whereby the grain was classified as either small or large based on the time series of its selected features. The accuracy of the classifier was measured by evaluating the algorithm's ability to classify particles as small or big. The classification was performed using a binary class separation method, where particles were detected as either small or large. The classifier accuracy is measured by:

$$\epsilon = \frac{\text{number of correct predictions}}{\text{number of predictions}}$$

In a system comprised of an equal number of small and large grains, ϵ typically varies from 0.5 to 1. $\epsilon = 0.5$ corresponds to a random prediction, and indicates an inability for the random forest to distinguish large from small grains. $\epsilon = 1$ reflects a perfect prediction, where the random forest correctly classifies all small and large grains.

We chose to use a random forest method in preference to other classifiers, such as neural networks, due to its higher degree of interpretability. In particular, random forests are able to rank the features as a function of their importance in the prediction. This allows us to detect which features are the most important to achieve classification, and therefore which features distinguish small from large grains.

The raw data collected was subjected to preprocessing using the Visual Studio Code interface with Python version 3.10.6. This step was crucial in preparing the data for classification. For the construction, training and testing of the random forest classifier, we used the Sklearn library in Python. Specifically, we employed the Sklearn.ensemble. RandomForest Classifier algorithm due to its ability to effectively handle complex datasets.

We have checked that similar prediction accuracy could be obtained using different machine learning method including Support Vector Method (SVM) and Artificial Neural Network. We chose the random forest against (ANN) for its higher degree of interpretability, enabling the detection of the importance of individual features in the classification. While SVM are also interpretablility and could have been used for this study, we chose random forests for their lower susceptibility to over fitting [37].

3 Features enabling classification

We propose two approaches to identify the features enabling classification. The first approach is "iterative": features are all used at first and then removed one by one. The second approach is "direct": it probes some selected combinations of features.

3.1 Iterative approach

The first step of this approach is to consider all of the grains in the flow and to use all of the available features for training and testing the classifier. These features include the norm of the grain acceleration $|\mathbf{a}|$ and of the total force it is subjected to $|\mathbf{f}|$, the grain position, velocity and rotational velocity.

With all these features, the classifier accuracy reaches 0.92. This implies that some of these features are different for large and small grains. Figure 2a shows the relative importance of each feature for the final classification: the higher the score the more important the feature is. Three features stand out: the acceleration $|\mathbf{a}|$, the force $|\mathbf{f}|$ and the vertical position z. Other features such as velocity and rotational velocity seem to not contribute significantly to the classification.

To demonstrate this, we conducted a resilience test whereby features are excluded one after the other, starting with those of least importance. Resulting classification accuracy are shown in Fig. 2a (inset). Using all 16 features (listed on the y axis of Fig. 2a) yields an accuracy of 0.92. Removing features of least importance (in order: v_y, then v_x,

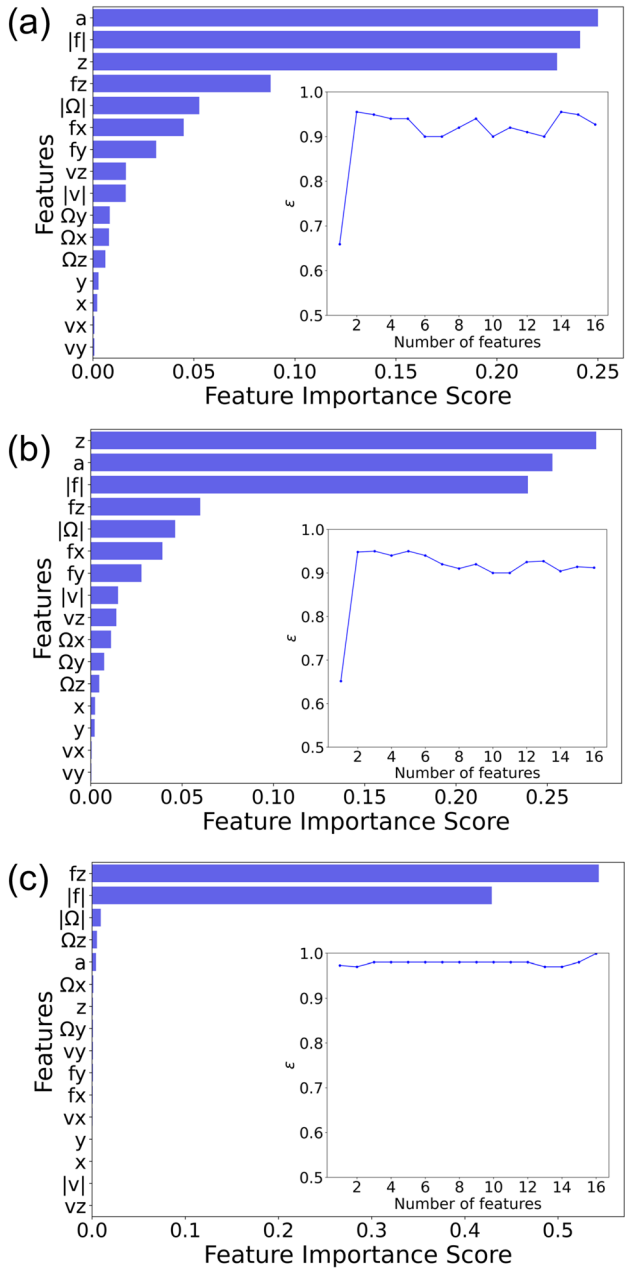

Fig. 2 Feature importance for the classification considering **a** all grains, **b** grains in the dense zones II and IV and **c** grains in the collisional zones I and III. (Main) relative importance of features when all features are feed to the classifier. (inset) iterative approach showing the classification accuracy evolution when features of the least importance are removed one after the other

then x etc.) does not significantly impact the classification accuracy. ϵ remains above 0.9 until two features are left: the acceleration $|\mathbf{a}|$ and the force $|\mathbf{f}|$.

However, once the force is removed, the classification based on acceleration only drops significantly to 0.67. This suggests that the information distinguishing large from small grains is contained in both their acceleration $|\mathbf{a}|$ and the force $|\mathbf{f}|$ they experience.

Table 1 Classification accuracy obtained with the "direct approach", using different features and combination of features

Features	Entire flow	Collisional	Dense
$\|\mathbf{f}\|$	*0.65*	**0.97**	*0.68*
$\|\mathbf{f}\|$ & $\|\mathbf{a}\|$	**0.94**	**0.96**	**0.95**
$\|\mathbf{a}\|$	*0.54*	*0.65*	*0.61*
x & y & z	*0.61*	*0.518*	*0.58*
$\|\mathbf{v}\|$ or v_z	*0.49 or 0.51*	*0.48 or 0.50*	*0.5 or 0.51*
$\|\Omega\|$ or Ω_z	*0.51 or 0.49*	*0.45 or 0.50*	*0.50 or 0.51*
$\|\mathbf{v}\|$ & v_x & v_y & v_z	*0.5*	*0.51*	*0.51*
$\|\Omega\|$ & Ωz & Ω_y & Ω_z	*0.51*	*0.46*	*0.52*

Successful classification ($\epsilon > 0.9$) is written in bold and unsuccessful in italic

We repeated the same iterative approach by selecting grains that are in the collisional zones (I and III) or in the dense zone (II and IV). Classification accuracy in Fig. 2b,c show that, in the dense zones, both force and acceleration are needed to achieve optimal classification while the other features play a negligible role. In contrast, only one feature—the vertical force—is sufficient to achieve classification in the collisional zones. This suggests that the information distinguishing small from large grains are different in dense and collisional flows.

3.2 Direct approach

With this alternative approach, classification accuracy is measured using individual features or some selected combinations of features. Results are summarised in Table 1 considering all grains, or grains belonging to the collisional or dense zones.

The first observation is that the position of the grains is not sufficient to distinguish small and large grains. This suggests an absence of significant size segregation.

The second observation is that the velocity (and rotational velocity) is also not a distinguishing feature of small and large grains. This suggests that large and small grains share a statistically similar velocity distribution in these bi-disperse flows. This differs from monodisperse flows, where a grain size effect on the velocity distribution was previously established as discussed in the introduction. One could expect that larger size ratio or different proportion of large grains could lead to differences in velocity distribution and therefore influence the classification efficiency. However, this remains to be established.

The third observation is that the grain acceleration only is not sufficient either to achieve classification. This contradicts the intuition that that larger, heavier and more inertial grains could exhibit lower accelerations than smaller grains.

The features yielding a successful classification (defined here to be $\epsilon > 0.9$) depend on the flow regime. In collisional zones, the force magnitude alone is sufficient. In dense flows, both force and acceleration magnitude are required. Force alone or acceleration alone are not sufficient. This suggests that the information distinguishing large and small grains is not contained in force or acceleration, but in their relationship.

3.3 Interpretation

To guide the interpretation of what the classifier is sensitive to, we turned to conventional statistics and measured the distribution of force, acceleration and velocity for large and small grains, in dense and collisional flows (Fig. 3).

In both dense and collisional flows, the distribution of velocities are similar for large and small grains. This is consistent with the fact that this feature alone did not warrant classification.

In collisional flows, the force distributions exhibit two distinct peaks, corresponding to the weight of small and large grains. The classifier appears to be capable of distinguishing these. In contrast, small and large grain accelerations both exhibit a similar peak at g, which explains why classification based on acceleration fails. These distributions of force and acceleration indicate a regime dominated by free falls in zone I and III.

In dense flows, large and small grains exhibit similar distributions of force and similar distributions of acceleration. Consistently, the classification failed with either of these features. Nonetheless, classification succeeded using both force and acceleration.

To help understand what the classifier detected, Fig. 4 presents some cross-correlation between features. The correlation between force and acceleration is poor in collisional flows and much higher in dense flows. This is consistent with (i) a regime of free fall where the acceleration is set by g and independent on the weight of the grains, and therefore of their size; and (ii) a regime with multiple contacts where acceleration is proportional to the contact forces via the grain mass, according to Newton's second law. Having two species of grains with differing masses means that there are two coexisting relationships between force and acceleration within the flow: $m_s|\mathbf{a}| = |\mathbf{f}|$ and $m_l|\mathbf{a}| = |\mathbf{f}|$, where $m_{s,l}$ is the mass of the small and large grains. The classifier appears to be able to detect and distinguish these two relationships. In other words, the classifier detects the difference in grain mass via the difference in correlation between force and acceleration.

The data presented in Fig. 5 provides compelling evidence for the existence of a dual correlation in the dense zones of the granular system. The figure displays a subset of data incluing all the grains which acceleration is lower than 50 m/s^2. It shows a clear linear trend between force and acceleration in the dense regime, in accordance with

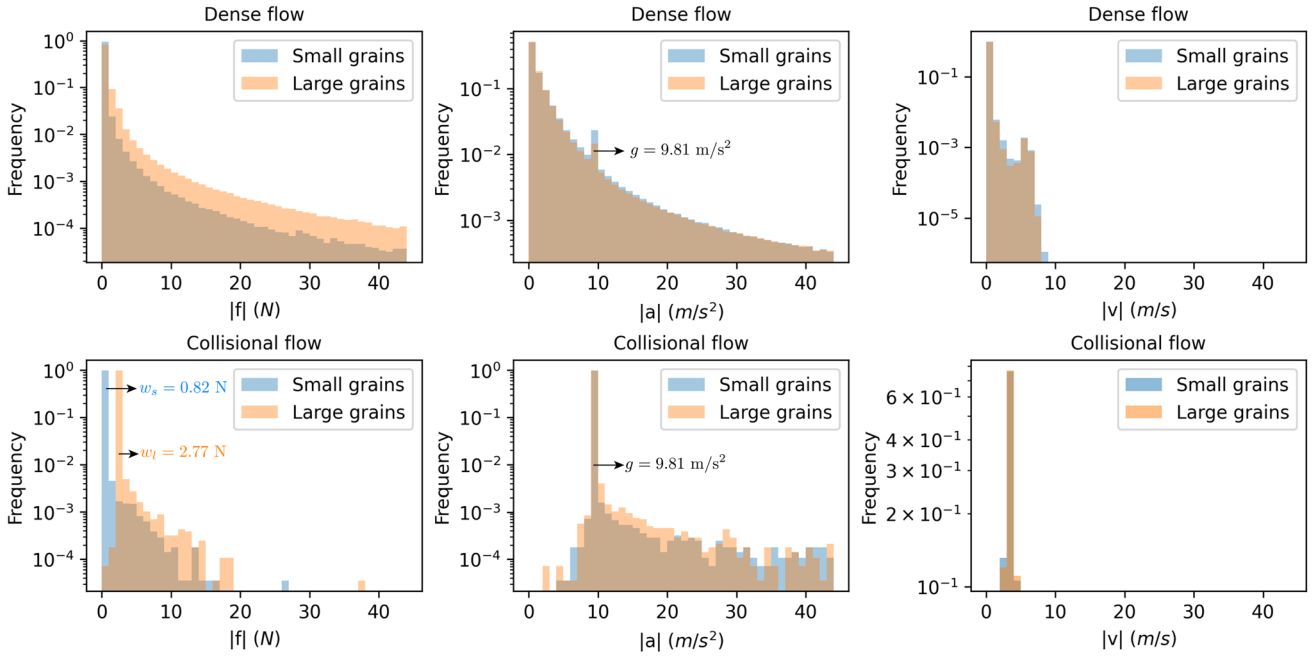

Fig. 3 Distribution of (left to right) force $|\mathbf{f}|$, acceleration $|\mathbf{a}|$ and velocity $|\mathbf{v}|$ of small grains (blue) and large grains (orange) considering dense zones II and IV (top row) and collisional zones I and III (bottom row). The weigth $w_{s,l}$ of small and large grains and the gravity are indicated for reference

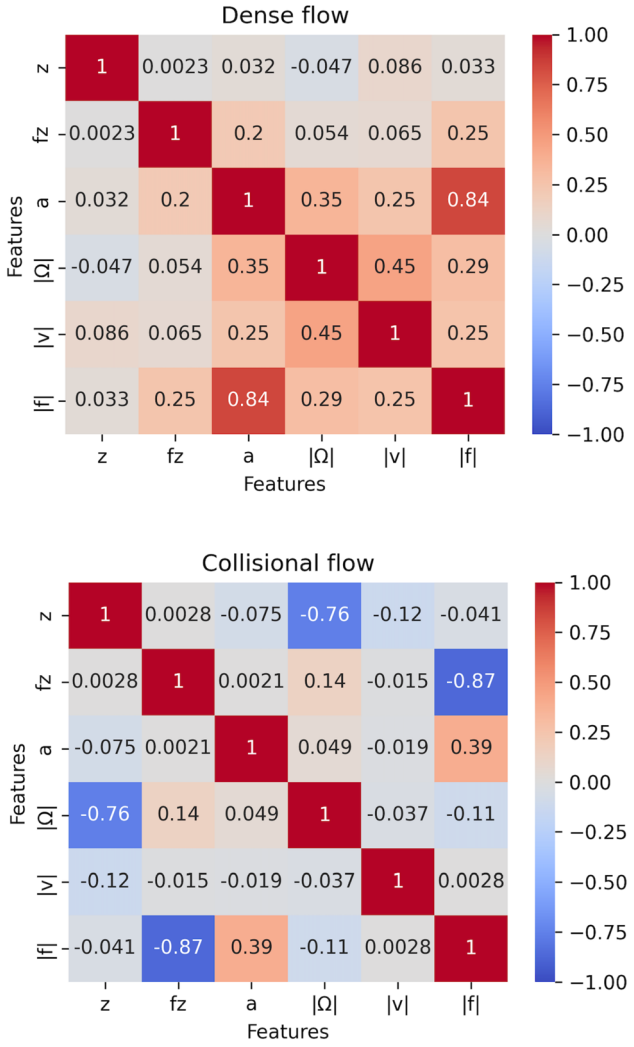

Fig. 4 Correlation between some selected features in dense and collisional zones

Newton's law of motion. It appears that most grain accelerations in the collisional zones equate gravity, and only a few grains that experience contacts exhibit this detectable dual correlation.

4 Conclusion

This study shows the potential for machine learning to help with the understanding of the mechanical behaviour of granular flows. Using the predictive ability of a random forest classifier, we were able to infer the difference and similitude in dynamical features of large and small grains in a bidisperse flow.

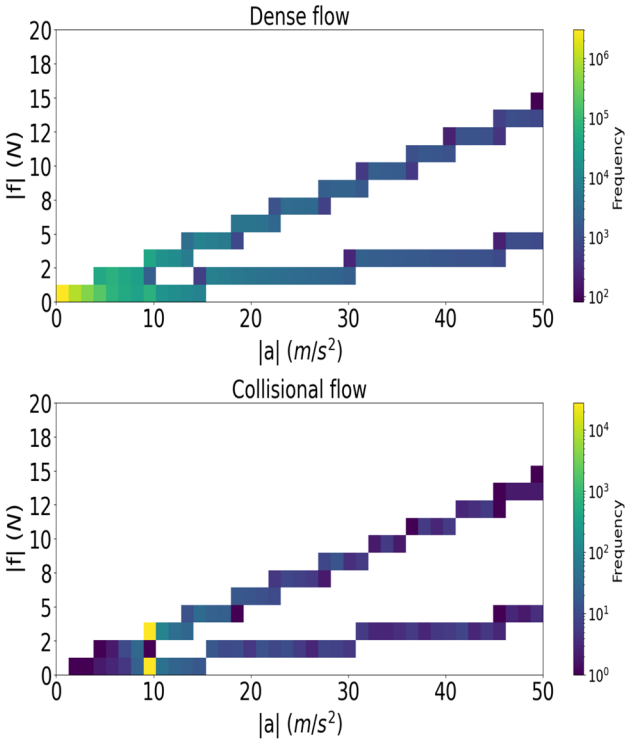

Fig. 5 Visualisation of the dual correlation between force and acceleration in a system with two grain sizes (and two grain masses): distribution of force $|\mathbf{f}|$ versus acceleration $|\mathbf{a}|$. Colors reflect the number of grains falling into a particular bin combination

Salient results include the lack of perceivable segregation, and similar velocity, angular velocity and acceleration between small and large grains. We also found that the classifier can detect not only differences in a single feature, but also a difference in the relationship between two features. Specifically, the classifier could detect Newton's second law relating grain acceleration and force via their size-dependent mass. This ability to detect differences in feature correlation may prove useful to improve classification and to gain further insights in the dynamics of granular flows.

This method is directly applicable to granular materials with different mixtures flowing in other geomteries. More generally, machine learning appears here to be a tool that can complement conventional statistical method to comprehend the behaviour of granular materials and other particulate fluids.

Funding Open Access funding enabled and organized by CAUL and its Member Institutions. Funding was provided by Australian Research Council (Grant No. DP200101927).

Declarations

Conflict of interest The authors declare that they have no conflict of interest.

References

1. Radjai, F., Jean, M., Moreau, J.J., Roux, S.: Force distributions in dense two-dimensional granular systems. Phys. Rev. Lett. **77**(2), 274 (1996)
2. Radjai, F., Roux, S.: Turbulentlike fluctuations in quasistatic flow of granular media. Phys. Rev. Lett. **89**(6), 064,302 (2002)
3. Rognon, P., Einav, I., Bonivin, J., Miller, T.: A scaling law for heat conductivity in sheared granular materials. Europhys. Lett. **89**(5), 58,006 (2010)
4. Rognon, P., Einav, I.: Thermal transients and convective particle motion in dense granular materials. Phys. Rev. Lett. **105**(21), 218,301 (2010)
5. Campbell, C.S.: Self-diffusion in granular shear flows. J. Fluid Mech. **348**, 85–101 (1997)
6. Losert, W., Bocquet, L., Lubensky, T., Gollub, J.P.: Particle dynamics in sheared granular matter. Phys. Rev. Lett. **85**(7), 1428 (2000)
7. Mueth, D.M.: Measurements of particle dynamics in slow, dense granular Couette flow. Phys. Rev. E **67**(1), 011,304 (2003)
8. MiDi, G.: On dense granular flows. Eur. Phys. J. E **14**(4), 341–365 (2004)
9. Da Cruz, F., Emam, S., Prochnow, M., Roux, J.N., Chevoir, F.: Rheophysics of dense granular materials: Discrete simulation of plane shear flows. Phys. Rev. E **72**(2), 021,309 (2005)
10. DeGiuli, E., McElwaine, J., Wyart, M.: Phase diagram for inertial granular flows. Phys. Rev. E **94**(1), 012,904 (2016)
11. Kharel, P., Rognon, P.: Vortices enhance diffusion in dense granular flows. Phys. Rev. Lett. **119**(17), 178,001 (2017)
12. Rognon, P., Macaulay, M.: Shear-induced diffusion in dense granular fluids. Soft Matter **17**(21), 5271–5277 (2021)
13. Chialvo, S., Sun, J., Sundaresan, S.: Bridging the rheology of granular flows in three regimes. Phys. Rev. E **85**(2), 021,305 (2012)
14. Azéma, E., Radjai, F.: Internal structure of inertial granular flows. Phys. Rev. Lett. **112**(7), 078,001 (2014)
15. Macaulay, M., Rognon, P.: Two mechanisms of momentum transfer in granular flows. Phys. Rev. E **101**(5), 050,901 (2020)
16. Miller, T., Rognon, P., Metzger, B., Einav, I.: Eddy viscosity in dense granular flows. Phys. Rev. Lett. **111**(5), 058,002 (2013)
17. Jop, P.: Rheological properties of dense granular flows. C. R. Phys. **16**(1), 62–72 (2015)
18. Zhang, Q., Kamrin, K.: Microscopic description of the granular fluidity field in nonlocal flow modeling. Phys. Rev. Lett. **118**(5), 058,001 (2017)
19. Gaume, J., Chambon, G., Naaim, M.: Microscopic origin of nonlocal rheology in dense granular materials. Phys. Rev. Lett. **125**(18), 188,001 (2020)
20. Gray, J.M.N.T.: Particle segregation in dense granular flows. Annu. Rev. Fluid Mech. **50**, 407–433 (2018)
21. Samadani, A., Pradhan, A., Kudrolli, A.: Size segregation of granular matter in silo discharges. Phys. Rev. E **60**(6), 7203 (1999)
22. Cliff, A., Fullard, L., Breard, E., Dufek, J., Davies, C.: Granular size segregation in silos with and without inserts. Proc. R. Soc. A **477**(2245), 20200,242 (2021)
23. Hill, K., Tan, D.S.: Segregation in dense sheared flows: gravity, temperature gradients, and stress partitioning. J. Fluid Mech. **756**, 54–88 (2014)
24. Jing, L., Kwok, C., Leung, Y.F.: Micromechanical origin of particle size segregation. Phys. Rev. Lett. **118**(11), 118,001 (2017)
25. Umbanhowar, P.B., Lueptow, R.M., Ottino, J.M.: Modeling segregation in granular flows. Annu. Rev. Chem. Biomol. Eng. **10**, 129–153 (2019)
26. Jaza, R., Mollon, G., Descartes, S., Paquet, A., Berthier, Y.: Lessons learned using machine learning to link third body particles morphology to interface rheology. Tribol. Int. **153**, 106,630 (2021)
27. Ren, C.X., Dorostkar, O., Rouet-Leduc, B., Hulbert, C., Strebel, D., Guyer, R.A., Johnson, P.A., Carmeliet, J.: Machine learning reveals the state of intermittent frictional dynamics in a sheared granular fault. Geophys. Res. Lett. **46**(13), 7395–7403 (2019)
28. Liao, Z., Yang, Y., Sun, C., Wu, R., Duan, Z., Wang, Y., Li, X., Xu, J.: Image-based prediction of granular flow behaviors in a wedge-shaped hopper by combing DEM and deep learning methods. Powder Technol. **383**, 159–166 (2021)
29. Cheng, H., Shuku, T., Thoeni, K., Tempone, P., Luding, S., Magnanimo, V.: An iterative Bayesian filtering framework for fast and automated calibration of dem models. Comput. Methods Appl. Mech. Eng. **350**, 268–294 (2019)
30. Cheng, Z., Wang, J., Xiong, W.: A machine learning-based strategy for experimentally estimating force chains of granular materials using X-ray micro-tomography. Géotechnique 1–44 (2023)
31. Rouet-Leduc, B., Hulbert, C., Lubbers, N., Barros, K., Humphreys, C.J., Johnson, P.A.: Machine learning predicts laboratory earthquakes. Geophys. Res. Lett. **44**(18), 9276–9282 (2017)
32. Torres-Serra, J., Rodríguez-Ferran, A., Romero, E.: Classification of granular materials via flowability-based clustering with application to bulk feeding. Powder Technol. **378**, 288–302 (2021)
33. Laudari, S., Marks, B., Rognon, P.: Classifying grains using behaviour-informed machine learning. Sci. Rep. **12**(1), 1–7 (2022)
34. Cheng, Z., Wang, J.: Estimation of contact forces of granular materials under uniaxial compression based on a machine learning model. Granul. Matter **24**, 1–14 (2022)
35. Cubuk, E.D., Schoenholz, S.S., Rieser, J.M., Malone, B.D., Rottler, J., Durian, D.J., Kaxiras, E., Liu, A.J.: Identifying structural flow defects in disordered solids using machine-learning methods. Phys. Rev. Lett. **114**(10), 108,001 (2015)
36. Kloss, C., Goniva, C., Hager, A., Amberger, S., Pirker, S.: Models, algorithms and validation for opensource DEM and CFD-DEM. Prog. Comput. Fluid Dyn. Int. J. **12**(2–3), 140–152 (2012)
37. Breiman, L.: Random forests. Mach. Learn. **45**, 5–32 (2001)

CHAPTER 6

Using Tracer Particle Kinematics to Predict Particle Size in Rotating Drums

---

Building upon our previous research, where we initially highlighted contrasts in granular particle trajectories and then advanced to exploring bi-disperse granular flows using machine learning classifiers, our third study takes a significant leap into the realm of comminution in ball mills. This progression reflects our overarching goal of applying the insights gained from granular particle behavior to practical, industrially relevant scenarios.

In the context of ball mills, where large metal balls crush ore particles, understanding and optimizing the comminution process is crucial, given its energy-intensive nature. Our research aims to tackle a key industry challenge: monitoring of particle size in the harsh mechanical environment of a ball mill. Traditional methods for measuring particle size under such conditions are either non-existent or impractical. Addressing this, our third study demonstrates that the acceleration of the grinding media, monitored via embedded accelerometers, can be an innovative solution to sense the particle size during operation. We utilize DEM simulations to show that a machine learning classifier can successfully determine the size of smaller 'ore' particles by analyzing the acceleration data of larger grinding media particles. This approach of 'kinematic sensing' is found to be effective across various particle size ratios, mixture ratios, and mill charges.

What makes this research significant is its potential impact on mineral processing. By providing a method to monitor particle size in real-time, it opens avenues for optimizing ball mill operations, leading to energy savings and increased efficiency. Furthermore, our findings have implications beyond practical applications. They offer a novel insight into the field of

rheology, especially in bi-disperse granular flows, by indicating that the kinematics of larger particles are influenced by the size of smaller particles. This observation could be pivotal in advancing rheological models for such flows. In essence, this research not only addresses a critical industrial need but also contributes to the broader scientific understanding of granular flow dynamics. It stands as a testament to the evolving nature of our studies, progressively bridging granular physics with real-world applications.

The following paper is comprised of a main material which is recently submitted to a journal 'Granular Matters' for review. Preprint of this material is available in: $https : //www.researchsquare.com/article/rs - 3909482/v1$

Using tracer particle kinematics to predict particle size in rotating drums

Sudip Laudari, Benjy Marks, Pierre Rognon

[a] *Particles and particles Laboratory, School of Civil Engineering, The University of Sydney, Sydney NSW 2006, NSW, Australia*

Abstract

Comminution is an energy intensive process. In ball mills, it is achieved by rotating a drum in which large metal balls crush ore particles. In-situ monitoring of particle size would be of considerable interest to optimize their operation. However, there is no established solution to measure particle size in such a harsh mechanical environment. We show here that the acceleration of the grinding media, which can be monitored using embedded accelerometers, can be used to sense the particle size during operation. In DEM simulations, we find that a machine learning classifier is able to detect the size of small "ore" particles solely based on the knowledge of the acceleration of larger grinding media particles. Results show that this kinematic sensing is effective over a wide range of particle size ratios, mixture ratio and mill charge. Beyond their practical interest in mineral processing, these results point out that the kinematics of large particles is affected by the size of the smaller particles, an observation which can help advance rheological models for bi-disperse granular flows.

Keywords: Ball-mill, particle size detection, machine learning, DEM

1. Introduction

Ball mills are commonly used as a primary grinder for mineral processing and cement production. They consist of a large rotating drum enclosing steel balls whose function is to crush large ore particles into smaller particles. Although specifics are application dependent, mills are typically large equipment with drum diameters up to a dozen metres. They transform coarse ore into fine submillimetric particles. The energy required to achieve this comminution is inversely proportional to the size of the fine particles [1, 2, 3]; it is substantial, as machines run continuously with power ratings of several MW. Optimizing their operation is thus a significant challenge: over-milling would produce finer particles than necessary and waste a vast amount of energy, while under-milling would produce ore particles that are too large to enable subsequent mineral extraction. The ability to monitor the ore size during operation is thus of significant interest to optimise the comminution process. However, sensors capable of monitoring particle size within operating mills are not readily available due to the harsh mechanical environment.

External sensors have been developed to gain some insights into the internal dynamics of mills whilst avoiding this harsh environment. For instance, the acoustic signals of sensors placed on the mill shell were related to features including feed size fraction [4], feed hardness [5], fill level and charge composition [6, 7]. Other externally measured quantities such as feed tonnage, bearing pressure, and spindle speed were successfully used to predict the mill energy consumption, including via machine learning methods [8, 9, 10, 11]. However, there is no evidence that these external sensors can allow to infer the ore size during operation.

An in-situ sensing method has been developed, which consists of embedding accelerometers into the grinding media to monitor their acceleration. This data was found to enable the determination of the load state of the mills [12, 13]. Whether this data also contain some information related to the ore particle size remains to be established. Nonetheless, findings in the behaviour of granular flows comprised of different particle sizes suggest it might. For instance, a bi-disperse granular materials may segregate within a rotating drum, with larger particles being located preferentially at the free surface and near the drum shell [14, 15, 16]. More generally, the flow dynamics of bi-disperse mixtures was found to depend on their size ratio [17, 18]. Finally, we evidenced in our recent studies that contrast in physico-mechanical properties of particles including size, density, Young's modulus and cohesion, could be detected from their trajectories and acceleration using machine learning classifier [19, 20].

In this paper we seek to determine whether the acceleration of the ginding media can be used as a proxy to detect the size of smaller particles. To this aim, we conducted discrete element method (DEM) simulations of a simplified mill comprised of a rotating drum containing a bi-disperse granular mixture. The large particles play the role of the grinding media and the small particles represent the ore. We then trained a machine learning classifier using the information on large particle acceleration to infer the size of the small particles. The simulation and machine learning methods are presented in Section 2. Section 3 introduces the capability of this method to perform a binary classification, that is to distinguish two flows with differing small particle sizes. Section 4 finally shows how this method can successfully perform a multiclass classification, that is inferring the size of small particles amongst several possibilities of small particle size.

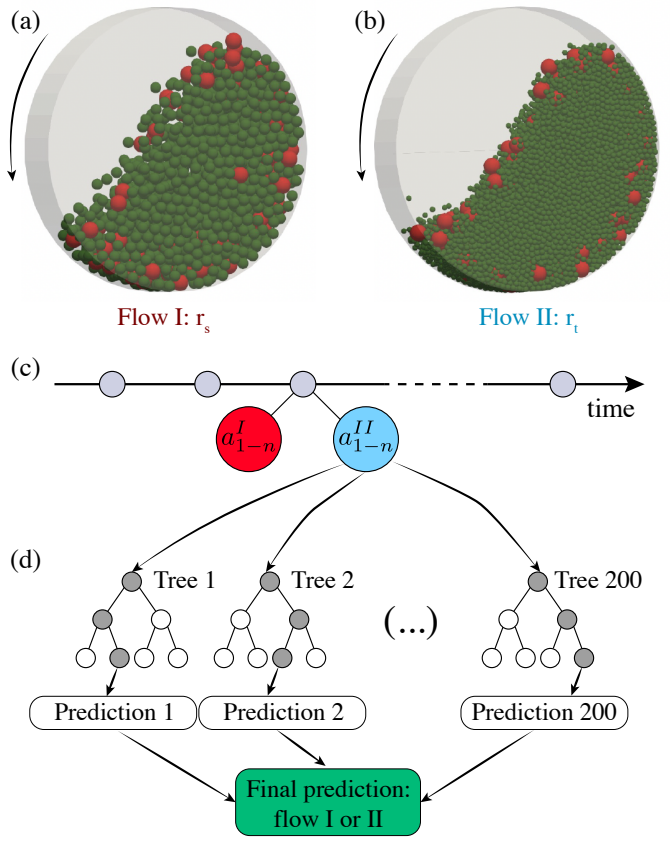

Figure 1: Binary classification of bi-disperse flows. (a,b) two identical flows are simulated using a DEM; they only differ by the size of the small particles (r_s or r_t). (c) Acceleration norm a of all n large particles is recorded during the flows at regular time intervals (grey circles). (d) Snapshots of large particle accelerations are fed to a random forest classifier for training and testing. For each snapshot, the classifier attempts to predict whether the flow comprises small particles of size r_s or r_t; the random forest classifier includes 200 trees of depth 9 - a depth of 3 is represented here for clarity.

2. Method

We developed the method described in figure 1 to assess whether the acceleration of large particles contains information enabling the detection of the size of the small particles. Bi-disperse flows are simulated using a DEM: each flow includes large and small particles. Flows differs by the size of the small particles. From this database, a machine learning classifier is then used to try and predict the small particle size based on large particle accelerations. The specifics of the DEM method and of the machine learning classifier are detailed below.

2.1. DEM simulation of bi-disperse flows in a rotating drum

We used LIGGGTHS to simulate bi-disperse flows in a rotating drum. The drum is 1 m in diameter and 0.2 m wide. The radius of large particles is the same in all simulations, r_B = 3 cm. The process of particle comminution is not included in the simulations. While it is possible to emulate it using DEM [21, 22, 23, 24], it is not the goal of this study. We instead consider two stages of the comminution process characterised by a change in small particle size. Simulations are thus performed in pairs: in the first simulation the small particle size is r_s and in the second the small particle size is r_t, with $r_s \geq r_t$; the total mass of the particles is the same in the two flows, reflecting mass conservation during comminution.

For simplicity, all particles have the same physical and mechanical properties. Their density is $\rho = 2.5{\times}10^3$kg/m^3. They interact via elasto-dissipative and frictional contacts characterised by a contact stiffness $k = 10^8$N/m, a coefficient of restitution $e = 0.6$ and a friction coefficient $\mu_p = 0.5$. The boundary of the drum are smooth and frictional, with a coefficient of friction of 0.3.

Simulations are performed by randomely seeding particles in the drum without contact. They then settle under the action of gravity while the drum is rotating. In all simulations, the rotation frequency of the drum is 0.2 Hz, which corresponds to a rotation period of 5 s. Simulations are performed for a duration of 20 rotations.

The fill ratio of the drum f measures the ratio of the volume of the particles to the volume of the drum. It is varied in the range 5% to 30%. Unless otherwise specified, results are presented for a fill ratio of 30%.

The bi-disperse mixture is characterised by the volumetric proportion of large particles ϕ, defined as the ratio of the volume of large particles to the volume of all particles. This proportion is varied from 0.05 to 0.7. The total number of particles varies from 10^3 to 14.10^3 depending on the fill ratio and on the size of the small particles.

2.2. Machine learning classifier

We used a machine learning classifier with the aim of distinguishing two flows with small particles of size r_s or r_t based on the acceleration of the large particles.

The feature which this classification is based on is the norm of the acceleration vector of individual large particles. No other information is provided. In particular, no information whatsoever regarding small particles is provided. Large particle accelerations are recorded during the flows at a frequency of 80 snapshots per rotation, unless otherwise specified. The classifier is trained and tested considering pairs of flows differing only by the size of the small particles, r_s or r_t. Each acceleration snapshot is used as either a training sample or testing sample. A k-fold algorithm is used to select at random training and testing samples with a proportion of 80% and 20%, respectively; training samples are never included in the testing set. This process is repeated five times with different subsets of training and testing samples. The final classification accuracy is defined as:

$$\epsilon = \frac{\text{Number of correct predictions}}{\text{Number of predictions}}. \quad (1)$$

where a prediction is whether a large particle acceleration snapshot belongs to a simulation with a small particle size r_s or r_t. A value of $\epsilon = 0.5$ corresponds to a random prediction, meaning that the classifier cannot distinguish between the two systems. A value of $\epsilon = 1$ is a perfect prediction, meaning that the classifier inferred the correct small particle size for all snapshots in the testing set.

Several machine learning classifiers are available to perform this task, including neural networks, support vector machines

and random forests. Both support vector machines and random forests have the benefit of a higher interpretability: the role of individual features to the success of a classification can be estimated. We chose here to use random forest as it is better suited to multiclass classification, which we will consider. We used the Sklearn Python library to that effect. We found that using 200 estimators (trees) and a maximum depth of 9 gave optimal classification accuracy.

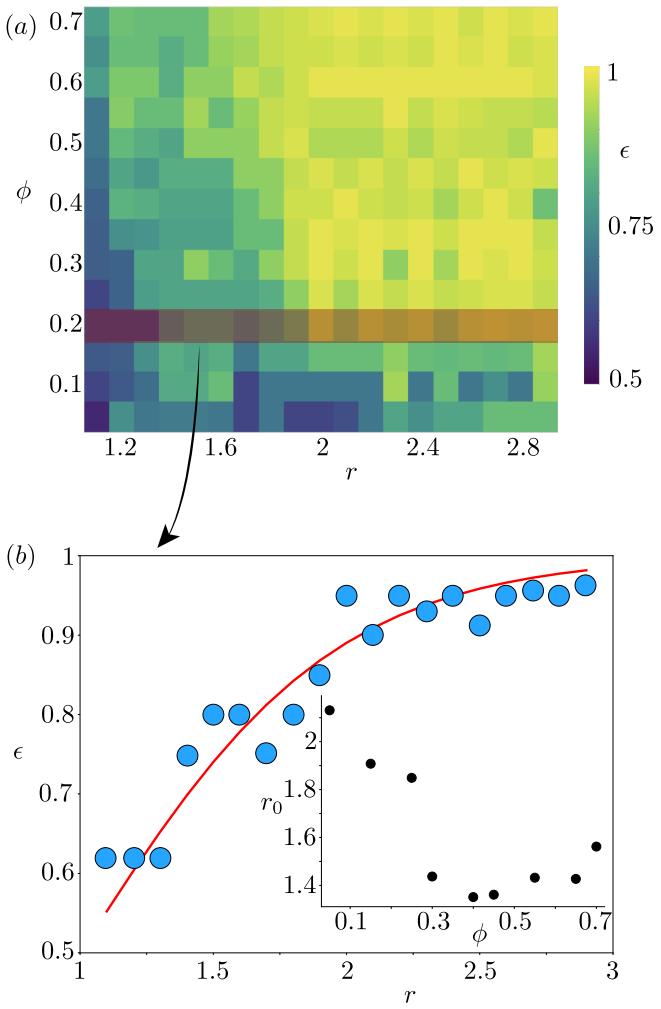

Figure 2: Particle size resolution in binary classifications. (a) Classification accuracy ϵ obtained for pairs of flows with a small particle size ratio $r = r_s/r_t$ and a proportion of large particles ϕ; Each pixel corresponds to a value of classification accuracy based on large particle acceleration, obtained for a pair of flows with a value of r and ϕ. (b) Classification accuracy as a function of the small particle size ratio r for $\phi = 0.2$; symbols are the results from the classifier and the red line is the best fit obtained with Eq. (2) using r_0 as a fitting constant. Inset: fitting constant $r_0(\phi)$ obtained by using the same method varying the proportion of large particles ϕ.

3. Binary classification

This section presents the classification accuracy obtained when attempting to distinguish two flows differing by the size of the small particles. The goal is to determine whether and under which conditions the particle sizes of the two flows can be distinguished. Parameters under scrutiny include the particle size ratio $r = r_s/r_t$, the proportion of large particles ϕ and the drum fill ratio f. We will also seek to establish the temporal resolution of this method, i.e. the minimum duration of data acquisition needed to achieve a successful classification.

3.1. Particle size resolution

To establish the particle size resolution of the classifier, we conducted a series of classifications covering size ratios r ranging from 1.1 to 3, and repeated the process for different proportion of large particles in the range $0.05 \leq \phi \leq 0.7$. The drum fill ratio is kept constant at 50% for all flows. Snapshots of large particle acceleration fed to the classifier are recorded at a frequency of 80 per rotation during 20 rotations, leading to a pool of 1 600 training and testing samples.

The resulting classification accuracies ϵ shown in figure 2a evidence a combined influence of r and ϕ. As expected, the lowest size contrast ($r = 1.1$) yields a poor classification accuracy ranging from 0.5 to 0.7 for all ϕ. The two mixtures being virtually identical, they cannot be distinguished. In contrast, the largest size contrast ($r = 3$) yields an excellent classification accuracy ranging from 0.8 to 1. This means that the acceleration of the large particles is sensitive to the size of the small particles in a way that can be detected by the classifier. Furthermore, figure 2a indicates that the classification is generally more accurate for a larger proportion of large particles ϕ. This may be attributed to the presence of fewer large particles at low ϕ, reducing the amount of data available to inform the classifier.

We propose to capture these accuracy dependencies by the following empirical function:

$$\epsilon(r, \phi) = \frac{1}{1 + \exp(-\frac{r-1}{r_0(\phi)-1})} \tag{2}$$

This function ranges from 0.5 for $r = 1$ to 1 when $r \to \infty$. $r_0(\phi) > 1$ represents a characteristic particle size ratio below which classification is poor. Figure 2b shows that the selected exponential function captures well the measured accuracies. Nonetheless, there is no physical rationale for this choice and other functions could equally well fit the data. The influence of the proportion of large particles is captured in the fitting constants $r_0(\phi)$, shown in the inset of figure 2b. Larger values of ϕ lead to smaller values of r_0, which denotes an enhanced particle size resolution.

3.2. Temporal resolution

The results discussed above were obtained using the large particle acceleration recorded during the entire simulated flows -20 rotations- at a frequency of 80 snapshots per rotation. We now seek to establish how using a shorter flow duration and fewer snapshots, which in turn reduces the amount of training data, affects the classification. For this purpose, we focus on a pair of flows with $r = 2$ and $\phi = 0.5$, for which the classification accuracy using the full data set is excellent: $\epsilon = 0.95$.

Figure 3 presents the classification accuracy obtained when considering the beginning of the flow up to a number of rotations ranging from 1 to 20. The recording frequency is 80

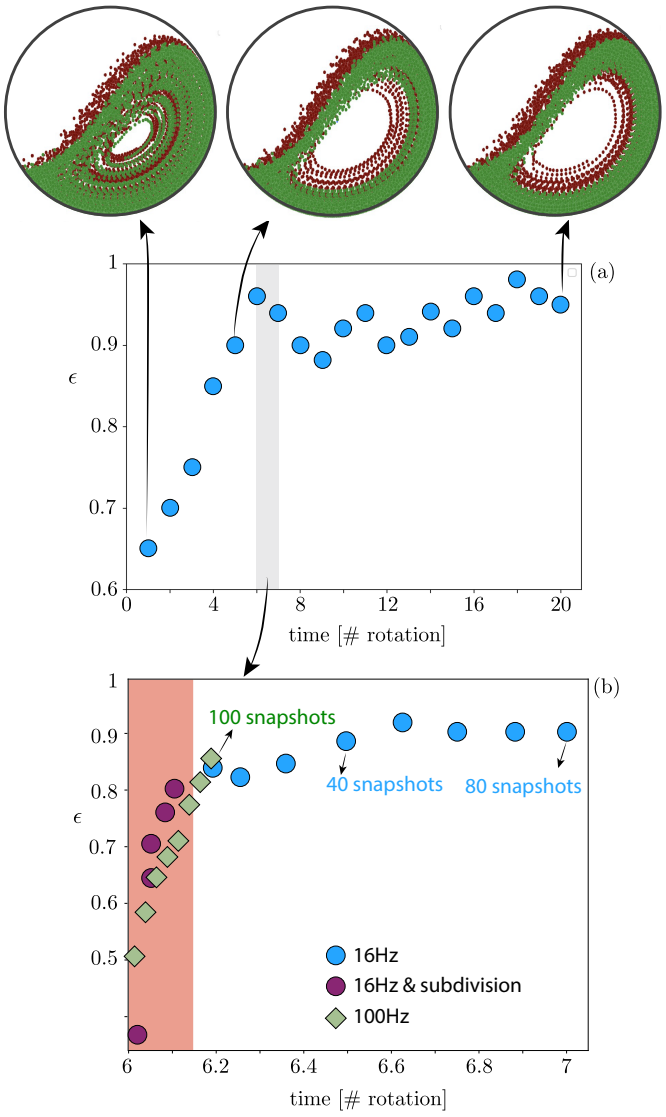

Figure 3: Time resolution of the binary classification using a pair of flows with $r = 2$, $\phi = 0.5$. (a) Accuracy obtained including an increasing period of time starting at the beginning of the flow, expressed in number of rotations (frequency of snapshots recording of 16 Hz). The three pictures represent the position of the large particles after 2, 5 and 20 rotations; in each picture the position of large particles in two flows with small particle size r_s (red) and r_t (green) are overlaid; small particles, which are predominantly located in the center of the flow, are not represented for clarity. (b) Accuracy measured during the 6^{th}*rotation* when the flow is segregated, using an increasing period of time. The recording frequency is 16 Hz (circles) or 80 Hz (diamonds). Purple circles represent a recording frequency of 16 Hz while snapshots are subdivided (see text).

snapshots per rotation. Results indicate that classification accuracy is poor when considering only the first rotations, and gradually increases to reach a plateau when 5 or more rotations are included.

Figure 3 also represents the position of the large particles in the pair of flows, taken after a number of rotation of 2, 5 and 20. These demonstrate a gradual development of size segregation, whereby large particles are predominantly located at the free surface and near the drum shell. However, this segregation takes time to develop: it is not fully developed after 2 rotations and seems fully developed after 5 rotations. This suggests that the ability of the classifier to sense the size of the small particles based on the large particle acceleration depends on the state of segregation. Accordingly, the effect of small particle size on large particle acceleration appears more pronounced in a segregated flow than in a non-fully segregated flow.

Figure 3 aims to highlight the minimum amount of data required to achieve classification during the fully segregated flow. To this aim, if focuses on the 6^{th} rotation. At first, classification is performed using all of the 80 snapshots recorded at a frequency of 16 Hz during this rotation. The resulting accuracy of 0.9 is nearly as good as the 0.95 accuracy obtained when including the 20 rotations of the flow. Further still, figure 3 indicates that classification is still possible when only including a fraction of rotation. Using as little as 0.2 of a rotation leads to an accuracy of 0.83.

Probing even shorter flow duration at a frequency of acquisition of 16 Hz is not possible as there are not enough snapshots available to form a testing set and a training set. To test whether classification is possible using such a short flow duration, we used two strategies: subdividing snapshots or increasing the recording frequency. The subdividing strategy consists of keeping the recording frequency unchanged but subdividing the data of each snapshots into 10 sub-snapshots, and used these for training and testing. These sub-snapshots thus contains the information of fewer large grains than the full snapshots. Using fewer and fewer of these sub-snapshots leads to sharp decrease in classification accuracy, as highlighted by the red zone on figure 3. This leaves two possible interpretations for the cause of this drop in accuracy: either there is not enough information, either the duration of the flow is too short. To discriminate between these two options, we performed classifications using a set of data recorded at a higher frequency of 100 Hz without subdivision. Even with this strategy, the classification accuracy sharply decreases for flow duration shorter than about 0.2 rotation. This decrease is similar to the one obtained with the subdivision strategy. This indicates that the temporal resolution of the classifier corresponds to a finite flow duration - a fraction of rotation of the order of 0.2- even with a higher recording frequency.

3.3. Effect of drum fill ratio

We finally consider whether the fill ratio of the drum affects the ability to detect small particle size. To this aim we focus on pairs of flows with $r = 2$ and $\phi = 0.5$, and vary the total mass of the mixture from 20kg to 120kg. This leads to fill ratios f varying from 5% to 30%.

Figure 4a shows that the classification accuracy is higher for higher fill ratios; it is poor below 20% and reaches 90% for larger fill ratios. It appears that this transition coincides with a degree of segregation in these flows. As illustrated in figures 4: a flow with a fill ratio of 30% becomes well segregated after 6 rotations. In contrast, flows with fill ratios of 5% and 15% remain poorly segregated. This further supports the conclusion that the acceleration of large particles is most affected by the size of the small particles in flows that are segregated.

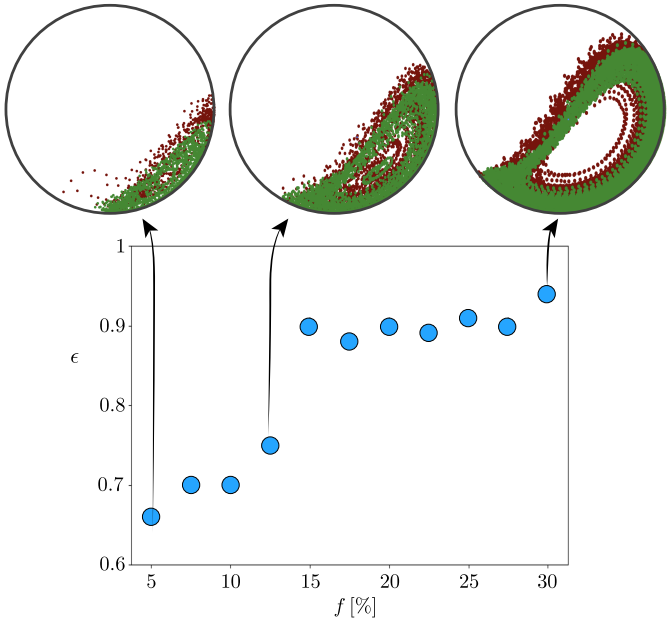

Figure 4: Sensitivity of the binary classification accuracy to the drum fill ratio f, ratio of the total volume of the particles to the drum volume. The accuracy ϵ is measured using 20 rotations for different fill ratios keeping $r = 2$, $\phi = 0.5$ constant. The three pictures represent the position of the large particles after 6 rotations in a pair of simulations with small particle size r_s (red) and r_l (green) with $f = 5\%$, 15% and 30%; small particles, which are located in the center of the flow, are not represented for clarity.

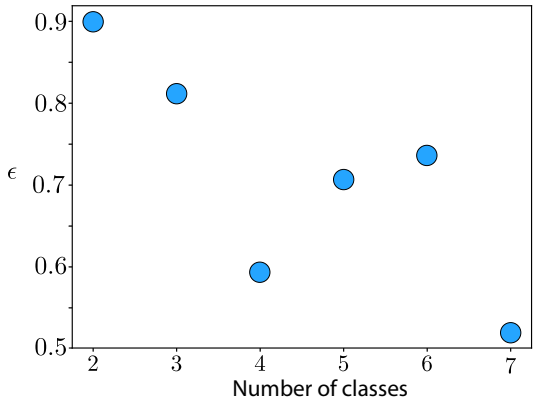

Figure 5: Multi-class classification: precision of the classification obtained for a flow with $r_s = 12$ mm using an increasing number of classes. As an example, 7 classes on the x-axis means that flows with $r_s = 12$ mm, 14 mm, 16 mm, 19 mm, 22 mm, 25 mm and 28 mm. are included; 3 classes means flows with $r_s = 12$ mm, 16 mm, 22 mm are included.

4. Multi-class classification

The previous section demonstrated how a random forest could successfully perform a binary classification based on the acceleration of the large particles. We now consider whether this ability can be extended to a multi-class classification, that is distinguishing the size of the small particles amongst a series of flows with differing small particle sizes.

To this end, we simulated a series of flows with similar fill ratio $f = 0.5$ and similar large particle proportion $\phi = 0.2$. The data fed to the classifier includes the entire flow duration and is recorded at a frequency of 16 Hz. A series of 7 flows is considered, including small particles size of 12 mm, 14 mm, 16 mm, 19 mm, 22 mm, 25 mm and 28 mm. The large particles size is 30 mm for all flows. Each of these flows will be referred to as a class.

Figure 5 shows the precision of the classification obtained when considering an increasing number of classes. The maximum precision is obtained when only two classes (in this case $r_s = 12$ mm and 14 mm) are included. This corresponds to a binary classification. The classification precision significantly decreases when more classes are introduced. It is only about 0.5 with 7 classes.

In a binary classification, a precision 0.5 means that 50% of the acceleration snapshots in the training set were attributed to the correct class, and the other 50% were incorrectly attributed to the other class. It implies that the classification is not possible. In contrast, in a multi-class classification, a precision of 50% means that 50% of the snapshots were correctly classified and that the remaining 50% were attributed to several other classes. As a result, a correct classification may still be possible for precision lesser than 50%. To demonstrate this, figure 6 shows the confusion matrix obtained with binary and multi-class classification. These matrices measure the percentage of snapshots attributed to any class for any given known class. For instance, on figure 6b represents the results of a classification involving five classes. The first row represents snapshots recorded from a flow with $r_s = 12$ mm. It shows that 68.4% of these snapshot were correctly attributed to this class while 16.98%, 11.79% and 2.83% of the snapshots were incorrectly attributed to the classes with $r_s = 16$ mm,22 mm and 25 mm, respectively.

This figure shows that a correct multi-class classification can be consistently be obtained by using a 'maximum-vote' criteria. The reason is that the diagonal element of this matrix are always greater than any other element of their row. This means that the actual class was consistently attributed the maximum number of votes compared to any other classes.

5. Conclusion

These results show that monitoring the acceleration of particles in ball mills may be an effective way to sense the size of small ore particles during operation. We proved this concept here considering a simplified, simulated system comprised of a bi-disperse mixture. The method based on machine learning appears to be robust, as it lead to successful grain size detection over a wide range of grain size, mixture ratio and fill ratio. We further found that this method could successfully perform multi-class classification, allowing to detect small particle size amongst many possibilities.

These results suggest that this proposed method is a promising tool to detect particle size in-situ during mills operations. It calls for further studies to confirm its applicability to real crushing applications. Importantly, comminution usually yields widely distributed ore particle sizes. A point of interest would be to establish whether the characteristic particle size of these distributions could be detected using this proposed method.

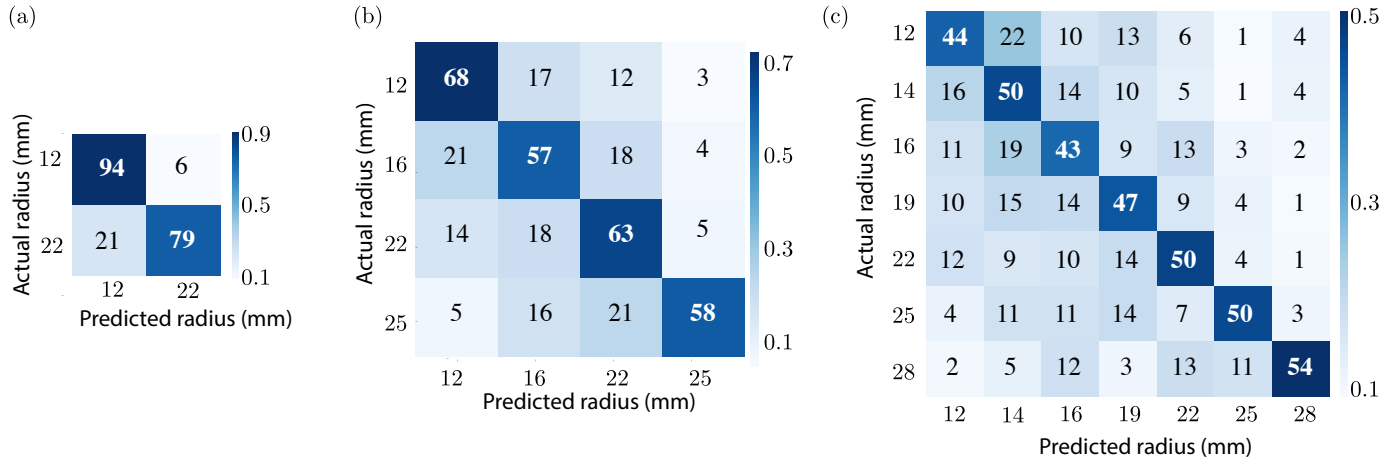

Figure 6: Confusion matrices in binary (a) and multi-class classifications considering 4 (b) and 7 (c) classes. Each class correpsond to flow with a different small particle size, as specified on the figures. The numbers in each cell represent the percentage of snapshots from the Actual class (row) attributed to the predicted class (columns); the sum of the cells on a line is 100%. The cells are colours according to this percentage following the displayed color bars. Diagonal elements correpspond to the proportion of correct prediction. As this proportion is consistently larger than any other class (any other cell on the same line), the multi-class classification is possible based on a maximum vote criteria.

Testing the effectiveness of the method including characteristics such as particle angularity, grinding media density and different mill speeds would also be required.

On a more fundamental stand, our results indicate that the large grain dynamics is affected by the small grain size in bidisperse granuluar flows, in particular when segregation has developed. This information can be of interest for the development of rheological models for granular flow undergoing segregation.

References

[1] F. C. Bond, The third theory of comminution, Trans. AIME, Min. Eng. 193 (1952) 484–494.

[2] S. Martins, Size–energy relationship in comminution, incorporating scaling laws and heat, International Journal of Mineral Processing 153 (2016) 29–43.

[3] J. Jeswiet, A. Szekeres, Energy consumption in mining comminution, Procedia CIRP 48 (2016) 140–145.

[4] K. B. Owusu, W. Skinner, R. K. Asamoah, Acoustic sensing and supervised machine learning for in situ classification of semi-autogenous (sag) mill feed size fractions using different feature extraction techniques, Powders 2 (2) (2023) 299–322.

[5] K. B. Owusu, W. Skinner, R. Asamoah, Feed hardness and acoustic emissions of autogenous/semi-autogenous (ag/sag) mills, Minerals Engineering 187 (2022) 107781.

[6] K. B. Owusu, M. Zanin, W. Skinner, R. K. Asamoah, Ag/sag mill acoustic emissions characterisation under different operating conditions, Minerals Engineering 171 (2021) 107098.

[7] D. K. Nayak, D. P. Das, S. K. Behera, S. P. Das, Monitoring the fill level of a ball mill using vibration sensing and artificial neural network, Neural Computing and Applications 32 (2020) 1501–1511.

[8] M. Góralczyk, P. Krot, R. Zimroz, S. Ogonowski, Increasing energy efficiency and productivity of the comminution process in tumbling mills by indirect measurements of internal dynamics—an overview, Energies 13 (24) (2020) 6735.

[9] S. Avalos, W. Kracht, J. M. Ortiz, Machine learning and deep learning methods in mining operations: A data-driven sag mill energy consumption prediction application, Mining, Metallurgy & Exploration 37 (2020) 1197–1212.

[10] P. López, I. Reyes, N. Risso, C. Aguilera, P. G. Campos, M. Momayez, D. Contreras, Assessing machine learning and deep learning-based approaches for sag mill energy consumption, in: 2021 IEEE CHILEAN Conference on Electrical, Electronics Engineering, Information and Communication Technologies (CHILECON), IEEE, 2021, pp. 1–6.

[11] M. Saldaña, L. Ayala, J. González, Modeling the dynamic of a sag milling system through regression models and neural networks, in: Proceedings of Fourth International Conference on Inventive Material Science Applications: ICIMA 2021, Springer, 2022, pp. 281–293.

[12] Z. Yin, Y. Peng, Z. Zhu, C. Ma, Z. Yu, G. Wu, Effect of mill speed and slurry filling on the charge dynamics by an instrumented ball, Advanced Powder Technology 30 (8) (2019) 1611–1616.

[13] T. Wang, W. Zou, R. Xu, H. Xu, L. Tao, J. Zhao, Y. He, Assessing load in ball mill using instrumented grinding media, Minerals Engineering 173 (2021) 107198.

[14] B. Yari, C. Beaulieu, P. Sauriol, F. Bertrand, J. Chaouki, Size segregation of bidisperse granular mixtures in rotating drum, Powder Technology 374 (2020) 172–184. doi:https://doi.org/10.1016/j.powtec.2020.07.030.

[15] S. Yang, Y. Sun, L. Zhang, J. W. Chew, Segregation dynamics of a binary-size mixture in a three-dimensional rotating drum, Chemical Engineering Science 172 (2017) 652–666.

[16] G. Seiden, P. J. Thomas, Complexity, segregation, and pattern formation in rotating-drum flows, Reviews of Modern Physics 83 (4) (2011) 1323.

[17] P. G. Rognon, J.-N. Roux, M. Naaïm, F. Chevoir, Dense flows of bidisperse assemblies of disks down an inclined plane, Physics of Fluids 19 (5) (2007).

[18] Y. Zhou, P. Ruyer, P. Aussillous, Discharge flow of a bidisperse granular media from a silo: discrete particle simulations, Physical Review E 92 (6) (2015) 062204.

[19] S. Laudari, B. Marks, P. Rognon, Classifying grains using behaviour-informed machine learning, Scientific Reports 12 (1) (2022) 1–7.

[20] S. Laudari, B. Marks, P. Rognon, Insights on the internal dynamics of bi-disperse granular flows from machine learning, Granular Matter 25 (4) (2023) 73.

[21] O. Ben-Nun, I. Einav, A. Tordesillas, Force attractor in confined comminution of granular materials, Physical review letters 104 (10) (2010) 108001.

[22] N. S. Weerasekara, M. S. Powell, P. Cleary, L. M. Tavares, M. Evertsson, R. Morrison, J. Quist, R. Carvalho, The contribution of dem to the science of comminution, Powder technology 248 (2013) 3–24.

[23] L. F. Orozco, D.-H. Nguyen, J.-Y. Delenne, P. Sornay, F. Radjai, Discrete-element simulations of comminution in rotating drums: Effects of grinding media, Powder Technology 362 (2020) 157–167.

[24] Q. Xie, C. Zhong, D. Liu, Q. Fu, X. Wang, Z. Shen, Operation analysis of a sag mill under different conditions based on dem and breakage energy method, Energies 13 (20) (2020) 5247.

CHAPTER 7

Kinematics Sensing in Experiemental Data

This chapter details the progression of our study from theoretical simulations to the practical implementation of the kinematics-based sorting method in conditions that mimic real-world scenarios. A prevalent concern in transitioning from theoretical to practical application lies in the utility and applicability of such methods to solve real-life problems. Additionally, there is a need to corroborate the findings obtained from computerized simulations with those from empirical, practical applications. To address these concerns, our approach involves two primary strategies. Firstly, we select a dataset that closely mirrors the conditions expected in practical settings, aligning with our system's configuration. Secondly, we undertake the validation of certain assumptions and the results derived from our studies, aiming to establish their validity in practical scenarios.

7.1 Experimental Set-Up & Data Collection

To test our kinematics-based sorting method, we started by collecting data from Maranic et al. (2021) [68] experimental work. This experiment, while not an exact match for our ball mill or silo DEM simulations, provided a valuable dataset for validating our theoretical approach.

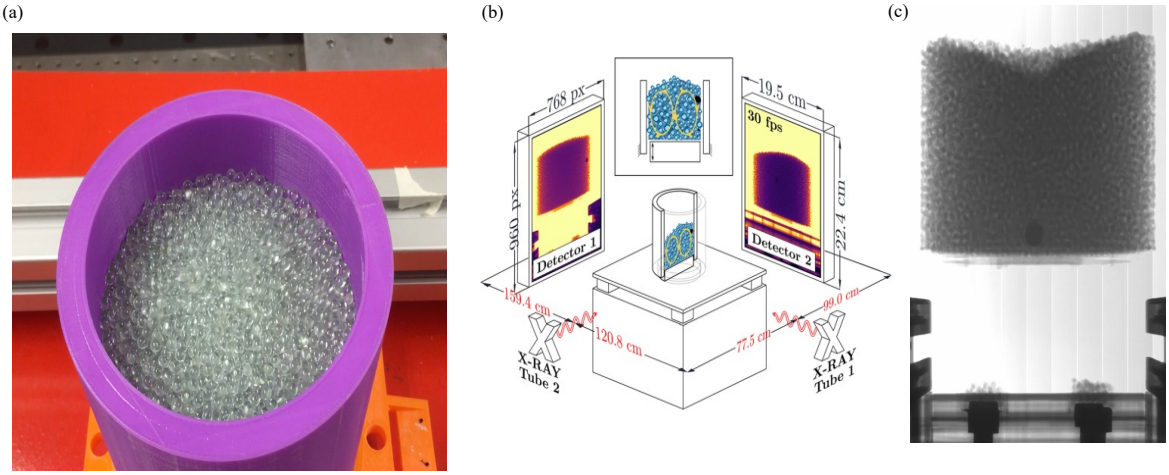

FIGURE 7.1: **A visualization of experimental setup[68]:** (a) A cylinder filled with glass beads. (b) Schematic of the experimental setup featuring two orthogonal X-ray tube/detector pairs capturing images of the granular medium, in motion due to a vibrating cylindrical piston beneath. (c) A solitary steal bead bead positioned at the base of the bead mixture while vibration is on.

In the experiment, a cylinder 100 mm in diameter was filled with glass beads up to a 60 mm height, weighing 710 grams and a steel tracer bead ranging from 2.5 mm to 8 mm in size was added into the cylinder, as shown in figure 7.1(c). The setup's spatial resolution was about 0.011 mm per pixel, giving us 273 pixels across the diameter of each tracer bead. The vibration needed for the experiment was provided by a Syntron V-50 electromagnetic vibrator operating at a frequency of 50 Hz and capable of using up to 530 W of power, strong enough to ensure the vibration effects were consistent regardless of the weight of the grains. Importantly, the vibrating stage's piston directly touched the grains but not the cylinder walls, reducing the transfer of vibrations.

In this process, we recorded the positions and velocities of steel tracer in all three dimensions, focusing on a dataset that captures the dynamics of different steel steal bead mixed with glass beads of the same size. This approach marks a departure from the proof of concept

employed in chapter 4 and chapter 6 of this thesis , where the emphasis was on small particles mixed with larger steel balls of the same size. The choice to utilize this specific dataset, despite its slight deviation from our earlier study, was driven by experimental challenges and time constraints. Nevertheless, this dataset was deemed suitable as it closely mirrors the phenomena under investigation in our current study. By incorporating this data, we aimed to bridge the gap between theoretical predictions and experimental evidence, facilitating a more effective learning process for our machine learning models based on actual experimental data. Following sections will elaborate detail view of analysis and explanation.

7.2 Analysis: Insight into Kinematics of steal bead Bead

This section delves into the kinematics of steel tracer within a granular beads, aiming to predict the size of these particles based on their velocities. By analyzing the trajectory of these particles, we leverage machine learning models to classify them into distinct size categories.

Type A	Type B	Input Features
5 mm	3 mm	Velocity (x-axis)
	4mm	Velocity (y-axis)
	8 mm	Velocity (z-axis)

TABLE 7.1: Information on steel tracers and input features. We divided the steel tracers into two groups, with the smaller size classified as Type A and the larger sizes as Type B. Velocity information was used to train the random forest model.

Initially, our analysis focuses on binary classification, where we categorize the steal bead into two size groups: 'Small' (2.5 mm) and 'Large' (3 mm, 4 mm, and 8.0 mm). Using the Random Forest algorithm, a well-established method in our prior studies, we examine the flow behavior and kinematic properties, specifically velocities in the x, y, and z directions, of these steel tracers.

This kinematic analysis reveals that at lower size ratios, the velocity differences among the particles are minimal. This finding suggests that the mixture and vibration intensity have negligible effects on particle sorting at smaller size ratios. However, as the size ratio increases,

the velocity differences become more distinct (see Figure 7.2, enhancing the machine learning model's ability to accurately determine the size of the steel tracers.

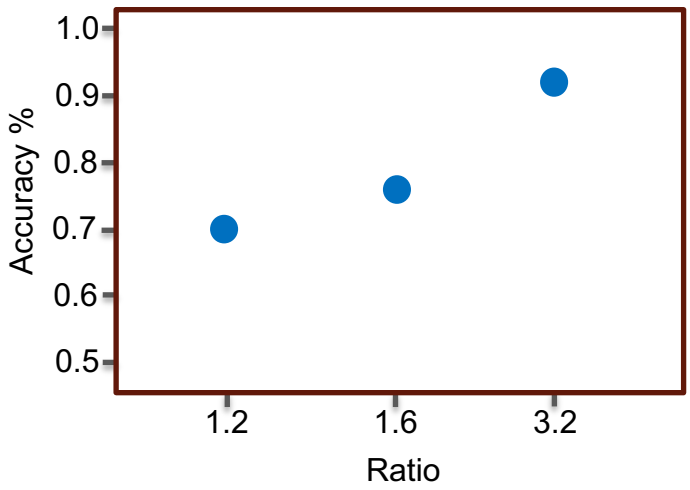

FIGURE 7.2: The graph demonstrates how sorting accuracy varies with the ratio of steel sizes, reflecting the proficiency of the kinematics-based machine learning model.

These results highlight the significant impact that both vibration and the presence of glass beads have on the flow of steal bead of varying sizes. A similar concept was explored in our Studies chapter 4 and chapter 6 where we examined the contrast in trajectories of bigger and smaller particles, and relationship between crusher ratios and particle size detection. This consistency across different binary classification tasks suggests that particle size can be predicted and categorized based on their kinematic properties. Additionally, figure 7.3 illustrates the importance of velocity components in the classification process. This explains that the variance that each features includes. In this analysis, we noticed that velocity of x axis is important during model training process however, excluding other features didn't improve the classification accuracy. This implies that, even though other features they carry out low variance, they are also important in training. Moreover, including other kinematics such as acceleration, forces may bring changes in this outcomes. Nevertheless, by understanding how velocities influence particle sorting, we can improve the accuracy and efficiency of our classification models, ultimately leading to better sorting techniques in various industrial applications.

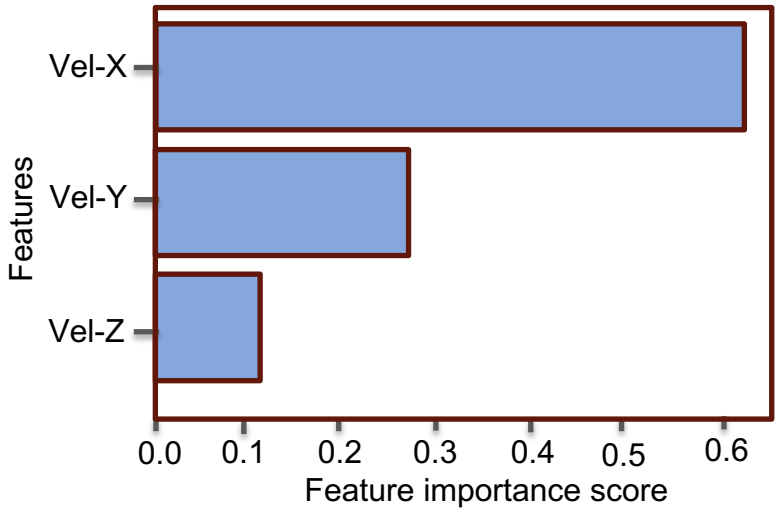

FIGURE 7.3: Feature importance scores reveal that the x-axis velocity component (Vel-X) is the most critical for classifying steal bead sizes, as opposed to y and z components (Vel-Y and Vel-Z).

In another part of our analysis, we incrementally introduce more classes during the model training process to visualize the impact of increasing complexity. Figure 7.4 illustrates how the model's performance adjusts as the number of classes increases. Importantly, our kinematic-based machine learning model demonstrates that introducing more classes reduces model accuracy. This reduction in accuracy is a consequence of the increased complexity in velocities when we add more steel tracer in training. For clear visualization, training information and size distribution are mentioned in following table.

Clas-2	Class-3	Class-4
2.5 mm	2.5 mm	2.5 mm
8 mm	3mm	3 mm
	4 mm	4 mm
		8 mm

TABLE 7.2: Binary to multi-class training information with group of steal bead sizes .

This observation is consistent with the findings from the latter part of our Study-3 (Chapter 6), where we examined the effects of complexity on model performance. The results highlight the challenge of maintaining high accuracy in the presence of increased class diversity and

underscore the importance of carefully selecting and engineering features to manage this complexity.

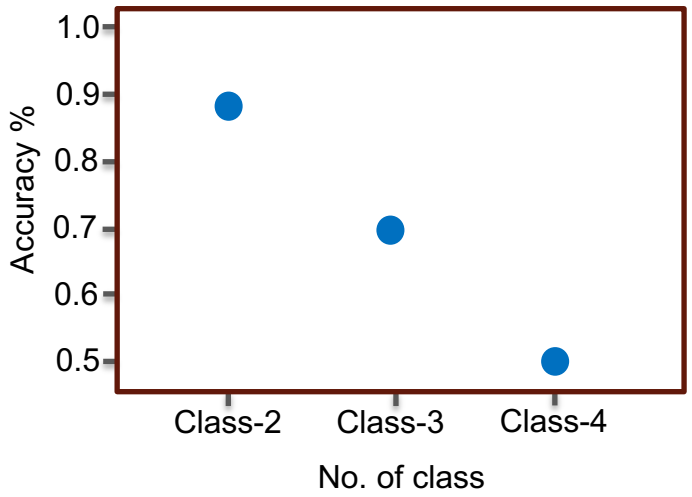

FIGURE 7.4: Complexity in classification when we increase number of classes step by step.

We also visualized the confusion matrix, depicted in Figure 7.4, to demonstrate the model's capability in accurately distinguishing various sizes of steel tracers. Observing the diagonal arrays, we achieved a higher percentage of correct predictions in binary classification, whereas the percentage reduced in multi-class classification. Despite this, it is evident that some particles are still predicted correctly more often than falsely. This reinforces the potential of our kinematic-based approach for practical sorting tasks, highlighting its applicability in scenarios that require precise size differentiation of particles based on their movement within a granular flow. The results suggest that, even as the complexity increases with more classes, our model retains a significant level of accuracy, demonstrating its robustness and effectiveness in real-world applications.

By focusing on the trajectory analysis of large particles and their classification based on velocity, this chapter aims to provide clear insights into the kinematic behavior of steel tracer and the effectiveness of machine learning models in predicting their size. Whether dealing with binary or multi-class classification, our approach emphasizes the critical role of kinematic data in enhancing the accuracy and reliability of particle sorting mechanisms. This chapter highlights how detailed velocity analysis can improve sorting processes, demonstrating that

kinematic features are invaluable for precise particle size differentiation within granular flows. Our findings reinforce the importance of integrating advanced machine learning techniques with kinematic data to develop more effective and efficient sorting systems.

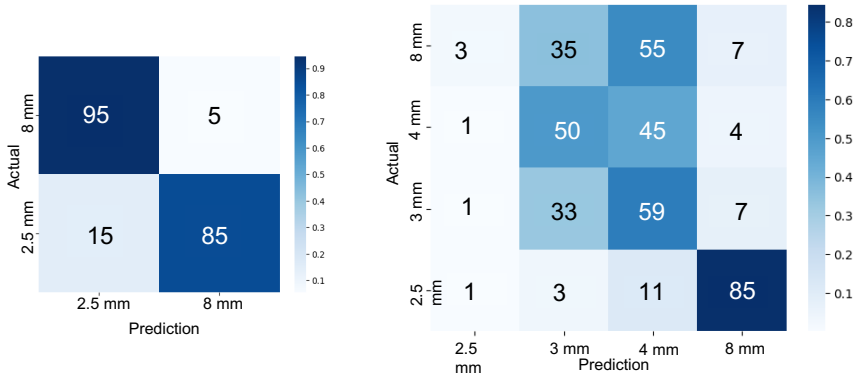

FIGURE 7.5: Confusion matrices demonstrating the performance of the machine learning model in classifying steal bead sizes. (Left) Binary classification showing high accuracy for two size classes. (Right) Multiclass classification depicting the model's predictive capability across four different size classes, with varying degrees of accuracy.

7.3 Future Outlook

This research establishes a foundational approach to particle sensing based on kinematic properties, utilizing experimental datasets to distinguish particles by their velocity characteristics and size ratios between beads and steel tracer. Our findings validate key aspects of our hypothesis, demonstrating the effectiveness of kinematic analysis in particle classification. However, several avenues for future research have emerged, highlighting opportunities to build upon and expand our current work.

Currently, our experiments rely on a relatively simplistic setup, focusing primarily on velocity-based features in a controlled environment. Future work should explore more complex and challenging experimental configurations to uncover nuanced phenomena within granular flow. For instance, incorporating three-dimensional motion tracking and introducing noise in the initial velocity vectors could provide deeper insights into particle behavior under more realistic

conditions. This would help to better understand the implications of increased dimensionality and noise on the classification accuracy and robustness of machine learning models.

Expanding the range of kinematic properties studied is another critical area for future research. In addition to velocity, analyzing acceleration, rotational velocities, and forces could offer a more comprehensive view of particle dynamics. These additional features might capture more subtle aspects of particle interactions and movements, potentially improving the model's ability to distinguish between different particle types.

Moreover, there is a clear need to generate datasets under a broader spectrum of conditions. This includes incorporating a variety of glass bead and steal bead sizes dimensions to enable a more comprehensive analysis of sorting mechanisms under varying conditions. Our current analysis primarily considers size and velocity; however, studying the effects of different shapes, densities, and surface roughness could further enhance our understanding of particle sorting.

Investigating the impact of vibration intensity on particle kinematics and sorting efficiency represents another promising area of research. Varying the intensity and frequency of vibrations could reveal how these factors influence the separation and classification of particles, providing valuable data to refine sorting techniques. Additionally, exploring the interactions between multiple particles in more complex flow environments could shed light on the collective behaviors that emerge in granular flows.

Such detailed analysis is crucial for unraveling the intricate behaviors of granular flows, contributing to the advancement of rheological studies. Ultimately, pursuing these directions could lead to significant innovations in the sorting of granular materials. By harnessing the full potential of machine learning technologies, we can refine and optimize sorting processes, leading to more efficient and accurate classification systems across various industrial applications.

Furthermore, integrating our kinematic-based approach with real-time sensing technologies could pave the way for automated sorting systems capable of adapting to dynamic conditions. This would not only enhance sorting efficiency but also reduce operational costs and improve

scalability. Collaborations with industry partners to test and implement these advanced sorting mechanisms in practical settings could accelerate the transition from theoretical research to real-world applications, driving technological advancements in particle sorting and beyond.

7.4 Summary

This chapter has traced the arc from the initial conceptual development to the empirical validation of our kinematics-based sorting method, rigorously tested against an experimental dataset. Our comprehensive approach to data collection and analysis has highlighted the transformative potential of machine learning in refining sorting processes. The effective use of ML algorithms to distinguish between steal bead based on their velocities not only demonstrates the practicality of our method but also lays a solid foundation for future research.

By meticulously analyzing the velocity characteristics and size ratios of particles, we have shown how machine learning can significantly enhance the accuracy and efficiency of sorting mechanisms. This research underscores the practicality and robustness of using kinematic properties for particle classification, providing a clear pathway for integrating these techniques into industrial applications.

Our findings validate the critical role of kinematic data in improving sorting accuracy and highlight the importance of expanding our analysis to include additional kinematic features such as acceleration and rotational velocities. This expanded approach could capture more nuanced aspects of particle behavior, leading to even more precise and reliable classification models.

Moreover, this work opens avenues for exploring more intricate experimental setups, promising significant advancements in sorting techniques applicable across a broad spectrum of industries. The insights gained from this research suggest that future studies should investigate the effects of varying experimental conditions, such as different particle shapes, densities, and surface roughness, to further refine and optimize sorting processes.

Through this work, we have established a benchmark for the integration of machine learning in kinematics-based sorting, heralding a new era of efficiency and precision in material classification. The methodologies and findings presented here set the stage for future innovations, where advanced ML techniques and detailed kinematic analyses combine to revolutionize particle sorting in various industrial contexts. By building on this foundation, future research can unlock new levels of performance and applicability, driving forward the capabilities of automated sorting systems.

CHAPTER 8

Conclusion

8.1 Conclusion

This thesis has presented a proof of concept that the kinematics of particles contain valuable information in granular flow, which can be used for detection and sorting. Initially focusing on the paths of individual particles, our research expanded to analyze the complex flow of particles of varying sizes and configurations. This provides insights for refining sorting techniques in contexts such as mineral processing, ore sorting, and many other applications. While machine learning (ML) predictions are particularly effective when segregation occurs, alternative or traditional methods could also be employed to detect different particle sizes. Traditional methods such as sieving, laser diffraction, or optical microscopy have long been established for accurately measuring particle sizes. These methods are highly reliable and provide detailed size distributions but often require manual intervention, can be time-consuming, and may not be suitable for real-time analysis. Realizing these challenges, our work introduces a novel sorting method based on the grain's kinematics, moving beyond traditional sorting criteria and challenges. This approach is especially beneficial for industries such as agriculture, pharmaceuticals, and mining, where sorting accuracy directly influences product quality and operational efficiency.

This study demonstrates that a deeper understanding of particle flow behaviors can significantly enhance sorting strategies. By analyzing these behaviors, we can effectively predict particle size and movements, laying the groundwork for more efficient sorting methodologies. This analysis highlights the intricate influence of kinematics on flow dynamics, offering valuable insights into particle segregation, sorting, and mixing. Importantly, our findings not

only refine existing sorting technologies but also open avenues for creating more sophisticated sorting solutions. Moreover, the results of this thesis can be extrapolated to broader real-world applications, which involve several considerations, such as assumptions, applications, and industrial sorting techniques. Additionally, in real-world processes and experiments, we can receive different types of data, including information on particles. This data is significantly large and complex, requiring a novel approach to gain insights. These insights can be fed into machine learning models developed in this study to classify particle properties and predict system behavior based on the observed data, optimizing industrial processes by improving particle sorting, predicting flow behavior, and preventing blockages in particle flow systems such as silos, thereby enhancing efficiency and reducing operational costs.

This work not only visualizes the potential of kinematics based approach in sorting task, it also gives an insightful exploration of granular flow including model sensitivity. For instance, we observed that the prediction accuracy for stiffness seemed to saturate at a value lower than 0.9. This may be attributed to the particles' behavior at lower stiffness and surface impact which is not sufficient to detect contrast in their trajectories. Similarly, isolating important features. In chapter-5, observing 'z' is an important feature, we found that the feature 'z' alone cannot provide better accuracy, and utilizing 'a' and 'z' together also showed a poor classification accuracy. Moreover, it highlights the recording frequency which plays a significant role in capturing the dynamics of different flow regimes. Realizing that, for dense flow regimes, lower frequencies (like 10 Hz for bigger particles) might be sufficient due to slower particle movements. However, detailed interactions might need higher frequencies, thus we decided to use 100 Hz. In gaseous flow regimes, higher frequencies (like 100 Hz for smaller particles) are essential to capture rapid dynamics. For intermediate flow regimes, a balanced approach is required, and sensitivity analysis can help determine the optimal frequency which was easily able to established the proof of concepts.

Although our approach shows significantly better performance and highlights the potential for developing new sorting methods, we also recognize its limitations. Managing different environmental conditions to extend the applicability of our approach to diverse industrial scenarios remains a critical challenge. Investigating the effects of various ambient conditions,

such as temperature, humidity, and varying particle concentrations, could provide more complex information that is difficult to measure, leading to challenges in different applications. Additionally, the resolution and sensitivity of existing in situ measurements of particle properties vary depending on the specific technology and method used. High-resolution techniques can achieve spatial resolutions down to a few micrometers or even nanometers. Sensitivity, which determines the smallest detectable change in particle properties, can also be highly precise, detecting minute variations in parameters such as size, velocity, and composition. Advanced imaging and sensing technologies, such as high-speed cameras, laser diffraction, and accelerometers, contribute to these capabilities, allowing for detailed and accurate characterization of particle properties in real-time, but also bringing challenges in analysis, especially in our approach. Currently, our approach relies on Discrete Element Method (DEM) simulations and small glass bead experiments. This also has certain limitations, as exploring different types of grains or irregular sizes remains unaddressed. We believe that the results would be affected by changing grain types due to their distinct flow dynamics. Additionally, measuring grain kinematics can be challenging and costly, which may render our methodology less suitable for some sorting applications.

Further exploration beyond our current assumptions, such as examining density ratios greater than 2, is necessary. The kinematic features derived from trajectories might not sufficiently capture the subtle differences caused by density variations, especially in the absence of a fluid medium where density differences would more prominently affect motion. While our approach shows promise, it is important to recognize its limitations. The current methodology primarily focuses on particles of specific sizes and materials, raising questions about its applicability to a broader range of particle types, including very small, soft, or highly deformable materials like bubbles or cells. Future research should address these limitations by testing the approach on a wider variety of particle types to evaluate its generalizability. Similarly, we conducted sequential analysis with particle sizes r_S and r_T to simplify the modeling process. We acknowledge that this approach may not fully capture the gradual transition of particle sizes in the transient regime. Addressing these in future studies could provide a more comprehensive understanding of particle dynamics and improve the robustness of the sorting methodology. Nevertheless, our main aim of this research is to search for a novel approach and establish a

proof of concept, successfully highlighting the potential of kinematics-based classification methods.

In our work, we demonstrated that particle properties can be inferred from their kinematics. This finding opens up many future research opportunities. One important direction is to collect more data and include additional features such as energy dissipation, particle deformation, interaction frequencies, and temperature including air-flow rate especially in drum. These additional features could greatly enhance the accuracy and robustness of our machine learning models.

Incorporating 3D motion and noise on initial velocity vectors would increase the complexity of the problem, requiring more sophisticated data collection and computational resources. However, this could ultimately lead to more accurate and robust classification of granular materials. Changing the configuration or dropping multiple particles simultaneously could further complicate the classification process, as trajectories will be influenced by more contacts. Future work should consider the impact of particle interactions on classification accuracy and explore ways to mitigate these effects. Similarly, the effect of density on classification accuracy was studied up to a rate of two. Our analysis indicated that higher density ratios might continue to exhibit poor classification performance. This suggests a need for more sophisticated feature extraction and data enrichment techniques to improve the accuracy and robustness of the classification models. This can be explore in future work.

To experimentally deduce forces in a granular system, sensors such as force plates or load cells integrated into the experimental apparatus (e.g., the base or walls of a silo) can be used. These sensors measure the forces exerted by the granular material. High-speed cameras and particle tracking software can capture particle motion, from which forces can be inferred using kinematic data and equations of motion. Additionally, accelerometers embedded within particles can provide direct measurements of forces, enriching the dataset and enhancing the robustness of the machine learning models and current approach can be used to analyze such dataset. Another crucial step is to create a comprehensive database that captures all types of variability. By using sensitivity analysis methods and other statistical techniques, we can make sure this database accurately represents real-world conditions. Developing new features

and labels that capture subtle differences in particle behavior will be essential for improving sorting algorithms.

Future work should also delve into integrating these algorithms with real-time monitoring systems, potentially revolutionizing sorting techniques by enabling machines to adapt to variations in particle flow on-the-fly, optimizing the sorting process for various materials without human intervention. Expanding the scope of kinematic properties analysis could uncover more nuanced relationships between particle dynamics and other factors, such as shape, resilience, and even chemical composition. This could lead to the development of multi-parameter sorting systems that are not only based on kinematics but also on a comprehensive profile of each particle, significantly enhancing the purity of sorted materials and leading to higher-quality end products.

Extrapolating the results of this study to practical applications requires careful consideration. While the kinematic-based approach shows potential, its implementation in real-world sorting systems must account for the complexities and variabilities of industrial environments. Exploring the use of deep learning algorithms, such as Convolutional Neural Networks (CNNs), could offer new avenues for enhancing sorting accuracy and efficiency by leveraging their ability to handle complex, high-dimensional data. CNNs are more robust to noise and can manage larger datasets, making them suitable for real-world applications, including image analysis.

In contrast to traditional methods, our approach leverages the nuanced kinematic properties of particles to enhance sorting accuracy and efficiency. While conventional techniques rely on easily measurable attributes such as size and color, our method delves deeper into the dynamic behavior of particles. This allows for the identification and classification of particles in more complex and variable environments. By addressing the limitations and exploring the proposed future directions, this research holds the potential to significantly advance the field of particle sorting, contributing to more efficient and precise industrial processes.

Bibliography

[1] *Research update: A new model accurately predicts three-dimensional sand flow — news.mit.edu*. https://news.mit.edu/2013/research-update-sand-modeling-0325. [Accessed 29-02-2024].

[2] FT Portmann, S Siebert, and P Döll. "MIRCA2000—Global monthly irrigated and rainfed crop areas around the year 2000: A new high-resolution data set for agricultural and hydrological modeling". In: *Global biogeochemical cycles* 24.1 (2010).

[3] M Meenu et al. "New Insights into Recent Trends and Emerging Technologies in Apple Sorting". In: *ACS Food Science & Technology* (2024).

[4] NE Sever et al. "Process analytical technology in solid dosage development and manufacturing". In: *Developing Solid Oral Dosage Forms*. Elsevier, 2009, pp. 827–841.

[5] C Robben and H Wotruba. "Sensor-based ore sorting technology in mining—past, present and future". In: *Minerals* 9.9 (2019), p. 523.

[6] C Robben et al. "X-ray-transmission based ore sorting at the San Rafael tin mine". In: *Minerals Engineering* 145 (2020), p. 105870.

[7] J Duran. *Sands, powders, and grains: an introduction to the physics of granular materials*. Springer Science & Business Media, 2012.

[8] DG Bucknall. "Plastics as a materials system in a circular economy". In: *Philosophical Transactions of the Royal Society A* 378.2176 (2020), p. 20190268.

[9] B Sharma et al. "Recycling of organic wastes in agriculture: an environmental perspective". In: *International journal of environmental research* 13 (2019), pp. 409–429.

[10] M Colledani et al. "Design and management of manufacturing systems for production quality". In: *Cirp Annals* 63.2 (2014), pp. 773–796.

[11] JW Vallance and SB Savage. “Particle segregation in granular flows down chutes”. In: *IUTAM Symposium on Segregation in Granular Flows: Proceedings of the IUTAM Symposium held in Cape May, NJ, USA June 5–10, 1999*. Springer. 2000, pp. 31–51.

[12] S Messal et al. “Sorting of finely-grinded granular mixtures using a belt-type corona-electrostatic separator”. In: *2015 IEEE Industry Applications Society Annual Meeting*. IEEE. 2015, pp. 1–5.

[13] C Pieper et al. “Numerical modelling of an optical belt sorter using a DEM–CFD approach coupled with particle tracking and comparison with experiments”. In: *Powder Technology* 340 (2018), pp. 181–193.

[14] Z Deng et al. “Continuum modelling of segregating tridisperse granular chute flow”. In: *Proceedings of the Royal Society A: Mathematical, Physical and Engineering Sciences* 474.2211 (2018), p. 20170384.

[15] V Dolgunin, A Kudy, and A Ukolov. “Development of the model of segregation of particles undergoing granular flow down an inclined chute”. In: *Powder technology* 96.3 (1998), pp. 211–218.

[16] E Alméras et al. “Statistics of velocity fluctuations in a homogeneous liquid fluidized bed”. In: *Physical Review Fluids* 6.3 (2021), p. 034301.

[17] S Balasubramanian, S Voropayev, and H Fernando. “Grain sorting and decay of sand ripples under oscillatory flow and turbulence”. In: *Journal of Turbulence* 9 (2008), N17.

[18] JM Ottino and DV Khakhar. “Mixing and segregation of granular materials”. In: *Annual review of fluid mechanics* 32.1 (2000), pp. 55–91.

[19] T Andersson. “Estimating particle size distributions based on machine vision”. PhD thesis. Luleå tekniska universitet, 2010.

[20] M Moaveni et al. “Machine vision based characterization of particle shape and asphalt coating in Reclaimed Asphalt Pavement”. In: *Transportation Geotechnics* 6 (2016), pp. 26–37.

[21] NS Visen. “Machine vision based grain handling system”. In: (2002).

[22] J Torres-Serra, A Rodrıguez-Ferran, and E Romero. “Classification of granular materials via flowability-based clustering with application to bulk feeding”. In: *Powder technology* 378 (2021), pp. 288–302.

[23] Z Liao et al. “Image-based prediction of granular flow behaviors in a wedge-shaped hopper by combing DEM and deep learning methods”. In: *Powder Technology* 383 (2021), pp. 159–166.

[24] AS Baumgarten and K Kamrin. “A general fluid–sediment mixture model and constitutive theory validated in many flow regimes”. In: *Journal of Fluid Mechanics* 861 (2019), pp. 721–764.

[25] R Delannay et al. “Granular and particle-laden flows: from laboratory experiments to field observations”. In: *Journal of Physics D: Applied Physics* 50.5 (2017), p. 053001.

[26] GM gdrmidi@ polytech. univ-mrs. fr http://www. lmgc. univ-montp2. fr/MIDI/. “On dense granular flows”. In: *The European Physical Journal E* 14 (2004), pp. 341–365.

[27] Y Forterre and O Pouliquen. “Granular flows”. In: *Glasses and Grains: Poincaré Seminar 2009*. Springer. 2011, pp. 77–109.

[28] PA Cundall and OD Strack. “A discrete numerical model for granular assemblies”. In: *geotechnique* 29.1 (1979), pp. 47–65.

[29] P Cleary. “Discrete element modelling of industrial granular flow applications”. In: *TASK Quarterly. Scientific Bulletin of Academic Computer Centre in Gdansk* 2.3 (1998), pp. 385–415.

[30] O Pouliquen. “Scaling laws in granular flows down rough inclined planes”. In: *Physics of fluids* 11.3 (1999), pp. 542–548.

[31] B Andreotti, Y Forterre, and O Pouliquen. *Granular media: between fluid and solid*. Cambridge University Press, 2013.

[32] MJ Jiang, HS Yu, and D Harris. “A novel discrete model for granular material incorporating rolling resistance”. In: *Computers and Geotechnics* 32.5 (2005), pp. 340–357.

[33] KM Hill, G Gioia, and VV Tota. “Structure and kinematics in dense free-surface granular flow”. In: *Physical Review Letters* 91.6 (2003), p. 064302.

[34] CS Campbell. “Granular material flows–an overview”. In: *Powder Technology* 162.3 (2006), pp. 208–229.

[35] JMNT Gray. “Particle segregation in dense granular flows”. In: *Annual review of fluid mechanics* 50 (2018), pp. 407–433.

[36] O Dubé et al. “Dynamics of non-spherical particles in a rotating drum”. In: *Chemical Engineering Science* 101 (2013), pp. 486–502.

[37] RP Behringer and B Chakraborty. “The physics of jamming for granular materials: a review”. In: *Reports on Progress in Physics* 82.1 (2018), p. 012601.

[38] P Sajeesh and AK Sen. “Particle separation and sorting in microfluidic devices: a review”. In: *Microfluidics and nanofluidics* 17 (2014), pp. 1–52.

[39] A Kudrolli. “Size separation in vibrated granular matter”. In: *Reports on progress in physics* 67.3 (2004), p. 209.

[40] T Mulder and J Alexander. “The physical character of subaqueous sedimentary density flows and their deposits”. In: *Sedimentology* 48.2 (2001), pp. 269–299.

[41] WD Fullmer and CM Hrenya. “The clustering instability in rapid granular and gas-solid flows”. In: *Annual Review of Fluid Mechanics* 49 (2017), pp. 485–510.

[42] E Opsomer et al. “Clustering and segregation in driven granular fluids”. In: *The European Physical Journal E* 37 (2014), pp. 1–6.

[43] D Puzyrev et al. “Machine learning for 3D particle tracking in granular gases”. In: *Microgravity Science and Technology* 32 (2020), pp. 897–906.

[44] GI Tardos, S McNamara, and I Talu. “Slow and intermediate flow of a frictional bulk powder in the Couette geometry”. In: *Powder Technology* 131.1 (2003), pp. 23–39.

[45] Z Zhou et al. “A new set of scaling relationships for DEM-CFD simulations of fluid–solid coupling problems in saturated and cohesiveless granular soils”. In: *Computational Particle Mechanics* 6 (2019), pp. 657–669.

[46] Y Forterre and O Pouliquen. “Flows of dense granular media”. In: *Annu. Rev. Fluid Mech.* 40 (2008), pp. 1–24.

[47] JH van der Linden, GA Narsilio, and A Tordesillas. “Machine learning framework for analysis of transport through complex networks in porous, granular media: A focus on permeability”. In: *Physical Review E* 94.2 (2016), p. 022904.

[48] R Stevens et al. *Ai for science: Report on the department of energy (doe) town halls on artificial intelligence (ai) for science*. Tech. rep. Argonne National Lab.(ANL), Argonne, IL (United States), 2020.

[49] E Kolb, P Cixous, and J Charmet. “Flow fields around an intruder immersed in a 2D dense granular layer”. In: *Granular Matter* 16.2 (2014), pp. 223–233.

[50] ME Larsen et al. “Using science to sell apps: evaluation of mental health app store quality claims”. In: *NPJ digital medicine* 2.1 (2019), p. 18.

[51] R Jaza et al. “Lessons learned using machine learning to link third body particles morphology to interface rheology”. In: *Tribology international* 153 (2021), p. 106630.

[52] NE Jackson, MA Webb, and JJ de Pablo. “Recent advances in machine learning towards multiscale soft materials design”. In: *Current Opinion in Chemical Engineering* 23 (2019), pp. 106–114.

[53] DV Voronin et al. “Detection of rare objects by flow cytometry: imaging, cell sorting, and deep learning approaches”. In: *International journal of molecular sciences* 21.7 (2020), p. 2323.

[54] T Peršak et al. “Vision-based sorting systems for transparent plastic granulate”. In: *Applied Sciences* 10.12 (2020), p. 4269.

[55] G Maier et al. “Motion-based material characterization in sensor-based sorting”. In: *tm-Technisches Messen* 85.3 (2018), pp. 202–210.

[56] S Maheswaran et al. “Development of machine learning based grain classification and sorting with machine vision approach for eco-friendly environment”. In: *Journal of Green Engineering* 10.3 (2020), pp. 526–543.

[57] M Erkinay Ozdemir et al. “Applying machine learning approach in recycling”. In: *Journal of Material Cycles and Waste Management* 23 (2021), pp. 855–871.

[58] TU Rehman et al. “Current and future applications of statistical machine learning algorithms for agricultural machine vision systems”. In: *Computers and electronics in agriculture* 156 (2019), pp. 585–605.

[59] JT McCoy and L Auret. “Machine learning applications in minerals processing: A review”. In: *Minerals Engineering* 132 (2019), pp. 95–109.

[60] AK Janakiraman, K Khanna, and S Ramkanth. “Role of Machine Learning in Automated Detection and Sorting of Pharmaceutical Formulations”. In: *Artificial intelligence in Pharmaceutical Sciences*. CRC Press, 2023, pp. 96–116.

[61] V Singh and SM Rao. “Application of image processing and radial basis neural network techniques for ore sorting and ore classification”. In: *Minerals Engineering* 18.15 (2005), pp. 1412–1420.

[62] D Wu et al. “Application of image texture for the sorting of tea categories using multi-spectral imaging technique and support vector machine”. In: *Journal of food engineering* 88.4 (2008), pp. 474–483.

[63] Z Xie, X Gu, and Y Shen. “A machine learning study of predicting mixing and segregation behaviors in a bidisperse solid–liquid fluidized bed”. In: *Industrial & Engineering Chemistry Research* 61.24 (2022), pp. 8551–8565.

[64] D Xu and Y Shen. “An improved machine learning approach for predicting granular flows”. In: *Chemical Engineering Journal* 450 (2022), p. 138036.

[65] C Kloss et al. “Models, algorithms and validation for opensource DEM and CFD–DEM”. In: *Progress in Computational Fluid Dynamics, an International Journal* 12.2-3 (2012), pp. 140–152.

[66] H Abdi and LJ Williams. “Principal component analysis”. In: *Wiley interdisciplinary reviews: computational statistics* 2.4 (2010), pp. 433–459.

[67] G Ma et al. “Role of particle crushing on particle kinematics and shear banding in granular materials”. In: *Acta Geotechnica* 13 (2018), pp. 601–618.

[68] Z Maranic et al. “A granular thermometer”. In: *Granular Matter* 23 (2021), pp. 1–15.

Appendices

1 Appendix

1.1 DEM Script

Below is a sample of our Discrete Element Method (DEM) script. In our study, we simulated particles in three different system configurations. The script presented here specifically pertains to the rotating drum simulation.

```
####Header for General commands#######################

atom_style granular      # Simulation of particles

boundary f p f           # fixed boundaries -> particles
   will be deleted if leaving the simulation box x, y, z

units si

communicate single vel yes  # default

newton off              # default



######################System variables###########

# Definition of boundaries
variable xmin equal -0.3
variable xmax equal  0.3

variable ymin equal -0.6
variable ymax equal  0.6

variable zmin equal -0.6
variable zmax equal  0.6
```

```
# Definition of the timestep

variable dt equal 0.000001     # timestep = 0.0001 second;
   Each iteration step represents 0.0001 seconds.


############Specific variables for current simulation
   #########

variable natoms equal 2   # 1 -> particle #2->drum parts

#### Variable for material properties ####

#### Young Modulus ####
variable youngmodulus1 equal 5e8  # N/mm
variable youngmodulus2 equal 5e8  # N/mm

#### Poisson ratio ####
variable poission1 equal 0.3
variable poission2 equal 0.3

#### Variable for contact properties ####

#### Coefficient of restitution ####
variable CoR11 equal 0.6
variable CoR12 equal 0.6
variable CoR21 equal 0.6
variable CoR22 equal 0.6

#### Sliding friction coefficient ####
```

```
variable sf11 equal 0.3
variable sf12 equal 0.3
variable sf21 equal 0.3
variable sf22 equal 0.0

#### Rolling friction coefficient ####
variable rf11 equal 0.6
variable rf12 equal 0.6
variable rf21 equal 0.6
variable rf22 equal 0.6


#### Variable for particle ####

variable radius_large equal  0.05   # m diameter = 10 cm,
   radius = 5 cm,    0.05m
variable radius_small1 equal 0.015  # m diameter = 3 cm,
   radius = 1.5 cm,   0.015m
variable radius_small2 equal 0.012  # m diameter = 2.4 cm,
   radius = 1.2 cm, 0.012m
variable radius_small3 equal 0.009  # m diameter = 1.8 cm,
   radius = 0.9 cm, 0.009m
variable radius_small4 equal 0.005  # m diameter = 1.0 cm,
   radius = 0.5 cm, 0.005m


variable frac_large equal 0.5       # 50%
variable frac_small1 equal 0.125    # 12.5%
variable frac_small2 equal 0.125    # 12.5%
variable frac_small3 equal 0.125    # 12.5%
variable frac_small4 equal 0.125    # 12.5%
```

```
variable density_large equal 7800   # kg/m   for large
   particles
variable density_small equal 2500   # kg/m   for small
   particles

#### Filling parameters ####

variable filltime equal 10      # seconds  # filltime to
   generate the particles

variable fillmass equal 80      # kg      # total mass of
   bulk material

variable fillmassrate equal ${fillmass}/${filltime}  # kg/s
    # mass rate for the particle generation

variable fillsteps equal ${filltime}/${dt}   # Transform
   time to iteration steps

variable rotatime equal 40      # seconds      # rotatime:
   how long will the drum rotate

variable rotasteps equal ${rotatime}/${dt}    # Transform
   time to iteration steps



#### Screw velocities ####

variable drumPeriod equal 4 # s  # Period of the drum
   rotation (time for 1 rotation)
```

```
###############Definition of simulation box#######

region reg block ${xmin} ${xmax} ${ymin} ${ymax} ${zmin} ${
   zmax} units box

create_box 2 reg

neighbor 0.004 bin     # default
neigh_modify every 1 check yes

neigh_modify delay 0      # default

################Definition of the contact models###########

pair_style gran model hertz tangential history
   tangential_damping on limitForce off

pair_coeff * *       # default

timestep ${dt}

fix integrator all nve/sphere      # default

fix gravi all gravity 9.81 vector 0.0 0.0 -1.0    # gravity
   of 9.81 m/s   in negative z direction

##################Definition of Material properties
   ################
fix m1 all property/global youngsModulus peratomtype ${
   youngmodulus1} ${youngmodulus2}
```

```
fix m2 all property/global poissonsRatio peratomtype ${
   poission1} ${poission2}

fix m3 all property/global coefficientRestitution
   peratomtypepair ${natoms} 0.6 0.6 0.6 0.6

fix m4 all property/global coefficientFriction
   peratomtypepair ${natoms} ${sf11} ${sf12} ${sf21} ${sf22}

fix m5 all property/global coefficientRollingFriction
   peratomtypepair ${natoms} ${rf11} ${rf12} ${rf21} ${rf22}


#######Generation and Loading of the Geometry .stl
   ##############
fix Drum  all mesh/surface file meshes/Drum.stl type 2   #
   Load Drum
fix Front all mesh/surface file meshes/Front.stl type 2  #
   Load Front face of the drum
fix Back  all mesh/surface file meshes/Back.stl type 2   #
   Load Back face of the drum

fix walls all wall/gran model hertz tangential history
   rolling_friction epsd2 mesh n_meshes 3 meshes Drum Front
   Back


#########Generation and Insertion of the particles
   ############
```

```
fix pts1 all particletemplate/sphere 49979693 atom_type 1
   density constant ${density_large} radius constant ${
   radius_large}
fix pts2 all particletemplate/sphere 15485863 atom_type 2
   density constant ${density_small} radius constant ${
   radius_small1}
fix pts3 all particletemplate/sphere 15485867 atom_type 2
   density constant ${density_small} radius constant ${
   radius_small2}
fix pts4 all particletemplate/sphere 32452843 atom_type 2
   density constant ${density_small} radius constant ${
   radius_small3}
fix pts5 all particletemplate/sphere 32452867 atom_type 2
   density constant ${density_small} radius constant ${
   radius_small4}

fix pdd1 all particledistribution/discrete 86028157 5 pts1 $
   {frac_large} pts2 ${frac_small1} pts3 ${frac_small2} pts4
    ${frac_small3} pts5 ${frac_small4}

fix ins_mesh all mesh/surface/planar file meshes/
   Insertionsface.stl type 1 scale 0.9

fix ins all insert/stream seed 67867979 distributiontemplate
    pdd1 &
        mass ${fillmass} massrate ${fillmassrate}
           overlapcheck yes all_in yes vel constant 0 0 -0.7
            &
        insertion_face ins_mesh extrude_length 0.2
```

```
########Dumping of the data for post-processing to visualize
   ########

shell mkdir post

# Definition of the dumptime

variable dumptime equal 0.05  # Every 0.05 s 1 image

variable dumpstep equal ${dumptime}/${dt}  # Transform time
   to iteration steps

# ======= ID ==========
variable nom string SAG012
# =====================

compute cout all pair/gran/local id force
compute cwall all wall/gran/local id force
dump dmpfrc all local 5000 particles/dump.force_*.liggghts
   c_cout[1] c_cout[2] c_cout[3] c_cout[4] c_cout[5] c_cout
   [6]
dump dmpfrcw all local 5000 wall/dump.wall_*.liggghts
   c_cwall[1] c_cwall[2] c_cwall[3] c_cwall[4] c_cwall[5]
   c_cwall[6]

dump dmpparticle all custom ${dumpstep} post/particles_*.
   liggghts id type x y z vx vy vz fx fy fz radius mass

dump dmpDrum all mesh/stl ${dumpstep} post/Drum*.stl Drum
      # dump Drum
dump dmpFront all mesh/stl ${dumpstep} post/Front*.stl Front
     # dump Front face
```

```
# dump dmpBack all mesh/stl ${dumpstep} post/Back*.stl  Back
       # dump Back face

variable acc atom sqrt(fx*fx+fy*fy+fz*fz)/mass
variable mv atom sqrt(vx*vx+vy*vy+vz*vz)
variable ke atom (mass*v_mv*v_mv)/2

dump dmp all custom/vtk 5000 post/chute_*.vtk id type type x
    y z ix iy iz vx vy vz fx fy fz omegax omegay omegaz
   v_acc mass radius v_mv v_ke

dump dumpstress all mesh/gran/VTK 5000 post/mesh_*.vtk
   stress wear
dump dmp0 all custom 5000 all/dump*.data id type x y z vx vy
    vz fx fy fz omegax omegay omegaz v_acc mass radius v_mv
   v_ke

fix ts_check all check/timestep/gran 5000 0.1 0.1
thermo_style custom step cpu atoms ke f_ts_check[1]
   f_ts_check[2] # f_ressort # ke
thermo 5000

######RUN the simulation filling and rotation#####
run ${fillsteps}
# run 1000000 upto

unfix ins

run ${fillsteps}

# run 7000000 upto
```

```
fix MoveDrum all move/mesh mesh Drum rotate origin 0 0 0
   axis 1. 0. 0. period  ${drumPeriod}   # Rotation of drum
fix MoveFront all move/mesh mesh Front rotate origin 0 0 0
   axis 1. 0. 0. period  ${drumPeriod}  # Rotation of front
   face
fix MoveBack all move/mesh mesh Back rotate origin 0 0 0
   axis 1. 0. 0. period  ${drumPeriod}   # Rotation of back
   face

run ${rotasteps}
```

1.2 Raw Data

Below is a sample of the raw data obtained after the simulation. Various variables were recorded for each particle at each timestep, including:

- **ATOMS:** id, type, x, y, z
- **Velocity components:** vx, vy, vz
- **Force components:** fx, fy, fz
- **Angular velocity:** omegax, omegay, omegaz
- **Additional variables:** v_acc, mass, radius, v_mv, v_ke

```
ITEM: TIMESTEP
5000
ITEM: NUMBER OF ATOMS
280
ITEM: BOX BOUNDS ff pp ff
-0.3 0.3
-0.6 0.6
-0.6 0.6
```

```
ITEM: ATOMS id type x y z vx vy vz fx fy fz omegax omegay
    omegaz v_acc mass radius v_mv v_ke
184 2 -0.0778772 -0.38891 0.00901387 0 -0 -0.7 0 0 0 0 0
   0 0 0.001309 0.005 0.7 0.000320704
273 2 -0.0170976 -0.373882 0.0229552 0 -0 -0.7 0 0 0 0 0
   0 0 0.001309 0.005 0.7 0.000320704
56 2 0.036779 -0.367034 0.0103949 0 -0 -0.7 0 0 0 0 0 0 0
    0.00763407 0.009 0.7 0.00187035
249 2 -0.0849144 -0.316865 0.0206543 0 -0 -0.7 0 0 0 0 0
   0 0 0.001309 0.005 0.7 0.000320704
12 2 -0.0522647 -0.333175 0.0199386 0 -0 -0.7 0 0 0 0 0 0
    0 0.0180956 0.012 0.7 0.00443342
51 2 -0.0720946 -0.326191 0.00767189 0 -0 -0.7 0 0 0 0 0
   0 0 0.00763407 0.009 0.7 0.00187035
269 2 0.0332578 -0.33816 0.00430453 0 -0 -0.7 0 0 0 0 0 0
    0 0.001309 0.005 0.7 0.000320704
215 2 0.0804706 -0.215071 0.00895304 0 -0 -0.7 0 0 0 0 0
   0 0 0.001309 0.005 0.7 0.000320704
272 2 0.0654333 -0.187984 0.0193755 0 -0 -0.7 0 0 0 0 0 0
    0 0.001309 0.005 0.7 0.000320704
74 2 -0.0399138 -0.145723 0.00923911 0 -0 -0.7 0 0 0 0 0
   0 0 0.001309 0.005 0.7 0.000320704
118 2 -0.0453649 -0.15669 0.0243243 0 -0 -0.7 0 0 0 0 0 0
    0 0.001309 0.005 0.7 0.000320704
199 2 0.0217286 -0.149216 0.00596309 0 -0 -0.7 0 0 0 0 0
   0 0 0.001309 0.005 0.7 0.000320704
201 2 0.0183066 -0.0986949 0.0239566 0 -0 -0.7 0 0 0 0 0
   0 0 0.001309 0.005 0.7 0.000320704
267 2 -0.0535696 -0.0760479 0.00517463 0 -0 -0.7 0 0 0 0
   0 0 0 0.001309 0.005 0.7 0.000320704
```

```
88 2 -0.0272239 -0.0388352 0.0127186 0 -0 -0.7 0 0 0 0 0
   0 0 0.001309 0.005 0.7 0.000320704
155 2 0.0598325 0.0130406 0.0185116 0 -0 -0.7 0 0 0 0 0 0
    0 0.001309 0.005 0.7 0.000320704
96 2 -0.0622675 0.045717 0.00812402 0 -0 -0.7 0 0 0 0 0 0
    0 0.001309 0.005 0.7 0.000320704
171 2 0.0370608 0.0554849 0.0176338 0 -0 -0.7 0 0 0 0 0 0
    0 0.001309 0.005 0.7 0.000320704
177 2 0.0378419 0.0458967 0.00868376 0 -0 -0.7 0 0 0 0 0
   0 0 0.001309 0.005 0.7 0.000320704
235 2 -0.0784085 0.162141 0.0242486 0 -0 -0.7 0 0 0 0 0 0
    0 0.001309 0.005 0.7 0.000320704
202 2 0.0266117 0.182016 0.0171058 0 -0 -0.7 0 0 0 0 0 0
   0 0.001309 0.005 0.7 0.000320704
165 2 0.0706301 0.230571 0.0104481 0 -0 -0.7 0 0 0 0 0 0
   0 0.001309 0.005 0.7 0.000320704
99 2 -0.0508104 0.252652 0.0201293 0 -0 -0.7 0 0 0 0 0 0
   0 0.001309 0.005 0.7 0.000320704
105 2 -0.0804017 0.258348 0.0207142 0 -0 -0.7 0 0 0 0 0 0
    0 0.001309 0.005 0.7 0.000320704
94 2 0.0563641 0.238168 0.0165982 0 -0 -0.7 0 0 0 0 0 0 0
    0.001309 0.005 0.7 0.000320704
42 2 -0.00587318 0.352314 0.0168493 0 -0 -0.7 0 0 0 0 0 0
    0 0.00763407 0.009 0.7 0.00187035
264 2 0.07234 0.404545 0.0130508 0 -0 -0.7 0 0 0 0 0 0 0
   0.001309 0.005 0.7 0.000320704
98 2 -0.0425603 -0.39721 0.0693307 0 -0 -0.7 0 0 0 0 0 0
   0 0.001309 0.005 0.7 0.000320704
111 2 -0.0229596 -0.400302 0.0353995 0 -0 -0.7 0 0 0 0 0
   0 0 0.001309 0.005 0.7 0.000320704
```

```
183 2 -0.0145826 -0.411856 0.0412822 0 -0 -0.7 0 0 0 0 0
   0 0 0.001309 0.005 0.7 0.000320704
143 2 -0.000617021 -0.354234 0.0401918 0 -0 -0.7 0 0 0 0
   0 0 0 0.001309 0.005 0.7 0.000320704
175 2 -0.0109397 -0.38186 0.0720515 0 -0 -0.7 0 0 0 0 0 0
    0 0.001309 0.005 0.7 0.000320704
```

1.3 Preprocessed Data

Below is a sample of the preprocessed data using Python, provided in TXT format. In this data, particle types were extracted as radius, and the remaining columns represent the information of each particle from each timestep. The information recorded depends on the desired kinematic properties.

For training, we used CSV file format for convenience.

```
radius  TIMESTEP-25000000   TIMESTEP-25005000   TIMESTEP
   -25010000       TIMESTEP-25015000       TIMESTEP
   -25020000
0.05    1.8403              2.47424
   1.89594                 11.6628
   12.8212
0.05    6.46278             4.62542
   4.06144                 8.73072
   2.39066
0.05    5.9569              7.41621
   4.82455                 5.49229
   6.81952
0.05    16.4227             2.11395
   1.82208                 1.33601
   0.91586
```

```
0.05    1.77208              1.78378
   1.81211                  4.26182
   14.9627
0.05    1.50092              0.364905
   1.21867                  6.13271
   4.71726
0.05    0.649307             2.75188
   0.60479                  9.38110
   7.98973
0.05    4.49499              3.86644
   7.43374                  10.1143
   3.58460
0.05    4.16968              6.67566
   3.07337                  10.9172
   5.82475
0.05    7.96389              15.3834
   28.3582                  1.10825
   8.49163
0.05    10.8307              12.4329
   15.1109                  9.55620
   11.9676
0.05    12.4165              7.15015
   16.5175                  1.27602
   1.67179
0.05    12.2098              2.2422
   3.14763                  0.84614
   2.22312
0.05    10.3762              9.99165
   6.71435                  1.74636
   3.61693
```

```
0.05    1.38996              1.77634
   2.26579                  6.46772
   8.47221
0.05    11.9347              0.831578
   6.58384                  14.4644
   10.1093
0.05    18.9461              14.1286
   5.94915                  5.59946
   10.2159
0.05    18.4704              14.471
   1.72473                  1.55002
   3.82520
```